

AN ABSTRACT OF THE THESIS

Se Kyoun Lee for the degree of DOCTOR OF PHILOSOPHY in

Mechanical Engineering presented on February 24, 1983

Title: THERMODYNAMIC ANALYSIS OF GEOTHERMAL ENERGY SYSTEMS WITH
FORCED RECOVERY FROM AQUIFERS

Abstract approved: _____

Redacted for Privacy

Gordon M. Reistad

A thermodynamic analysis of forced geoheat recovery from aquifers has been accomplished. The system investigated consists of a single recharging-discharging well pair, in a horizontally extensive aquifer, with either power generation or space heating as surface applications. The space heating systems investigated are (i) direct heating, (ii) heat pumps and (iii) a combination of direct heating and heat pumps. The thermodynamic performance parameters considered are the effectiveness (Second Law Efficiency) and fossil fuel savings.

Previous work on this problem has considered only the surface system with a specified temperature at the wellhead. Also, in the previous work, the surface system was either power generation only or heating only. This thesis includes the subsurface system in the analysis and the surface application of this work is treated as an important parameter. Due to the interaction between the surface and subsurface systems, the load conditions and geologic conditions play important roles in determining the optimum operation.

The analysis indicates that the well separation should be large enough to insure a constant production temperature during the project life time. For high temperature resources (higher than about 435 K), power generation yields the best performance and is therefore recommended. The relative desirability of the combination (heating and heat pumps) requires consideration of the load condition, resource temperature and other geologic conditions. Such evaluations for these automatically determine the appropriate ranges of direct heating. The optimum operation of each system is also dependent on the same parameters as well as the injection temperature.

Analysis also has been done on a given well system with a small well separation. In such a case, operation must be continued after thermal breakthrough in order to obtain a moderate output for the life of the system. Power generation and the combination do not have good performance with this model. Direct heating, with careful control of flow rate, appears to be the preferred system. For low temperature resources, heat pumps can only be used with careful control of the flow rate and injection temperature.

THERMODYNAMIC ANALYSIS OF GEOTHERMAL ENERGY
SYSTEMS WITH FORCED RECOVERY FROM AQUIFERS

by

Se Kyoum Lee

A THESIS

submitted to

Oregon State University

in partial fulfillment of
the requirements for the
degree of

Doctor of Philosophy

Completed February 24, 1983

Commencement June 1983

APPROVED:

Redacted for Privacy

Professor of Mechanical Engineering in charge of major

Redacted for Privacy

Head of Department of Mechanical Engineering

Redacted for Privacy

Dean of Graduate School

Date thesis is presented February 24, 1983

Typed by Se Kyoun Lee

ACKNOWLEDGEMENTS

I would like to thank my major professor Dr. Gordon M. Reistad for the many hours of help he provided throughout the study of this thesis.

I would like to express my gratitude to my wife, Hyun, and my daughter, Angie, who have have suffered such a long student life with me. Without the endless love of my parents, In-Sop and Kyung-Ok, who continuously have supported and encouraged me, this work could not have been accomplished.

The computer center is greatly appreciated for the grant of computer time for this research.

TABLE OF CONTENTS

1.	INTRODUCTION	1
1.1	Background	1
1.1.1	General	1
1.1.2	Classification of Systems	2
1.2	Performance of Geothermal Systems	4
1.3	Problem Statement	5
2.	HOT WATER AQUIFERS	10
2.1	Fluid Flow in Aquifers	11
2.2	Production Temperature of Production-Reinjection Well Systems	17
2.2.1	Production Temperature of a Doublet	24
2.2.2	Production Temperature of a Doublet with Decreasing Injection Temperature	29
2.2.3	Production Temperature of a Doublet with Increasing Flow Rate	34
2.3	Head Loss through Aquifers	38
3.	SYSTEM MODELS AND PERFORMANCE PARAMETERS	50
3.1	The Subsurface Systems	50
3.1.1	The Aquifer and Well Systems	50
3.1.2	Geothermal Fluid Pump Work	51
3.2	Power Generation	53
3.3	Space Heating	59
3.3.1	Direct Heating	59
3.3.2	Heat Pump	60
3.3.3	Combination	63
4.	CONSTANT FLOW MODEL	66
4.1	Preliminaries	67
4.2	Direct Heating	74
4.3	Power Generation	76
4.4	Combination	82
4.5	Heat Pump System	90

5.	INCREASING FLOW MODEL	101
5.1	Preliminaries	101
5.2	Selection of Applicable Systems	103
5.2.1	Direct Heating	109
5.2.2	Heat Pump System	111
6.	CONCLUSIONS AND RECOMMENDATIONS	118
	BIBLIOGRAPHY	122
	APPENDIX I	124
	APPENDIX II	127
	APPENDIX III	132

LIST OF FIGURES

<u>Figure No.</u>		<u>Page</u>
1.1	Schematic of forced geoheat recovery system by well pair.	9
2.1	(A) Visualization of a stream channel. (B) Energy balance on a stream channel element.	20
2.2	Stream channel element.	25
2.3	Dimensionless temperature at the production well of a doublet in an extensive aquifer with no regional flow.	27
2.4	Stream lines and the position of thermal front of a doublet.	28
2.5	Schematic flow diagram of a geothermal energy system with constant flow rate and decreasing injection temperature for maintaining a constant system load.	30
2.6	Dimensionless temperature at the production well of a doublet with constant flow rate and decreasing injection temperature for maintaining a constant system load.	33
2.7	Schematic flow diagram of a geothermal energy system with constant injection temperature and increasing flow rate for maintaining a constant system load.	35
2.8	Dimensionless temperature at the production well of a doublet with constant injection temperature and increasing flow rate for maintaining a constant system load.	39
2.9	Stream channel of a doublet. The flow rate within the stream channel is denoted by q_j , the spreading angle of the stream channel at the injection well is denoted by $\Delta\theta_j$, and the position of thermal front is denoted by B . The injection and production well are designated by A and C respectively.	43
2.10	Head loss as a function of time. Data for this calculations are given in Section 2.3.	46

<u>Figure No.</u>		<u>Page</u>
2.11	Comparisons of the results between the detailed and simple head loss calculations. Solid line is the result from the detailed one and dotted line is the result from simple one.	48
3.1	Simple schematic of binary cycle system with the energy source from the forced geoheat recovery.	54
3.2	Sub-critical cycle without superheating.	55
3.3	Typical temperature profile in the sub-critical heat exchanger without superheating.	55
3.4	Flow diagram of direct heating system.	62
3.5	Flow diagram of heat pump system.	62
3.6	Flow diagram of combination.	62
4.1	The performance of direct heating.	75
4.2	Energy available and conversion efficiency as functions of injection temperature.	78
4.3	Effectiveness as a function of injection temperature in the power generation.	79
4.4	Optimum effectiveness as a function of resource temperature.	80
4.5	Comparison of the direct heating and power generation for a range of T_o .	81
4.6	Optimum power as a function of flow rate.	83
4.7	Comparison of the performance of direct heating and combination at a given load condition.	84
4.8	Effectiveness ratio(ϵ_r) for a range of T_o and L_H (k = 200 mD case).	86
4.9	Effectiveness ratio(ϵ_r) for a range of T_o and L_H (k = 100 mD case).	87
4.10	Effectiveness ratio(ϵ_r) for a range of T_o and L_H (k = 50 mD case).	88
4.11	The effectiveness and fossil fuel saving for a range of L_H for a combination.	89

<u>Figure No.</u>		<u>Page</u>
4.12	Maximum favorable load conditions for a range of T_o (combination).	91
4.13	Optimum injection temperature and optimum flow rate as functions of heating load for combination ($k = 200$ mD case).	92
4.14	Optimum injection temperature and optimum flow rate as functions of heating load for combination ($k = 100$ mD case).	93
4.15	Optimum injection temperature and optimum flow rate as functions of heating load for combination ($k = 50$ mD case).	94
4.16	Effectiveness of heat pump system as a function of injection temperature for specified load conditions.	96
4.17	Maximum favorable load conditions for a range of T_o (heat pump).	97
4.18	Optimum injection temperature and optimum flow rate as functions of heating load for heat pump system ($k = 200$ mD case).	98
4.19	Optimum injection temperature and optimum flow rate as functions of heating load for heat pump system ($k = 100$ mD case).	99
4.20	Optimum injection temperature and optimum flow rate as functions of heating load for heat pump system ($k = 50$ mD case).	100
5.1	Production temperature, flow rate and pump work of geothermal fluid as a function of time for the Increasing Flow Model.	105
5.2	Optimum injection temperature (T_i), system inlet temperature (T_s) and net power output as functions of initial flow rate for Increasing Flow Model.	106
5.3	Performance comparisons of power generation and direct heating for the Increasing Flow Model.	108
5.4	Performance diagram of combination: (A) $T_o = 330$ K case (B) $T_o = 350$ K case	110

<u>Figure No.</u>		<u>Page</u>
5.5	Load curve of direct heating system (D = 300 m case).	112
5.6	Load curve of direct heating system (D = 500 m case).	113
5.7	Performance diagram of heat pump.	115
5.8	Performance diagram of heat pump ($T_o = 315$ K case).	116
5.9	Performance diagram of heat pump ($T_o = 310$ K case).	117

LIST OF TABLES

<u>Table No.</u>		<u>Page</u>
2.1	Values used for the Calculation of Head Loss through Aquifers.	45
4.1	The Values of Parameters used for the System Performance Calculations.	72

THERMODYNAMIC ANALYSIS OF GEOTHERMAL ENERGY SYSTEMS WITH FORCED RECOVERY FROM AQUIFERS

1. INTRODUCTION

1.1 Background

1.1.1 General

A geothermal resource can be simply defined as a reservoir in the earth's crust from which thermal energy can be extracted economically and utilized for generating electric power or heating. Radioactive decay of unstable isotopes such as uranium, thorium and potassium continuously generate thermal energy within the earth[1] and the thermal energy content of the earth is estimated to be 13×10^{30} Joules. However, under normal geothermal conditions, it is not economical to exploit this enormous heat reservoir. High temperature zones within the earth's crust and the availability of fluid in these zones are essential in exploiting geothermal energy. The normal geothermal gradient is only about 3 K per 100 m within the earth's crust. However, in some regions of the world, the geothermal gradient is much greater than the normal one. These anomalous regions which generally are associated with young volcanism are usually regarded as geothermal resources. High temperature alone is not sufficient for a geothermal resource to be exploited. The high temperature zone must be filled with fluid at a depth which can be reached by drilling and the fluid must be

available in great quantities. This zone must also have a great contact area between the rock and fluid in order to have efficient heat exchange between them. Only water or steam occurs in the necessary quantities in nature. The hot water or the steam can be exploited through drilling holes.

1.1.2 Classification of Systems

Geothermal resources are conveniently divided into four basic types: the vapor-dominated systems; the hot water geothermal systems; the geopressured systems; and the hot dry rock systems.

Vapor-dominated systems: These can be subdivided into two types: dry steam systems or wet steam systems. Dry steam systems are relatively rare, however the most important and successful geothermal power developments in the world today are associated with the development of these systems (in Larderello, Italy; in The Geysers, California; in Matsukawa, Japan). In such systems, the continuous phase within the pore space is that of steam. Temperatures are typically in the range of 490–520 K. Wet steam systems are the underground reservoirs of hot water which have temperatures close to the boiling temperature at the pressure in the reservoir. Upon the opening of a well into the reservoir, the pressure can be released thus allowing the production of a mixture of steam and water. Temperatures are usually in the range of 450–640 K.

Hot water geothermal systems are sometimes called low temperature geothermal systems. Water temperature is sufficiently below the

boiling temperature at that pressure in the reservoir, thus allowing the production of liquid geothermal fluid. In order to have a purely liquid state production down-hole pumps may be required. The temperature varies from 330 to 450 K.

Geopressured geothermal systems are reservoirs located in deep sedimentary strata in regions where rock compaction has taken place over extended periods of time, and where an effective shale seal has formed. Under conditions of such shale compression which squeezes water out of the shale matrix into adjacent sand bodies, the water acquires an internal pressure greater than the ordinary hydrostatic pressure at that depth. The attractiveness of this form of resource lies in the fact that three types of energy may be extracted: hydraulic energy (by virtue of the high pressure), thermal energy (by virtue of the high temperature) and fossil energy (by virtue of dissolved methane gas). Temperatures as high as 510 K have been encountered in some geopressured reservoirs in the Gulf Coast of the United States with wellhead pressures as high as 76000 kPa or more.

Hot dry rock systems exist where the geothermal temperature gradient is high within the earth's crust without any fluid availability to store or transport the thermal energy. Considerable research effort is presently being devoted to methods of introducing cold water into hot dry rock systems with natural or artificially induced fractures, and extracting heated water through a pattern of appropriately drilled holes in the vicinity of the injected holes.

Superheated or saturated steam from geothermal resources is the most important source of geothermal power generation. Hot water from geothermal resources can be used for either power generation or heating depending on the resource temperature and other site specific conditions. It is generally considered that electricity generation is not presently economically feasible for resources with temperatures below about 423 K. Geothermal resources with temperatures below 423 K can be used for direct heating. If the resource temperature is too low for direct heating applications a heat pump system may be used to upgrade the thermal energy of geothermal fluid[2].

1.2 Performance of Geothermal Systems

In the geothermal energy systems, several system variables such as well flow rate, allowable temperature drop and type of application greatly influence their thermodynamic performances. Several authors have considered these problems so far.

Reistad et al.[3] have analyzed the thermodynamic performance of several types of geothermal systems. Their work is based on the assumptions of liquid state geothermal fluid and given flow rate at constant temperature. On this basis, they have shown the optimum type of heating system which maximizes the effectiveness¹ as a function of resource temperature. The effectiveness comparison of

¹ For complete definition, see Chapter III.

each system is based on the calculations of optimum allowable temperature drop of each system.

Walter[4] has considered the optimization problem of geothermal power generation. His analysis is also based on the assumptions of liquid state geothermal fluid and given flow rate. Using the iso-butane binary cycle system, optimum turbine inlet pressure which maximizes the effectiveness is shown in his work as a function of resource temperature (turbine inlet pressure is strongly a function of temperature drop of geothermal fluid).

On the other hand, Steidel[5] has considered the optimum well flow rate which maximizes the available power at the wellhead from either dry steam or wet steam fields.

1.3 Problem Statement

The above studies are mostly limited to the performances of the surface systems. However, what actually happens in the subsurface system can affect the overall performances significantly and such subsurface performances may be closely related to the system variables. Unfortunately, many features of the subsurface system are still obscure. Also there are many different features that could occur depending on the given geologic conditions.

The particular geothermal energy resource considered in this work is a homogeneous aquifer bounded top and bottom by impermeable aquicludes. The aquifer is assumed to be saturated with hot water and this hot water is assumed to be produced as a purely liquid

state at the wellhead. It is further assumed that the used geothermal fluid is reinjected back into the producing reservoir. The flow characteristics and heat exchanging characteristics of such types of geothermal energy resources are relatively well known. Such features will be addressed in Chapter II.

Reinjection of used geothermal fluid into the producing reservoir has been proposed by many investigators as an effective way to avoid or alleviate the following problems which might be associated with a specific geothermal energy system:

- 1) Disposal of used geothermal fluid with minimum environmental impact
- 2) Land subsidence due to the reduced pressure in the reservoir fluid withdrawal
- 3) Depletion of fluid in the reservoir

This procedure also permits the partial recovery of the thermal energy contained in the rock materials in the aquifer. However, reinjection creates a zone of relatively cold water around each injection well. These zones will grow with time and will eventually reach the production wells. After thermal breakthrough occurs, the production temperature starts to decrease drastically. It is thus important to design the system of production-reinjection wells in order to prevent the cold region breakthrough before a specified time. If continued operation after thermal breakthrough is desired, more careful control of flow rate and temperature drop of geothermal fluid is required to maximize the performance of overall

operation because these variables are closely related to the production temperature after thermal breakthrough.

For such type of energy resource, it may be readily seen that the interactions between the surface conversion system and the subsurface energy resource play important roles in determining the overall system performance. Reinjection temperature and flow rate are considered as important interaction parameters. For instance, reinjection temperature is an important factor in determining the performance of the surface system. As reinjection temperature increases, conversion efficiency (for power generation or heat pump) increases but the amount of energy available in the system decreases. Also reinjection temperature greatly affects the subsurface performance. Low reinjection temperature causes the growing of a high viscosity zone around the reinjection well which means the required pump work for the geothermal fluid circulation becomes high. Buoyancy effect which reduces the pump work when cold water is reinjected is also not small for the aquifers at the depths of order of several thousand meters. This pump work reducing effect is high when reinjection temperature is low. Considering the low available energy of thermal water, it is evident that pump work is an important factor for the overall performance. Flow rate is also closely related to the pump work and the amount of energy yielded in the surface system. The time required for the thermal breakthrough is also mainly a function of flow rate. If continued operation after thermal breakthrough is desired (especially when the well separation

is limited to small dimension), both quantities, reinjection temperature and flow rate, play more important roles for the subsurface performance because these quantities largely determine the production temperature after thermal breakthrough. Including the geothermal energy resource in the overall performance analysis thus brings about such interaction problems between the surface and subsurface systems which also give rise to many interesting new problems.

This thesis aims at a more complete thermodynamic analysis of the geothermal systems by including the geothermal energy reservoir. The primary object of the present work is to evaluate the range of system variables which provide the best range of overall performance. The thermodynamic performance parameters considered in this work are the effectiveness and fossil fuel savings. These concepts will be explained in Chapter III.

Figure 1.1 shows the system being investigated which consists of one production and one reinjection well. Hot geothermal fluid produced at the production well enters the surface system which may be either an electric or a non-electric application. Used geothermal fluid is reinjected back into the same reservoir through the reinjection well. This results in a cold zone growing around the reinjection well. The geothermal applications being investigated here are electricity generation and residential heating. Direct heating, combination of direct heating and heat pumps and heat pumps alone are all considered as potential heating systems.

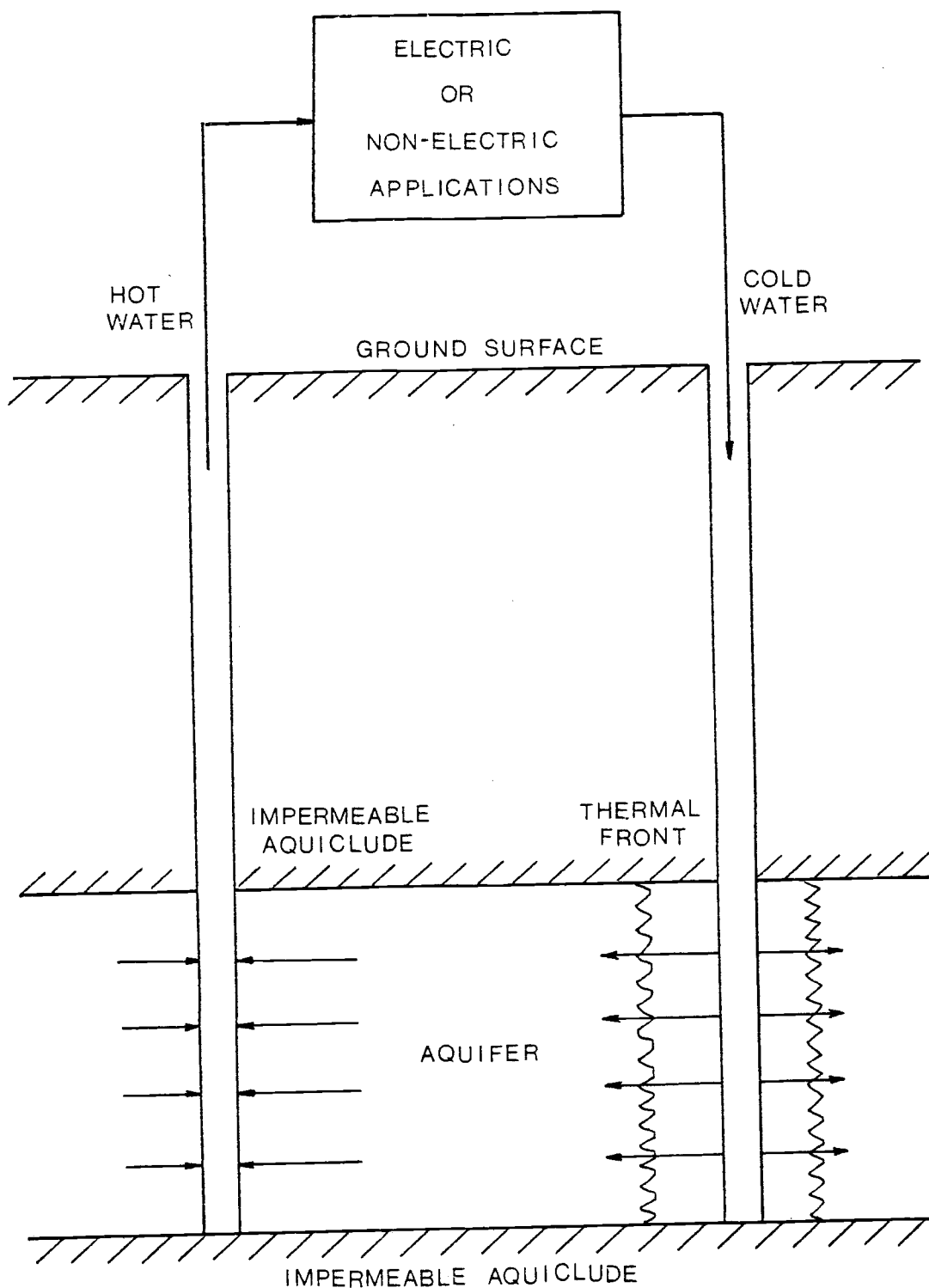


Figure 1.1. Schematic of forced geoheat recovery system by well pair.

2. HOT WATER AQUIFERS

Aquifers are underground formations which transmit and store water in pore space within rocks. Most readily exploitable geothermal energy in the western United States resides in the aquifers saturated with hot water. Aquifers bounded top and bottom by impermeable materials are called confined aquifers.

Depending on the type of geothermal fluid extraction, three categorizations may be possible: the free flow systems; the partially forced systems; and the forced geoheat recovery systems. In the free flow systems, sufficient pressure head of geothermal fluids maintains the required borehole flow. The partially forced systems involve down-hole pumping to compliment the natural pressure head of the geothermal fluids to maintain or increase the borehole flow. The third type, forced geoheat recovery systems rely on an artificial recharge of the used geothermal fluids into the producing reservoir. Thus in the forced geoheat recovery systems, the well systems must consist of production and reinjection wells and the pumping work is essential. The advantages and problems of reinjection of used geothermal fluids into the producing aquifers were already discussed in Chapter I.

The geothermal energy resources of interest in this work are forced geoheat recovery systems of confined aquifers. Two major characteristics must be understood in such systems before going to detailed analyses; the flow characteristics and the heat

exchanging characteristics in aquifers. These two phenomena will be discussed in Section 2.1 and Section 2.2. In Section 2.3, head loss through aquifers will be discussed.

2.1 Fluid Flow in Aquifers

The ground-water flow is governed by Darcy's law which may be expressed as

$$V = -K \frac{dh}{dl} \quad (2.1)$$

where V is the Darcy velocity², h is the hydraulic head and l is the length along the flow path. The proportionality constant K is called the hydraulic conductivity. The kinetic energy term which is proportional to the square of the velocity is neglected in h because ground-water velocities are very small, at least in laminar flow.

Thus

$$h = z + \frac{p}{\rho g} + \text{arbitrary constant} \quad (2.2)$$

where z is the elevation above an arbitrary datum plane, p is the pressure sustained by the fluid, ρ is the density of the fluid and g is the gravitational constant.

The hydraulic conductivity K is related to the intrinsic

² The Darcy velocity is a fictitious flow velocity or a specific discharge which is defined as $V=Q/A_c$ where Q is the volume flow rate and A_c is the cross sectional area of a porous medium. To find the true velocity between the grains, V must be divided by porosity ϕ which is defined as a void space fraction of a given volume of porous medium. Unless otherwise specified, the velocity in this work refers to the Darcy velocity.

permeability k of the medium by

$$K = \frac{k \rho g}{\mu} \quad (2.3)$$

in which μ is the viscosity of the fluid. As is evident from Equation (2.1), K has the dimensions of a velocity. The darcy unit is adopted as a measure of the intrinsic permeability k which has the dimensions of an area. One darcy is equal to $0.987 \times 10^{-12} \text{ m}^2$.

Darcy's law, originally given for one-dimensional flow only, can be generalized to apply to three dimensional flow. For a homogeneous and isotropic porous medium,

$$V_x = -K \frac{\partial h}{\partial x}, \quad V_y = -K \frac{\partial h}{\partial y}, \quad V_z = -K \frac{\partial h}{\partial z} \quad (2.4)$$

where V_x , V_y , V_z are the velocity components of x , y , z axis respectively in the Cartesian coordinate system.

From this it is seen that $\Phi = Kh$ is really velocity potential—a function whose negative gradient gives the velocity vector. Equation (2.4) may be conveniently combined into the single vector equation as

$$\bar{V} = -\nabla\Phi. \quad (2.5)$$

Equation (2.4) or Equation (2.5) may be considered as a substitute for the Navier-Stokes equations in this type of flow problem.

The validity of Darcy's law falls in the region of laminar flow where the Reynolds number is less than 1. Reynolds number has been established in the flow through porous media, namely

$$N_R = \frac{V d \rho}{\mu} \quad (2.6)$$

in which d is the characteristic length which is usually chosen as any reasonable average diameter of the grains in the porous medium.

Combining Equation (2.4) with the equation of conservation of mass, the equation for ground-water flow in a homogeneous, isotropic porous medium can be established. The equation of conservation of mass in the porous medium can be shown³ as

$$\frac{\partial(\rho V_x)}{\partial x} + \frac{\partial(\rho V_y)}{\partial y} + \frac{\partial(\rho V_z)}{\partial z} = - \frac{\partial(\rho \phi)}{\partial t} . \quad (2.7)$$

For incompressible fluid and rigid porous medium, both ρ and ϕ may be taken as constant. For such a case, Equation (2.7), by combining with Equation (2.4), becomes

$$\frac{\partial^2 h}{\partial x^2} + \frac{\partial^2 h}{\partial y^2} + \frac{\partial^2 h}{\partial z^2} = 0 \quad (2.8)$$

which is the so-called Laplace's equation. In the ground-water flow through aquifers, the compressibilities of both the fluid and aquifer are usually not neglected. The compressibility of the fluid $\hat{\beta}$ is related to the fluid density by

$$\rho \hat{\beta} \frac{\partial p}{\partial t} = \frac{\partial \rho}{\partial t} . \quad (2.9)$$

³ The equation of conservation of mass in the porous medium takes the same form as that of fluid dynamics except the porosity, ϕ , which comes into play in the storage term. See Davis and DeWiest [6] for the derivation of Equation (2.7).

The compressibility of aquifer is essentially due to the vertical compression or expansion of aquifer which causes the changes in porosity. By introducing the concept of vertical compressibility of the granular skeleton of the medium

$$\alpha = -\frac{dz/z}{d\sigma_z} \quad (2.10)$$

where z is the vertical length and σ_z is the vertical stress of the medium, it can be shown[6] that

$$\frac{\partial \phi}{\partial t} = -(1-\phi)\alpha \frac{\partial \sigma_z}{\partial t} \quad (2.11)$$

By combining Equations (2.4), (2.9) and (2.11) with the Equation (2.7), the final equation of ground-water flow can be established. Detailed analyses are shown in the textbook by Davis and DeWiest[6]. Therefore, it may be enough to present simply their final equation here. The final equation of ground-water flow is

$$\frac{\partial^2 h}{\partial x^2} + \frac{\partial^2 h}{\partial y^2} + \frac{\partial^2 h}{\partial z^2} - g\hat{\beta}\rho \frac{\partial h}{\partial z} = \frac{S_s}{K} \frac{\partial h}{\partial t} \quad (2.12)$$

in which $S_s = \rho g[(1-\phi)\alpha + \phi\hat{\beta}]$ is called the specific storage.

The $\partial h/\partial z$ term may be neglected for most cases since the multiplier β is very small for liquid water. The right-hand side becomes zero in the steady state. Thus it is seen again that the steady state equation becomes Laplace's equation for such cases. For two-dimensional flow,

$$\frac{\partial^2 h}{\partial x^2} + \frac{\partial^2 h}{\partial y^2} = \frac{S_s}{K} \frac{\partial h}{\partial t} \quad (2.13)$$

is obtained from Equation (2.12). Two-dimensional flow cases arise in the problem of horizontal aquifers of uniform thickness which are completely filled with fluids and pierced by wells penetrating the whole thickness. For two-dimensional steady flow, the two-dimensional Laplace's equation

$$\frac{\partial^2 h}{\partial x^2} + \frac{\partial^2 h}{\partial y^2} = 0 \quad (2.14)$$

can be obtained. Two-dimensional steady flow makes it possible to use the powerful tools of hydrodynamics. The concept of velocity potential $\Phi = Kh$ as is seen in Equation (2.5) is valid for the medium of constant K . By means of the Cauchy-Riemann equation, the conjugate harmonic function ψ (stream function) can be determined such that the complex potential function $W(z) = \Phi(x,y) + i\psi(x,y)$ is an analytic function of the complex variable, $z = x + iy$.

When steady state is established, the effect of initial conditions disappear and the flow is fully governed by boundary conditions only. Therefore, steady state establishment requires sufficient time elapsing. However, if perfect incompressibilities of both fluids and aquifers can be assumed, the velocity of propagation of disturbances in the porous medium can be infinite. Such a case would result in an instant establishment of steady state and each state caused by changing boundary conditions may be assumed as a continuous succession of steady state [7] appropriate to the corresponding instantaneous values of the boundary conditions. Therefore, the time variable does not appear in the governing

equation for this case. For ground-water flow, both fluid and medium may be somewhat compressible. However, the required time for the establishment of steady state is relatively small if the flow dimensions are moderate and the medium is completely filled with liquid. Muskat[7] has shown that the establishment of steady state would take a time of the order of

$$t \sim \frac{\phi \hat{\beta} \mu r_e^2}{4k} \quad (2.15)$$

where r_e is the flow dimension. For the production-reinjection well system, the separation between the wells may be considered as the flow dimension even though the aquifers themselves are considered to be very large or infinite. This can be done since the features of particular interest are the mutual interactions of the wells. The water at 343 K shows a compressibility value of $4.5 \times 10^{-10} \text{ sec}^2 \text{ m/kg}$ and viscosity of $0.42 \times 10^{-3} \text{ kg/msec}$. Thus for a system with $\phi=0.2$, $k=200 \text{ mD}$ and $r_e=300 \text{ m}$, t is found to be only 1.2 hours if the aquifers are filled with water at the temperature of 343 K. This value is very small in relation to the overall problem.

The concept of continuous succession of steady state thus may be applied for most practical cases except when flow dimensions are very large⁴ or significant amount of vapors are present⁵ in the ground-water systems.

⁴ The time required for the establishment of steady state is proportional to the square of flow dimension as is seen from Equation (2.15).

⁵ It is shown[7] that the normal compressibility of water can be raised to an effective value 10 times as great by a distributed gas volume of only 4.5%, at 100 atm.

Often in the geothermal well systems, the required borehole flow may change to meet the required load. Especially when the continued operation after the thermal breakthrough is desired, the borehole flow may be required to increase continuously due to the production temperature decreasing. However, the increasing rate may be very small considering the large time scale of geothermal well operation, usually several tens of years. Hence, for moderate dimensions of geothermal well systems(usually several hundred meters of well separation cases), the assumption of steady state or continuous succession of steady state can be applied if the aquifers are completely filled with liquid water. Also it is possible to use Laplace's equation for most practical cases. Especially for the two-dimensional flow case, the complex potential function is available.

2.2 Production Temperature of Production-Reinjection Well Systems

A simple mathematical model for investigating the non-steady temperature behavior of a pumped aquifer during reinjection of a fluid at a temperature different from that of the native water has been developed by Gringarten and Sauty[8]. Their model is based upon many simplified assumptions, from which analytical solutions can be obtained. Assumptions of their model are listed below:

- 1) The aquifer is assumed to be horizontal and of uniform thickness b . The cap rock and bed rock are impermeable to flow and of infinite extent in the vertical direction. The system is thus symmetrical with respect to the midplane of the aquifer.

- 2) The flow field is assumed to be two-dimensional steady state with wells fully penetrated the aquifer. The total injection rate Q is constant and equal to the total production rate. Thus the flow field due to the recharging and discharging wells is superimposed on a natural system of areal parallel flow.
- 3) Initially, the water and rock in the aquifer and the cap rock and bed rock are at the same temperature T_0 . At time $t=0$ the temperature of the injected water is set equal to T_i and is maintained constant thereafter. Thermal equilibrium is supposed to take place instantaneously between the water and the rock in the aquifer.
- 4) Horizontal conduction is neglected in the aquifer. Furthermore, the aquifer is assumed to be thin enough that the temperature is always uniform in the vertical direction.
- 5) Horizontal conduction is also neglected in the cap rock and bed rock.
- 6) The cap rock or bed rock temperature is assumed to be equal to the aquifer temperature at the point of contact.
- 7) The product of the density and the heat capacity for both the water and the rock, and the cap rock vertical thermal conductivity, are constant. Differences in viscosity between the injected water and the native water are neglected. A "no-mixing" condition and piston-like displacement are assumed in the aquifer.

The above assumptions thus allow each stream channel leaving a particular well to be treated independently. The production temperature is a mixed temperature of water from all of the stream channels that reach the production well.

The temperature corresponding to a particular stream channel bounded by stream lines ψ and $\psi+d\psi$, can be described by a one-dimensional function $T_w^\psi(S,t)$ in the aquifer and by a two-dimensional function $T_R^\psi(S,z,t)$ in the cap rock or bed rock, S being the stream channel area from the corresponding injection well(Figure 2.1.A).

From the energy balance on an element of stream channel between the areas S and $S+dS$ from the injection well (Figure 2.1.B) the governing differential equation for the water temperature can be written as

$$\frac{q}{2} \rho_w C_w \frac{\partial T_w^\psi(S,t)}{\partial S} + \frac{b}{2} \rho_A C_A \frac{\partial T_w^\psi(S,t)}{\partial t} = K_R \frac{\partial T_R^\psi(S,z,t)}{\partial z} \Big|_{z=0} \quad (2.16)$$

where q is the flow rate within the stream channel, $\rho_w C_w$ is the volumetric heat capacity of water, $\rho_A C_A = \phi \rho_w C_w + (1-\phi) \rho_r C_r$ is the aquifer volumetric heat capacity ($\rho_r C_r$ being the volumetric heat capacity of the rock in the aquifer and ϕ being the porosity of aquifer), K_R is the cap rock thermal conductivity and b is the thickness of the aquifer. The cap rock temperature is governed by

$$\frac{\partial^2 T_R^\psi(S,z,t)}{\partial z^2} = \frac{\rho_R C_R}{K_R} \frac{\partial T_R^\psi(S,z,t)}{\partial t} \quad z \geq 0 \quad (2.17)$$

where $\rho_R C_R$ is the cap rock volumetric heat capacity. Equation (2.16) can be treated as a boundary condition of Equation (2.17). Other boundary and initial conditions are

$$T_R^\psi(S,0,t) = T_w^\psi(S,t) \quad (2.18)$$

$$T_w^\psi(0,t) = T_i \quad (2.19)$$

$$T_R^\psi(S,\infty,t) = T_o \quad (2.20)$$

$$T_R^\psi(S,z,0) = T_w^\psi(S,0) = T_o \quad (2.21)$$

where T_i is the injection temperature.

The simultaneous solution of Equations (2.16) and (2.17)

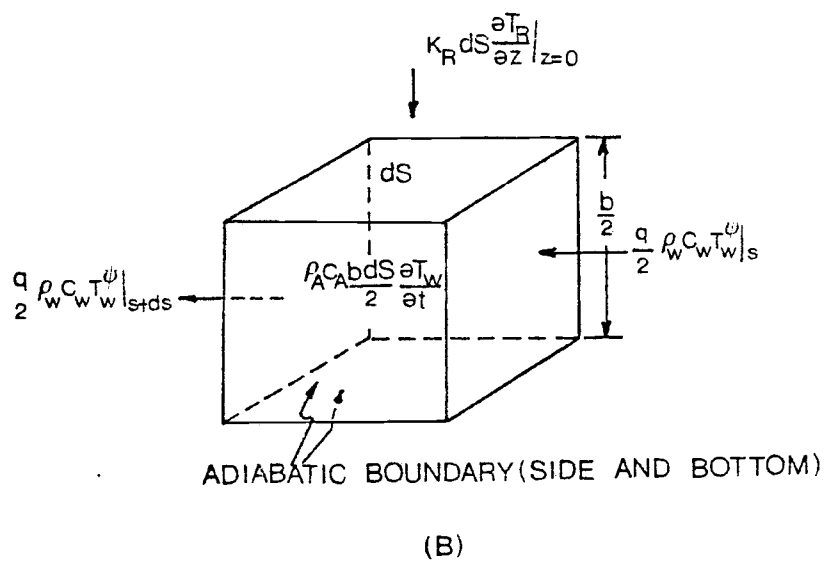
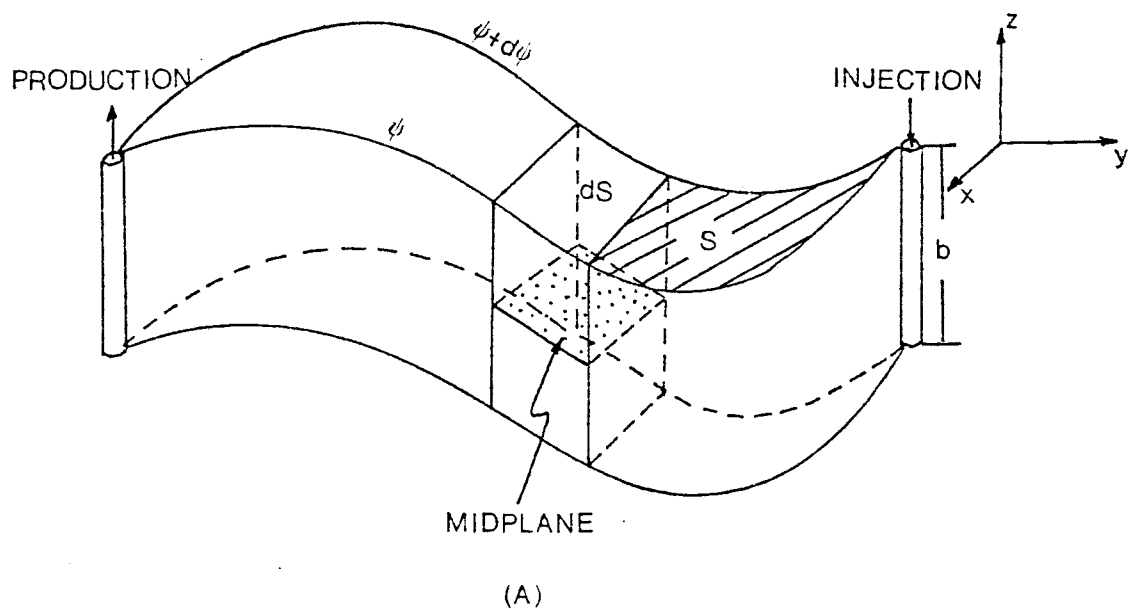


Figure 2.1. (A) Visualization of a stream channel. (B) Energy balance on a stream channel element.

subject to conditions (2.18)-(2.21) is easily obtained[9,10].

The result for the water temperature is

$$\frac{T_o - T_w^\psi(S,t)}{T_o - T_i} = \text{erfc} \left[\frac{S (\rho_R C_R K_R)^{1/2}}{q \rho_w C_w} \frac{1}{\{t - (\rho_A C_A / \rho_w C_w) (bS/q)\}^{1/2}} \right]. \quad (2.22)$$

The water temperature at the production well within an elementary stream channel, $T_w^\psi(t)$, is obtained by substituting the total stream channel area between two wells, S_{\max} , for S in Equation (2.22).

The non-dimensional expression of the result is

$$\frac{T_o - T_w^\psi(t)}{T_o - T_i} = \text{erfc} \left[\frac{S_{\max}/D^2}{q/Q} \left\{ \lambda \left(t_D - \frac{S_{\max}/D^2}{q/Q} \right)^{-1/2} \right\} \right] \quad (2.23)$$

where $\lambda = \frac{\rho_w C_w \rho_A C_A Q b}{\rho_R C_R K_R D^2}$, $t_D = \frac{\rho_w C_w Q t}{\rho_A C_A D^2 b}$, D is some characteristic length and Q is the production rate of the production well. S_{\max} and q are actually differential elements. By defining A as an area bounded by the stream line ψ and some arbitrary datum stream line, S_{\max} can be expressed as dA . Also $d\psi$ can be defined as q . Substituting S_{\max}/q in Equation (2.23) by $dA/d\psi$ results in

$$\frac{T_o - T_w^\psi(t)}{T_o - T_i} = \text{erfc} \left[\frac{d(A/D^2)}{d(\psi/Q)} \left\{ \lambda \left(t_D - \frac{d(A/D^2)}{d(\psi/Q)} \right)^{-1/2} \right\} \right]. \quad (2.24)$$

The production temperature at the production well at a given time t_D is then obtained by intergrating the right-hand side of Equation (2.24) with respect to ψ for all stream channels that have reached the production well at t_D :

$$\frac{T_o - T_w(t)}{T_o - T_i} = \int \text{erfc} \left[\frac{d(A/D^2)}{d(\psi/Q)} \left\{ \lambda \left(t_D - \frac{d(A/D^2)}{d(\psi/Q)} \right)^{-1/2} \right\} \right] d\left(\frac{\psi}{Q}\right) \quad (2.25)$$

Equation (2.25) is Gringarten and Sauty's general solution. It can be evaluated only after the flow pattern for a particular well system and set of assumptions is prescribed. Once the flow pattern is known the term $d(A/D^2)/d(\psi/Q)$ can be evaluated. This evaluation is usually done by numerical computations except in very simple cases.

It should be noted that small scale details of the aquifer temperature field cannot be predicted well from the above model due to many simplified assumptions. However, it is generally believed that the prediction of the production temperature from the above equation is not bad. Actually, the horizontal heat conduction results in thermal dispersion and smoothing the thermal front. The gravitational effect due to the density difference between injected water and native water results in the thermal front tilting with the cold temperature front advancing faster near the bottom of the aquifer than that near the top when injected water temperature is lower than that of the native water. These effects generally accelerate the advancement of the thermal front. The viscosity difference between the injected water and native water affects the flow field and also the thermal front movement. When cold water is injected in a single recharging-discharging well pair, the flow rate in the stream channel close to the straight line leading from the injection to the production well decreases because of the growing resistance to the flow due to the relatively high viscosity of the injected cold water in this stream channel. This results in

the retarding of the movement of the thermal front. On the other hand, if injected water is warmer than the aquifer, the opposite effect will occur[8].

Good prediction of thermal breakthrough time by Gringarten and Sauty's model can be expected in the cold water injection case due to such opposite effects. The prediction of production temperature after thermal breakthrough based on this model also may not be bad due to the averaging effect of water temperature from all stream channels which reach the production well. Therefore, it is determined that the temperature profile calculated this way is appropriate for the purpose of this thesis.

The numerical solutions can be obtained from the general solution, Equation(2.25), by specifying the particular flow pattern. The term, $d(A/D^2)/d(\psi/Q)$, can be usually obtained from numerical computations, but in some few simple cases, analytical evaluations are possible. The production temperature profile in a single recharging-discharging well pair(called a "doublet" hereafter) will be shown in Section 2.2.1. It is evident that the surface load will decrease after thermal breakthrough if flow rate and injection temperature are kept constant. To maintain a constant load after thermal breakthrough, some new operation with changing either flow rate or injection temperature or both after thermal breakthrough must be required. The production temperature for such cases will be investigated in Section 2.2.2 and Section 2.2.3. The case of decreasing injection temperature with constant flow rate will be

shown in Section 2.2.2 and increasing flow rate with constant injection temperature case in Section 2.2.3.

2.2.1 Production Temperature of a Doublet

Equation (2.25) has been applied to a doublet(single recharging-discharging well pair) in an extensive aquifer with no areal flow.

The complex potential function $W(z)$ is available to describe the flow field[11]. The production well is located on the x-axis at a point with coordinates $(-a,0)$ and the injection well at a point on the x-axis $(+a,0)$ (see Figure 2.2). With the source and sink approximation(source being the injection well and sink being the production well), $W(z)$ is expressed as:

$$\begin{aligned} W(z) &= \frac{Q}{2\pi b} \ln(z-a) - \frac{Q}{2\pi b} \ln(z+a) \\ &= \phi + i\psi \end{aligned} \quad (2.26)$$

Thus

$$\phi = \frac{Q}{4\pi b} \ln \left[\frac{(x-a)^2 + y^2}{(x+a)^2 + y^2} \right] \quad (2.27)$$

$$\psi = \frac{Q}{2\pi b} \theta \quad \text{where } \theta = \angle APB \text{ (Figure 2.2)}. \quad (2.28)$$

From Equation (2.28), it is seen that stream line is a segment of a circle connecting the production and injection wells. The term $d(A/D^2)/d(\psi/Q)$ in Equation (2.25) can readily be found for such a case from the geometrical relations(dA being the hatched area in Figure 2.2). The well separation in this case is considered as a

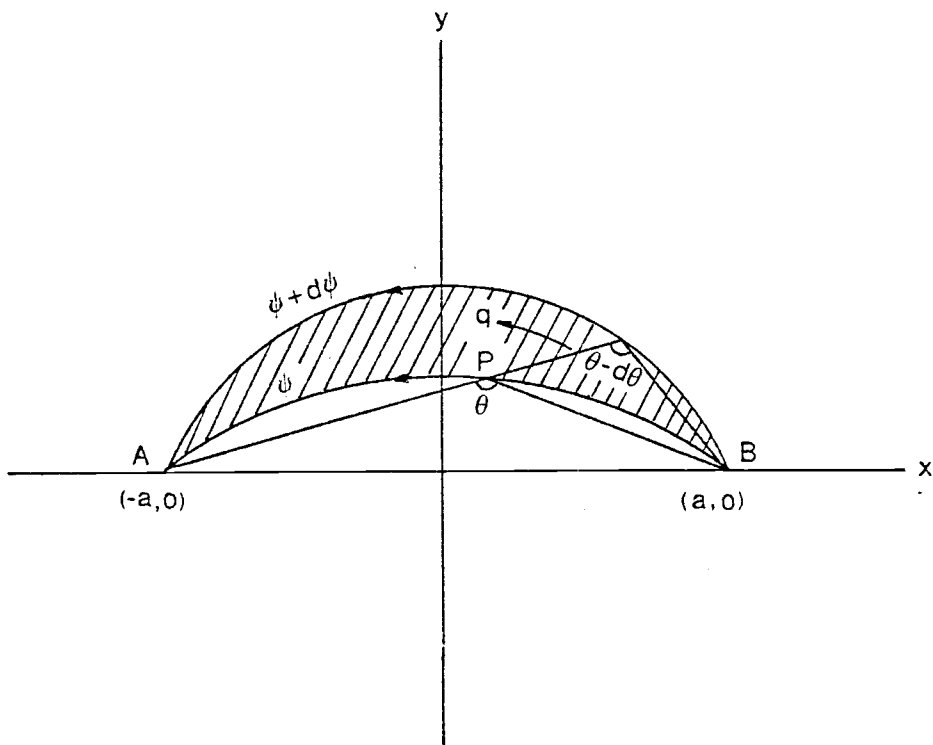


Figure 2.2. Stream channel element.

characteristic length (thus $D=2a$). The area bounded by the arc APB and x-axis can be expressed as a function of θ as:

$$A = \left(\frac{a}{\sin \theta} \right)^2 \left(\pi - \theta + \frac{\sin 2\theta}{2} \right) \quad (2.29)$$

The term $d\psi$ is, in this case,

$$d\psi = - \frac{Q}{2\pi} d\theta. \quad (2.30)$$

Thus

$$\frac{d(A/D^2)}{d(\psi/Q)} = f(\theta) \quad (2.31)$$

where

$$f(\theta) = \frac{\pi \cos \theta}{\sin^3 \theta} (\pi - \theta + \sin \theta \cos \theta) + \pi. \quad (2.32)$$

Then the general solution, Equation (2.25), becomes

$$T_{wD}(\lambda, t_D) = \frac{1}{\pi} \int_0^\pi \operatorname{erfc} \left[\frac{f(\theta)}{(\lambda \{t_D - f(\theta)\})^{1/2}} \right] d\theta \quad (2.33)$$

where $T_{wD} = \frac{T_o - T_w(t)}{T_o - T_i}$.

Figure 2.3 shows the numerical solution of T_{wD} . From this figure, it is seen that the heat transfer by conduction from the cap rock and bed rock is very small for the value of λ greater than 300. (In the forced operation cases, λ values often exceed 300.) The curve of $\lambda=\infty$ is the case in which there is no heat exchange by conduction between the aquifer and cap rock and bed rock ($K_R=0$). Thermal breakthrough occurs at $t_D=\pi/3$. Figure 2.4 shows the stream line and

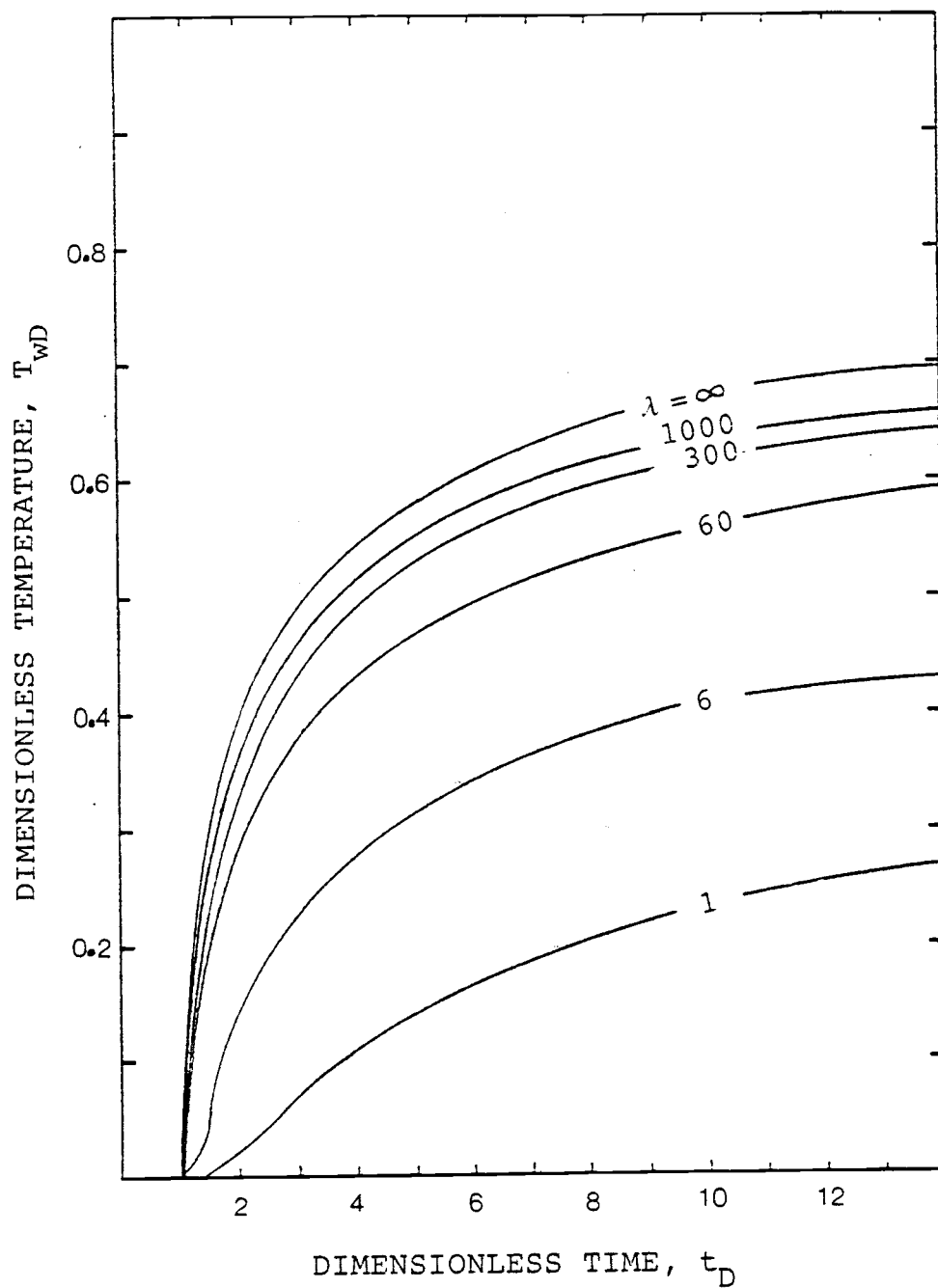


Figure 2.3. Dimensionless temperature at the production well of a doublet in an extensive aquifer with no regional flow.

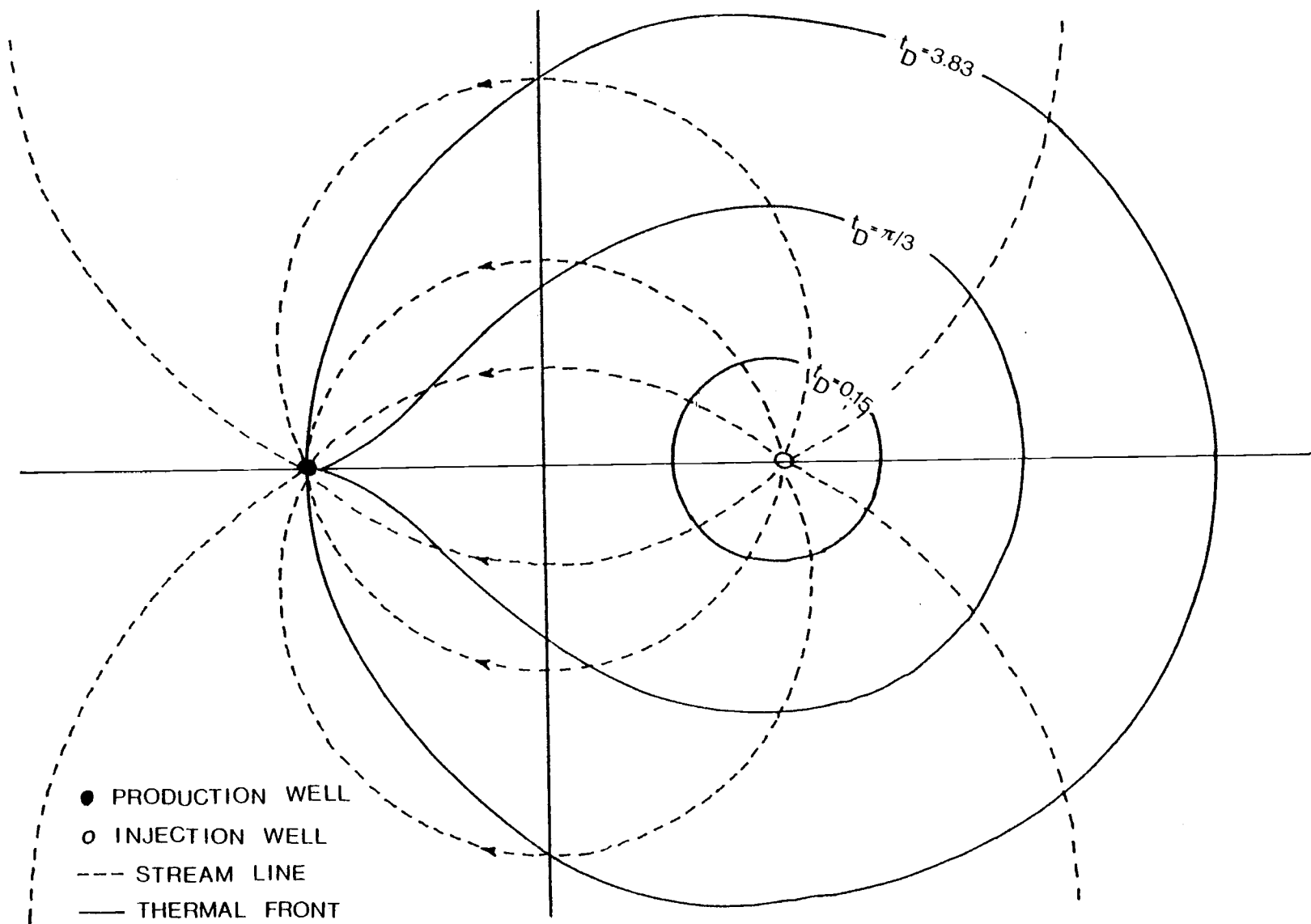


Figure 2.4. Stream lines and the position of thermal front of a doublet.

the position of thermal front before breakthrough, at breakthrough and after breakthrough.

2.2.2 Production Temperature of a Doublet with Decreasing Injection Temperature

As is indicated before, surface load of a doublet will decrease after thermal breakthrough. One possible way of yielding a constant load after thermal breakthrough without changing the flow rate is maintaining a constant temperature difference between the production and injection wells. Then it is evident that the injection temperature should decrease as the production temperature decreases.

Figure 2.5 shows the schematic diagram of this system. An appropriate amount of cold water from the system outlet is extracted and mixed with the produced water to lower the production temperature to T_{s1} , the constant system inlet temperature. To maintain a constant system flow rate, the same amount must be extracted from the system inlet. This amount is mixed with the system outlet fluid at a temperature T_{s2} before injection. As a result, the injection temperature increases, the effect of which will be shown later at the production well as an increased production temperature. Thus the operation of the surface system can be under constant conditions over the system life. If the system life time is designed to be ended at or before the thermal breakthrough, certainly extraction is not necessary. The amount of extraction from the system is really a function of design temperatures, T_{s1} , T_{s2} and the system life time. Also the extraction should approach zero at the end of the system life. The production

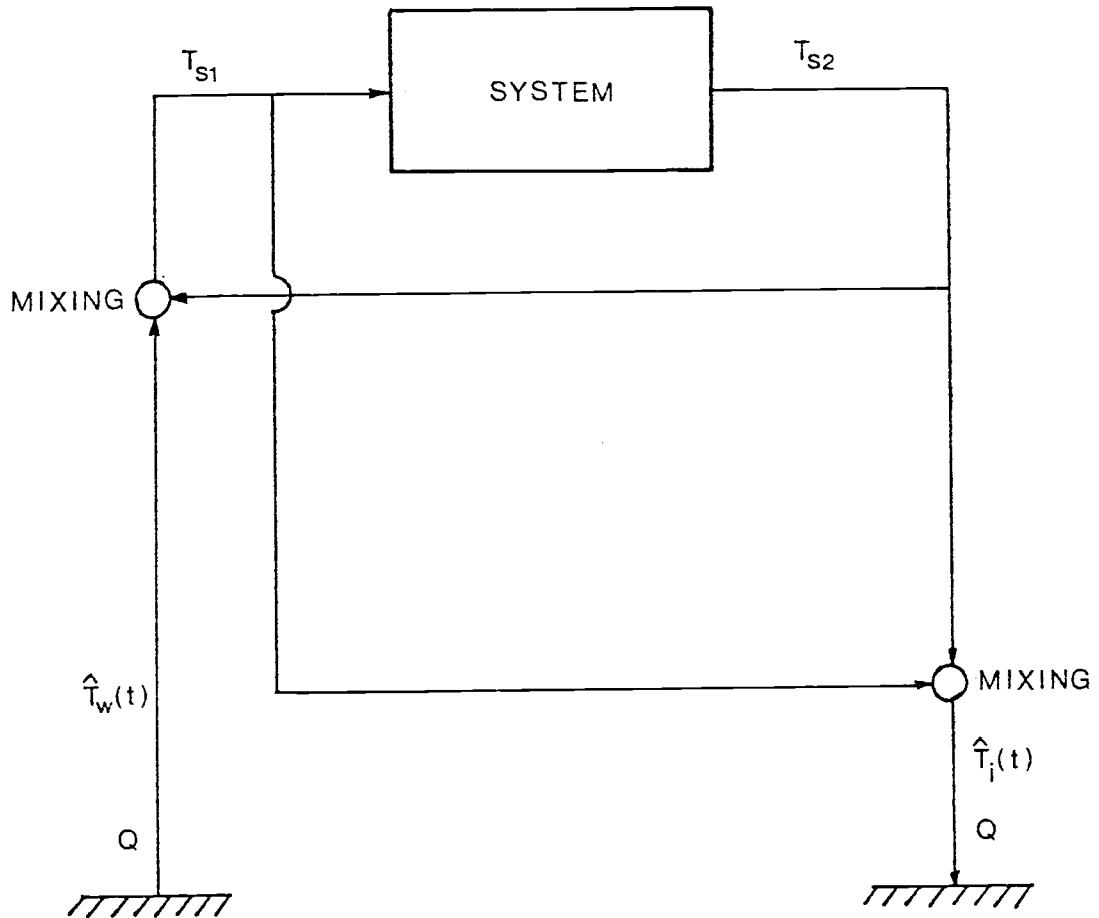


Figure 2.5. Schematic flow diagram of a geothermal energy system with constant flow rate and decreasing injection temperature for maintaining a constant system load.

temperature of such a system will be investigated with the same aquifer model as presented in Section 2.2.1.

Equations (2.16) through (2.21) can be applied here except for the boundary condition (2.19). The boundary condition in this case is a time dependent one. Duhamel's superposition intergral can be applied for such a case[12] to modify the solution (2.25).

Let T_i be the initial injection temperature and T_w be the production temperature of a constant injection temperature case. The non-dimensional production temperature, $T_{wD} = (T_o - T_w)/(T_o - T_i)$, is truly the solution of Section 2.2.1. The actual injection temperature should deviate from T_i after thermal breakthrough and the corresponding production temperature also deviates from T_w for maintaining a constant load. Let \hat{T}_w be the production temperature corresponding to the actual injection temperature \hat{T}_i . Then

$$\hat{T}_w - \hat{T}_i = T_{s1} - T_{s2} = T_o - T_i = \text{constant}. \quad (2.34)$$

The non-dimensional expression of \hat{T}_w is defined as:

$$\hat{T}_{wD} = \frac{T_o - \hat{T}_w}{T_o - T_i} \quad (2.35)$$

Duhamel's superposition integral for such a case can readily be applied. Thus

$$\hat{T}_{wD}(t_D) = T_{wD}(t_D) + \int_0^{t_D} \hat{T}_{wD}(t_D - \tau_D) \frac{dT_{wD}}{d\tau_D} d\tau_D \quad (2.36)$$

where t_D is the non-dimensional time as defined in Section 2.2.

Solution of Equation (2.36) can be obtained from the following

characteristic of this system. The effect of injection temperature of this system is shown at the production well with a time delay. The delayed time is actually the thermal breakthrough time which is $\pi/3$ in non-dimensional form. From this characteristic, the following are known:

$$\hat{T}_{wD} = T_{wD} = 0 \quad 0 \leq t_D \leq \frac{\pi}{3} \quad (2.37)$$

$$\hat{T}_{wD} = T_{wD} \quad \frac{\pi}{3} \leq t_D \leq \frac{2\pi}{3} \quad (2.38)$$

Therefore, the integration limits of Equation (2.36) change as:

$$\hat{T}_{wD}(t_D) = T_{wD}(t_D) + \int_{\pi/3}^{t_D - \pi/3} \hat{T}_{wD}(t_D - \tau_D) \frac{dT_{wD}}{d\tau_D} d\tau_D \quad (2.39)$$

To solve this equation, \hat{T}_{wD} must be known from $\hat{T}_{wD}(\pi/3)$ to $\hat{T}_{wD}(t_D - \pi/3)$. Since $\hat{T}_{wD} = T_{wD}$ for $t_D \leq 2\pi/3$ and T_{wD} is already known, \hat{T}_{wD} can be calculated up to $t_D = \pi$. With this, \hat{T}_{wD} up to $t_D = 4\pi/3$ can be calculated again. Through such repetitions, calculations of \hat{T}_{wD} at the desired point can be performed. Since T_{wD} is a function of t_D and λ , \hat{T}_{wD} is also a function of t_D and λ . The results of numerical calculations are shown in Figure 2.6.

It is evident that this modified operation does not affect the thermal breakthrough time, which occurs again at $t_D = \pi/3$ in this case, since the modification starts at thermal breakthrough. The steepness of each curve's slope can be explained from the definition of \hat{T}_{wD} , Equation (2.35). Because \hat{T}_{wD} is based upon the initial injection temperature while the actual injection temperature decreases after thermal breakthrough to keep a constant temperature

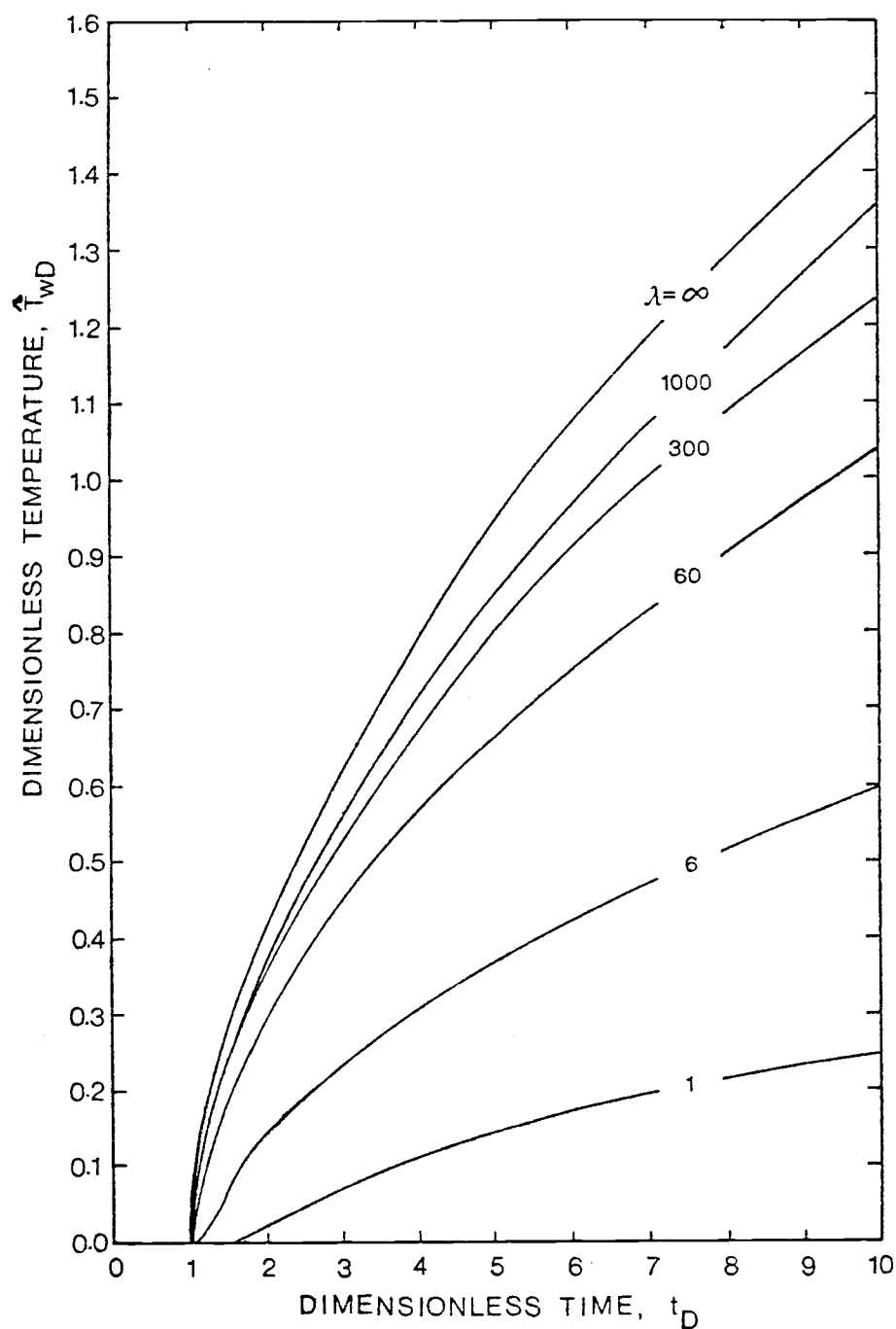


Figure 2.6. Dimensionless temperature at the production well of a doublet with constant flow rate and decreasing injection temperature for maintaining a constant system load.

difference between the production and injection, \hat{T}_{wD} can exceed 1. The value of \hat{T}_{wD} equal to 1 means the production temperature is equal to the initial injection temperature.

2.2.3 Production Temperature of a Doublet with Increasing Flow Rate

The other way of maintaining a constant load without changing the injection temperature is increasing flow rate appropriately after thermal breakthrough. This can be accomplished by a system such as shown in Figure 2.7. Feed back fluid circulates through the system in order to maintain a constant system inlet temperature T_s and constant system flow rate Q_s over the life of the system. By mixing with this feed back fluid, the temperature of the produced water decreases to T_s , constant system inlet temperature. Feed back flow rate should continuously decrease and approach to zero at the end of system life. If system life is designed to be ended at or before thermal breakthrough, feed back fluid is certainly not necessary.

The production temperature of this system will be investigated with the aquifer model of Section 2.2 and following assumptions.

- 1) The flow pattern change due to the flow rate increasing may not be significant.
- 2) The amount of heat transfer by conduction from the cap rock and bed rock is small.

As is indicated in Section 2.1, the concept of continuous succession of steady state can be applied for most practical cases. Therefore,

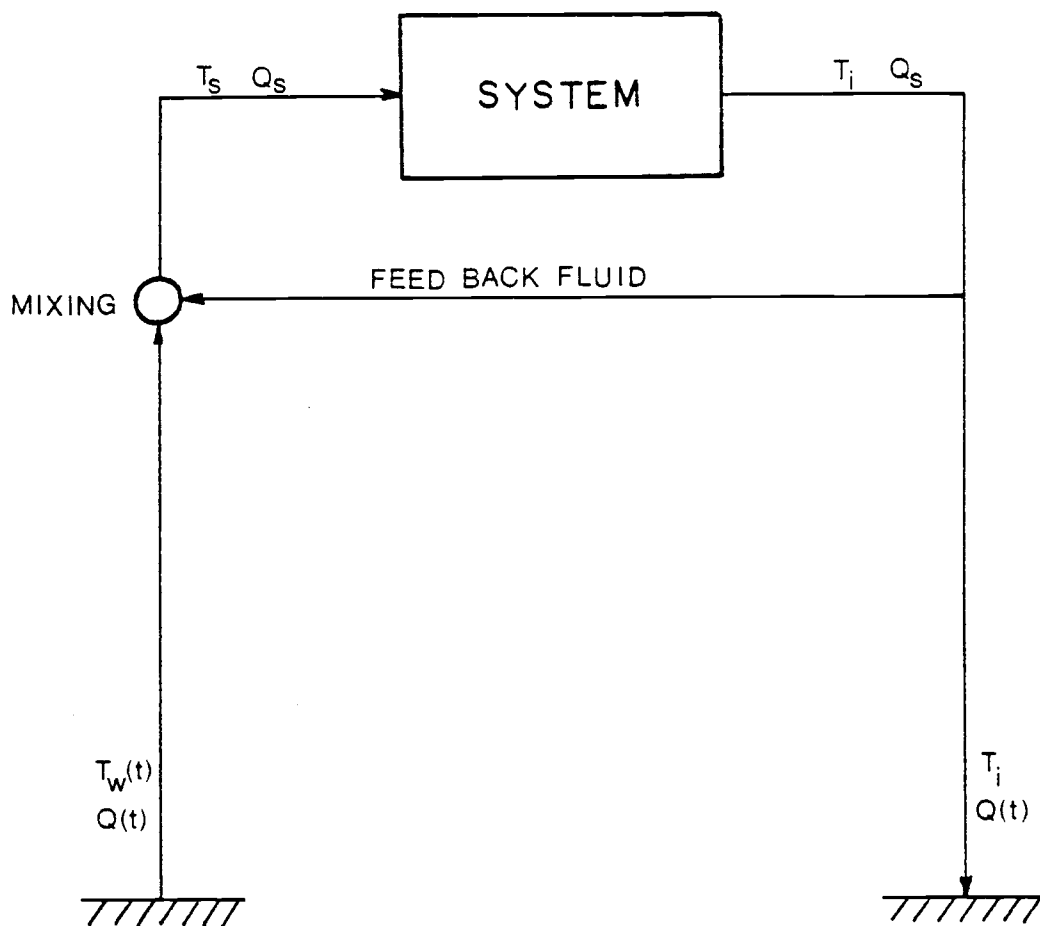


Figure 2.7. Schematic flow diagram of a geothermal energy system with constant injection temperature and increasing flow rate for maintaining a constant system load.

the flow pattern change can be assumed to be small and the element of stream channel(Figure 2.2) used for the calculation of production temperature in Section 2.2.1 is assumed to be valid here as far as the flow rate of both wells are kept equal. Also, it is seen from Figure 2.3 that the heat transfer by conduction is not significant for λ values greater than several hundred.

As is seen from the governing differential equation, Equation (2.16), for the aquifer temperature, flow rate change due to the water temperature change results in the non-linear differential equation. However, if heat conduction from the cap rock is neglected ($K_R = 0$), Equation (2.16) can be rewritten as:

$$\frac{\rho_w C_w}{2} \frac{\partial T_w^\psi}{\partial S} + \frac{b}{2} \rho_A C_A \frac{\partial T_w^\psi}{\partial \int q dt} = 0 \quad (2.40)$$

The above equation is linear and T_w is expressed as a function of S and $\int q dt$ (total recharged or discharged amount from $t=0$ through the stream channel element). Therefore, the solution of Equation(2.40) must be the solution of $\lambda = \infty$ case in Figure 2.3 by interpreting the non-dimensional time t_D in a different way as:

$$t_{D,av} = \frac{\rho_w C_w \int_0^t Q dt}{\rho_A C_A D^2 b} \quad (2.41)$$

Including the conduction effect from the cap rock and bed rock can be done by assuming that the production temperature of variable flow rate case is close to that of constant flow rate case if total recharged or discharged amount is the same. This assumption is really based upon the assumption 2) mentioned above and may be

good for the large λ value cases. By introducing Equation (2.41) and λ_{av} which is defined as

$$\lambda_{av} = \frac{\rho_w C_w \rho_A C_A b \int_0^t Q dt}{K_R \rho_R C_R D^2 t} \quad (2.42)$$

the production temperature can be calculated with Equation (2.33).

Thus

$$T_{wD}(\lambda_{av}, t_{D,av}) = \frac{1}{\pi} \int_0^\pi \operatorname{erfc} \left[\frac{f(\theta)}{(\lambda_{av} \{t_{D,av} - f(\theta)\})^{1/2}} \right] d\theta \quad (2.43)$$

where $T_{wD} = (T_o - T_w) / (T_o - T_i)$.

As is evident from Equation (2.41) and Equation (2.42), $t_{D,av}$ does not increase uniformly with time and λ_{av} is not constant because flow rate is not constant. Therefore, it is desired to have a solution which is expressed as a function of λ_I and t_{DI} which are based upon the initial flow rate. Thus

$$\lambda_I = \frac{\rho_w C_w \rho_A C_A b}{K_R \rho_R C_R D^2} Q_I \quad (2.44)$$

$$t_{DI} = \frac{\rho_w C_w}{\rho_A C_A D^2 b} Q_I t \quad (2.45)$$

where Q_I is the initial flow rate or flow rate before thermal breakthrough. Conversions of $t_{D,av}$ and λ_{av} to t_{DI} and λ_I are possible because the flow rate increasing is unique to yield a constant system load. The relation of flow rate to the initial flow rate is

$$\rho_w C_w Q (T_w - T_i) = \rho_w C_w Q_I (T_o - T_i) \quad (2.46)$$

or

$$Q = \frac{Q_I}{1 - T_{wD}} . \quad (2.47)$$

By combining Equations (2.41), (2.42), (2.43), (2.44) and (2.45) with Equation (2.47), T_{wD} can be expressed as a function of λ_I and t_{DI} . Such calculations have been done by numerical computations. The results are shown in Figure 2.8 as a function of t_{DI} and λ_I .

Again it is seen that this operation does not affect the thermal breakthrough, which occurs still at $t_D = \pi/3$, since the flow rate starts to increase at that time. The characteristics of this temperature profile are actually the same as those of Figure 2.3. The only difference appears in the shape of each curve which approaches rapidly to 1 in this case. Such a difference is due to the transformations of coordinate system (from $t_{D,av}$ to t_{DI}) and the parameter of each curve (from λ_{av} to λ_I).

2.3 Head Loss through Aquifers

Pump work for the circulation of geothermal fluid is largely due to the head loss through aquifers. Head loss, h_L , of a doublet in a homogeneous, laminar flow field is given[6]⁶ by

$$h_L = \frac{Q}{K\pi b} \ln \frac{D}{r_w} \quad (2.48)$$

⁶ What has been shown in this reference is drawdown at the production well, which is half of that of Equation (2.48). Therefore, total head loss (drawdown + excess injection pressure head) in a homogeneous flow field must be two times the drawdown.

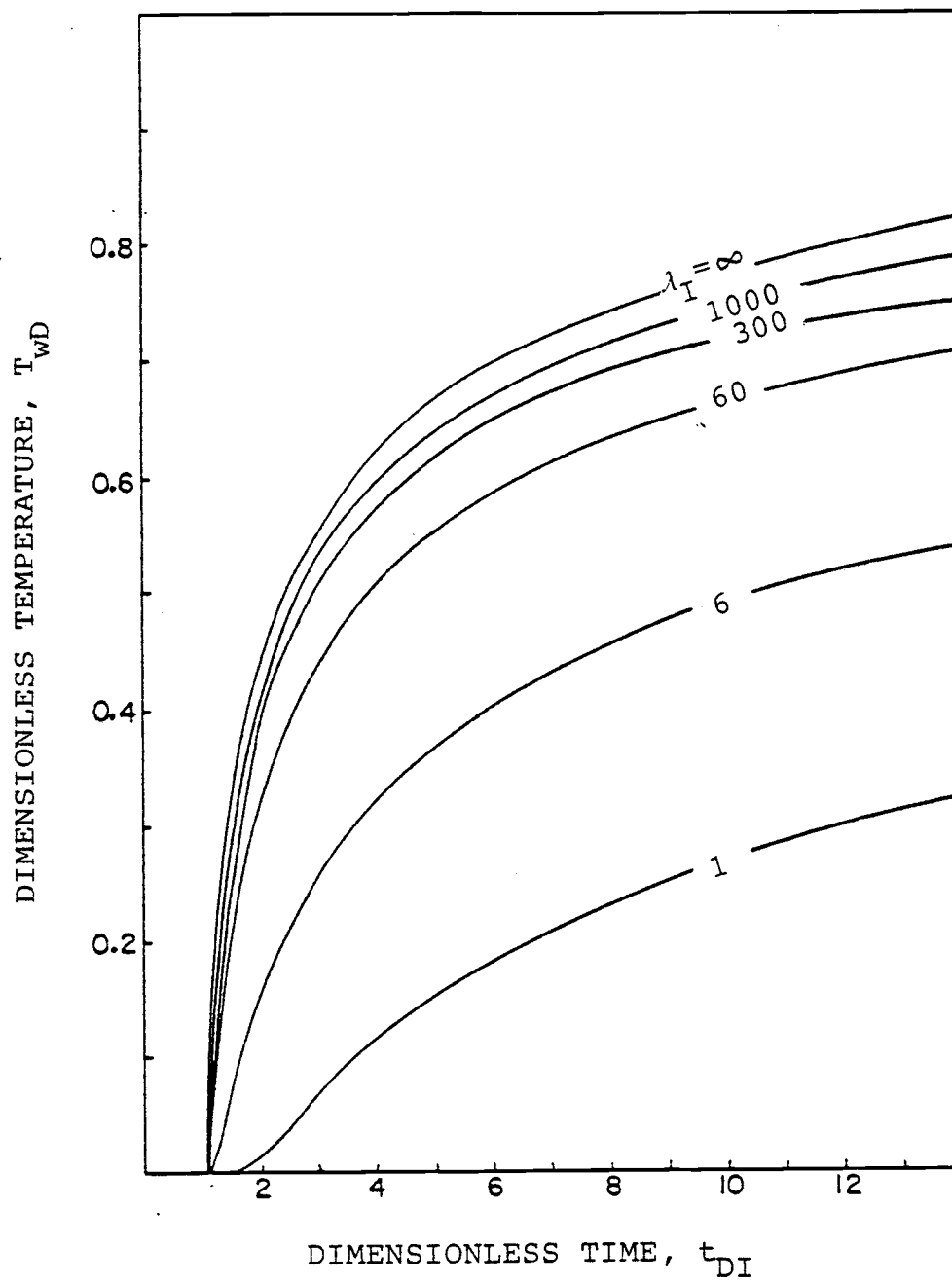


Figure 2.8. Dimensionless temperature at the production well of a doublet with constant injection temperature and increasing flow rate for maintaining a constant system load.

where r_w is the radius of well. In the forced geoheat recovery systems, injection temperature is always different from the aquifer temperature (injection temperature is lower than aquifer temperature in the power generation or heating cases and higher in the air cooling case). Therefore, a different viscosity region is growing around the injection well as the injection is proceeding. The hydraulic conductivity K in Equation (2.48) is inversely proportional to the viscosity of water as is seen from Equation (2.3). The viscosity of water is directly obtained from the Bingham formula[13]:

$$\frac{1}{\mu} = 21.482 [(T - 281.585) + \{8078.4 + (T - 281.585)^2\}^{\frac{1}{2}}] - 1200 \quad (2.49)$$

In this equation, μ is given in kg/msec with T in K. Thus it is seen that the viscosity of water is a strong function of temperature. For instance, the viscosity of water at 300 K is about 4 times that of water at 400 K. Therefore, if injection is proceeding at 300 K in an aquifer originally at 400 K, the region which is formed around the injection well at an injection temperature has a hydraulic conductivity about 1/4 that of the region occupied by the hot water. Head loss through the aquifer then grows from the initial head loss corresponding to the hydraulic conductivity at 400 K in Equation (2.48) and approaches to the final head loss corresponding to the hydraulic conductivity at 300 K as injection continues. The final head loss is about 4 times the initial head loss in this case

if flow rate is kept constant.

Perhaps the most rigorous way to study the unsteady behavior of the head loss through aquifers is to carry out coupled energy-mass transport calculations. The approach used in this section is a less rigorous one, the result of which is adequate for the purpose of this work. Here, the objective is to get some quantitative idea of the role of injection temperature on the unsteady behavior of head loss through the aquifer. In this approach, the well system is assumed to be a doublet and the position of the thermal front is assumed to be established by the steady flow model of Section 2.2. Further, it is assumed that the region bounded by the thermal front is entirely at the injection temperature, which may not be a bad assumption for the high λ cases. Actually the head loss between the injection and production well can be found through the line integration of Darcy's law, Equation (2.1), following any stream channel if the exact flow rate through that stream channel is known. Thus

$$h_L = \int \frac{V}{K(T)} dl \quad (2.50)$$

where V is the Darcy velocity and the hydraulic conductivity K is a function of temperature as was indicated previously. Due to a coupled effect of the growing of the thermal boundary and the variation of flow rate, which was explained briefly in Section 2.2, such an integration usually fails to give a reasonable result because V is determined from the flow rate within that stream channel. Therefore, the concept of resistance is introduced.

Resistance of a particular stream channel is defined as

$$R_j = \frac{h_L}{q_j} \quad (2.51)$$

where q_j is the flow rate within that stream channel (see Figure 2.9).

By combining Equation (2.51) with Equation (2.50), R_j can be rewritten as:

$$R_j = \int \frac{V}{K(T)q_j} dl \quad (2.52)$$

The advantage of introducing the concept of resistance is readily apparent from Equation (2.52). In Equation (2.50), V is not known unless q_j is known. However, V/q_j of Equation (2.52) does not depend on q_j because V is proportional to q_j at a given position. Therefore, by assuming any flow rate and calculating the corresponding Darcy velocity, V/q_j can be evaluated. This is truly a function of a position only. The situation is now similar to the electric parallel circuit. Information on the electric circuit analogy of ground water flow is available in the literature [6,14,15,16]. With such an analogy (h_L being the electric potential, R being the electric resistance and q being the electric current), the total resistance, R_{tot} , of the flow field can be calculated by

$$\frac{1}{R_{tot}} = \sum_{j=1}^n \frac{1}{R_j} \quad (2.53)$$

Then h_L is obtained by

$$h_L = QR_{tot} \quad (2.54)$$

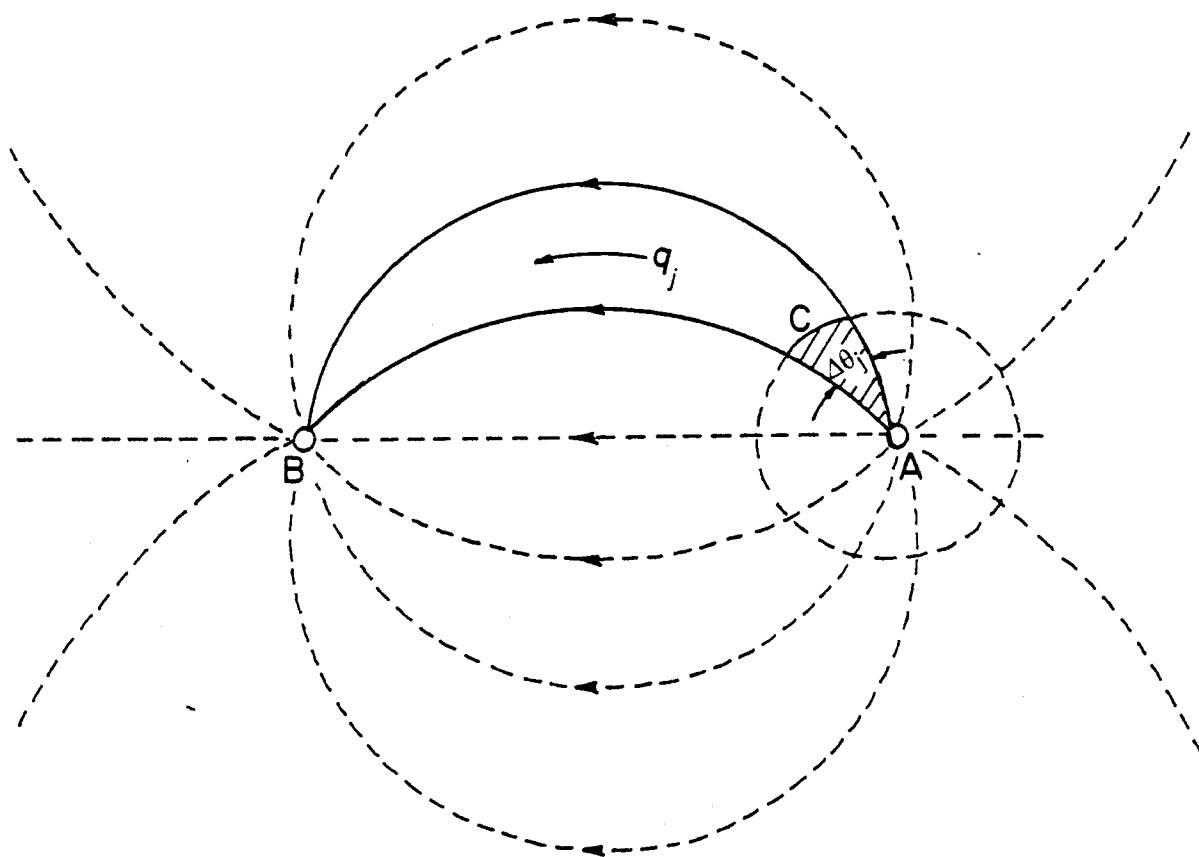


Figure 2.9. Stream channel of a doublet. The flow rate within the stream channel is denoted by q_j , the spreading angle of the stream channel at the injection well is denoted by $\Delta\theta_j$, and the position of thermal front is denoted by C. The injection and production well are designated by A and B respectively.

where $Q = \sum_{j=1}^n q_j$. Only two values of K , $K(T_o)$ and $K(T_i)$, are considered in Equation (2.52) because it is assumed that the region bounded by the thermal front is entirely at the injection temperature. Thus Equation (2.52) by introducing true fluid velocity V_w which is obtained by dividing V by porosity ϕ becomes

$$R_j = \frac{\phi}{q_j K(T_i)} \int_A^C V_w dl + \frac{\phi}{q_j K(T_o)} \int_C^B V_w dl \quad (2.55)$$

where A, B and C designate the position of injection well, production well and thermal front (see Figure 2.9). The integration limits of the last term (B and C) in the above equation can be transformed to A and B by using the following relation:

$$\frac{\phi}{K(T_o)} \int_A^B V_w dl = \frac{Q}{K(T_o) \pi b} \ln \frac{D}{r_w} \quad (2.56)$$

This equation is really the Equation (2.48) which is valid in the constant temperature flow field. Thus

$$\frac{\phi}{K(T_o) q_j} \int_C^B V_w dl = \frac{Q}{K(T_o) \pi b q_j} \ln \frac{D}{r_w} - \frac{\phi}{K(T_o) q_j} \int_A^C V_w dl. \quad (2.57)$$

Assuming that q_j is proportional to $\Delta\theta_j$ of Figure 2.9 (which is true for a flow field of constant temperature) as $q_j = Q\Delta\theta_j/2\pi$, Equation (2.55) becomes

$$R_j = \frac{2\pi\phi}{K(T_i) Q \Delta\theta_j} \left[1 - \frac{K(T_i)}{K(T_o)} \right] \int_A^C V_w dl + \frac{2}{K(T_o) b \Delta\theta_j} \ln \frac{D}{r_w}. \quad (2.58)$$

In the above equation V_w is obtained from the steady flow model.

R_j must be evaluated for all stream channels. By combining Equation (2.58) with Equation (2.53) and Equation (2.54), the required head

loss can be obtained as a function of time. Such an analysis must be done by numerical computations.

A computerized analysis has been carried out for the data of Table 2.1. The production model is assumed to be an increasing flow rate model to maintain a constant surface load. The calculation of production temperature has been done at each year to determine the required flow rate. The flow field has been generated with 20 stream channels from the injection to the production well. The calculation of R_j has been performed according to Equation (2.58) for each stream channel. Total resistance and head loss at each year have been calculated. The results of such calculations over 20 years are shown in Figure 2.10. It is seen from this figure that the head loss rapidly increases as the injection starts. This means a significant portion of head loss occurs at the region near the injection well, where the fluid velocity is very high and the aquifer is essentially cooled down to the injection temperature. Head loss is relatively steady during 1 ~ 3 year even though the thermal boundary is growing. Increasing of head loss is again seen near the thermal breakthrough.

TABLE 2.1. VALUES USED FOR THE CALCULATION OF HEAD LOSS THROUGH AQUIFERS

T_o	423 K	$\rho_w C_w$	4 MJ/m ³ K
T_i	340 K	$\rho_R C_R$	2 MJ/m ³ K
k	200 mD	D	300 m
ϕ	0.2	r_w	0.15 m
b	100 m	Q_I	0.05 m ³ /sec
K_R	1.157 J/m sec K		

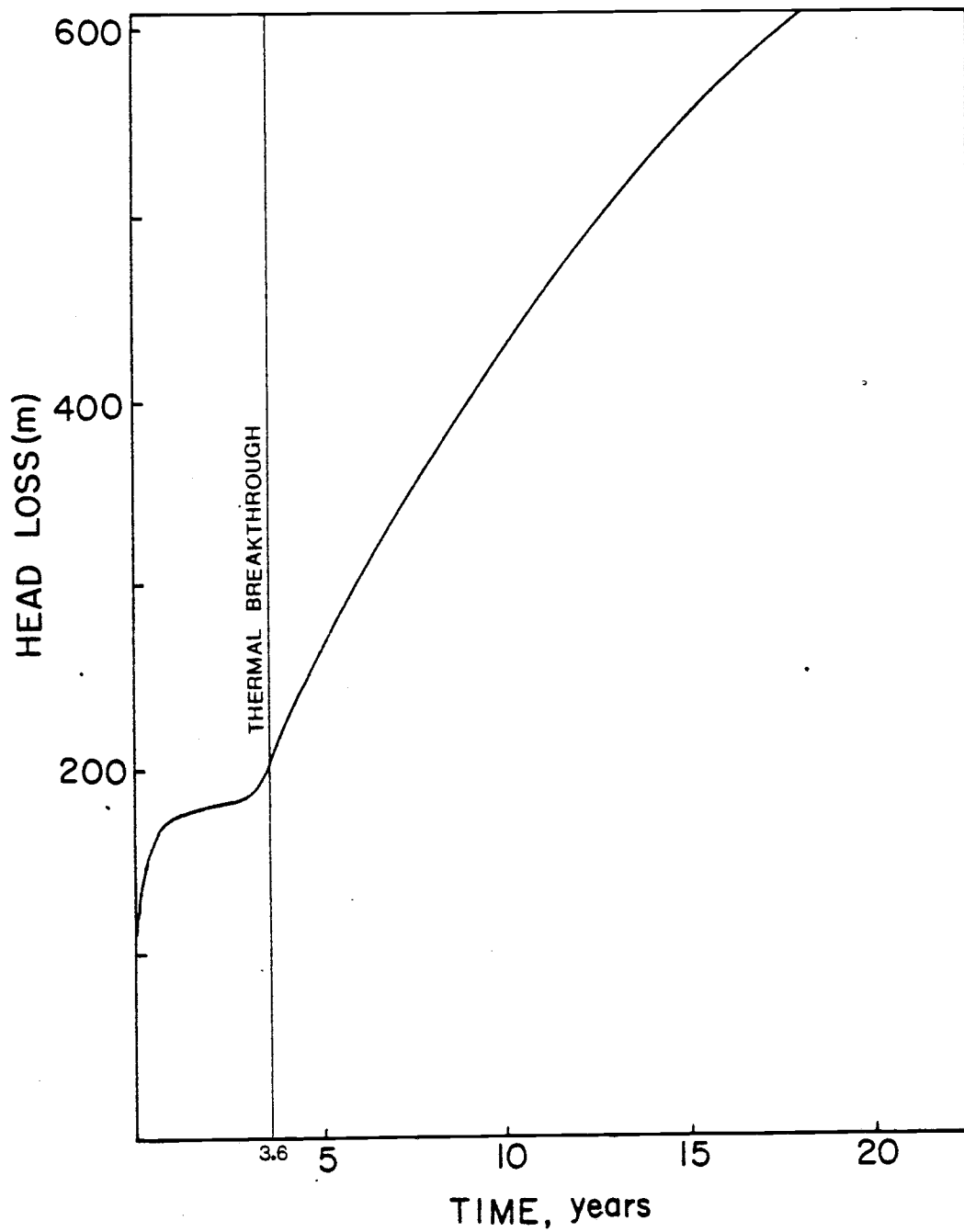


Figure 2.10. Head loss as a function of time. Data for this calculations are given in Section 2.3.

Thermal breakthrough occurs at $t = 3.6$ year in this case. After thermal breakthrough, head loss again increases rapidly due to the flow rate increasing.

Such an analysis requires involved computerized calculations. A simple method has been tried and it has turned out to agree well with the previous analysis. In this method, the calculation of excess injection pressure head at the injection well has been done by assuming that the aquifer is at the injection temperature (T_i) while the drawdown calculation is done with the entire aquifer at the production temperature (T_w). Then the corresponding head loss can be obtained by combining both quantities. Thus

$$h_L = \left(\frac{1}{K_i} + \frac{1}{K_w} \right) \frac{Q}{2\pi b} \ln \frac{D}{r_w} . \quad (2.59)$$

In the above equation, K_i and K_w are the hydraulic conductivity at the injection temperature and production temperature respectively. The comparison of this result with the previous one is shown in Figure 2.11. From this figure, it is seen that both results agree relatively well. However, it should be noted that the simple method cannot predict the unsteady behavior of head loss before thermal breakthrough.

The analyses of this chapter are based upon the assumption of laminar flow in the aquifer, where the Reynolds number as defined by Equation (2.6) is less than 1. This means the temperature and head loss analyses of this chapter cannot be applied when the flow rate exceeds some value. Another viewpoint about such a limit of

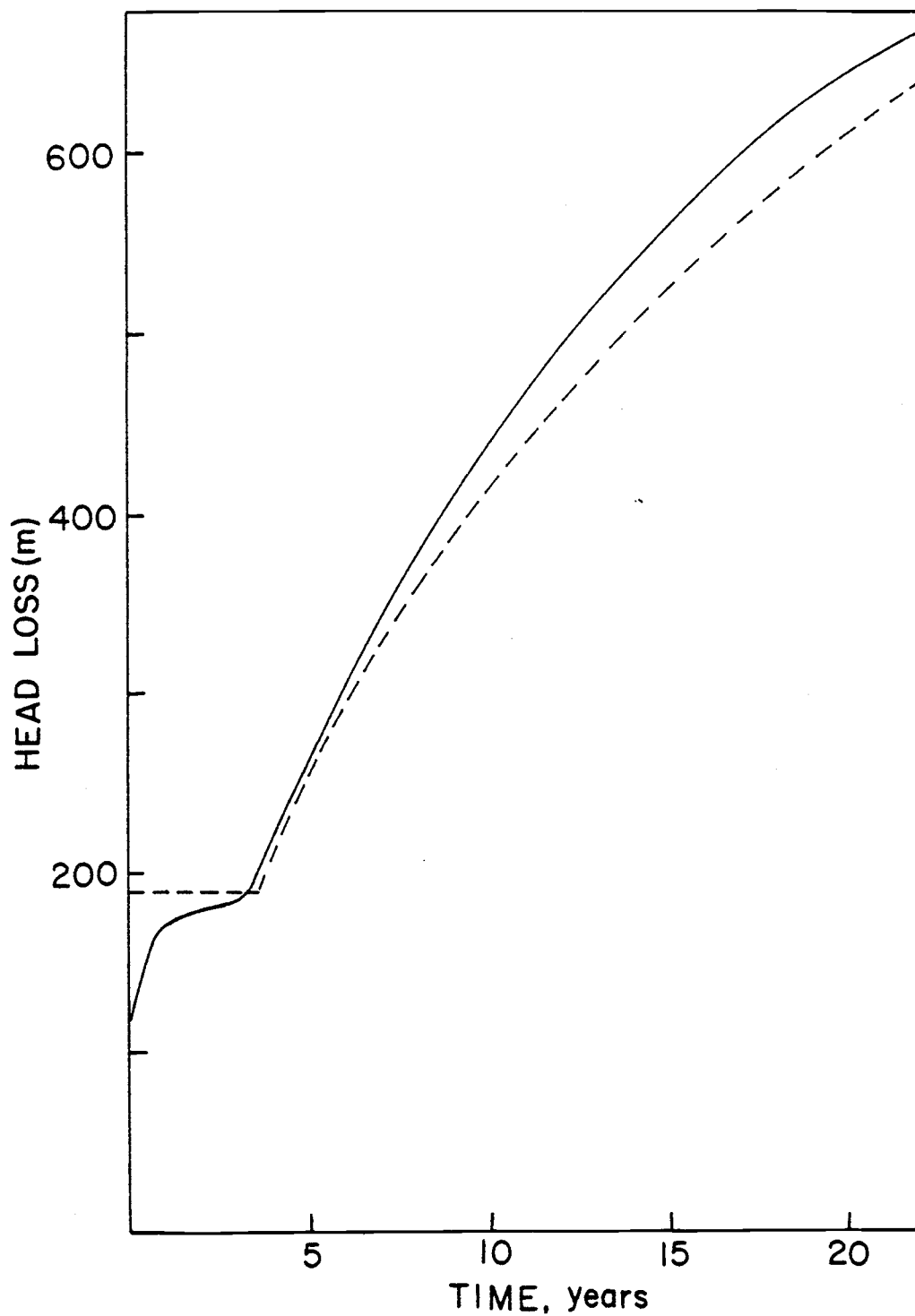


Figure 2.11. Comparisons of the results between the detailed and simple head loss calculations. Solid line is the result from the detailed one and dotted line is the result from simple one.

flow rate comes from the phenomenon of hydraulic fracturing in the aquifer which often occurs in the forced geoheat recovery systems due to too high pressure around the injection well. Hydraulic fracturing causes the deviation of stream lines from those considered thus far. The limits of flow rates from these two viewpoints have been considered in Appendix I.

As noted in Appendix I, however, such limits on the flow rate are critical only near the well bore and as the point of interest is moved from the well bore, these influences decrease very rapidly. Therefore, most of the flow field has laminar flow and no fracturing even if flow rate limits at aquifer entrance are exceeded. It is thus seen that there should be no serious problem in applying the results of this chapter for most practical cases where the flow rate per well bore is usually less than $0.1 \text{ m}^3/\text{sec}$.

3. SYSTEM MODELS AND PERFORMANCE PARAMETERS

The systems involved in this work are (i) either power generation, direct heating or heat pumps for the surface system and (ii) the aquifer with associated wells for the subsurface system. The main interest of this work is the thermodynamic performance, and consequently each model is developed in a manner that will be simple, but adequate for portraying the thermodynamic aspects. As a result, detailed design aspects were not necessarily considered in the modeling of each system. Sections 3.1, 3.2 and 3.3 are devoted to the system modeling. The performance parameters considered in this work are discussed in Section 3.4.

3.1 The Subsurface Systems

3.1.1 The Aquifer and Well Systems

The aquifer model considered in this study is a confined aquifer with extensive horizontal dimensions and no regional flow⁷. The aquifer is assumed to be saturated with liquid. Such a system falls in the category of hot water geothermal systems (see Chapter I) which show usually low temperature production. Therefore, the reservoir temperature in this study is considered to range up to 470 K. The associated well system is assumed to be a doublet (single recharging-discharging well pair). The temperature behavior and the

⁷ The influence of regional flow upon the production temperature is very small for most deep confined aquifers[8].

head loss analyses in such a system have been done in Chapter II. The assumption of extensive horizontal dimensions is really a technical fiction, for no aquifer can be indefinitely unbounded. However, if the aquifer is large enough and the well separation small enough, the stream lines will be effectively undisturbed and a finite aquifer will behave almost like an infinite reservoir. The application of this model is appropriate for such a system. For the case of many doublets in a given large aquifer with a sufficient distance between each location, this model also can be applied. It is beyond the scope of this work to examine the deviations of temperature and pressure behavior due to the finiteness of horizontal dimensions of the aquifer or the distance between each location.

3.1.2 Geothermal Fluid Pump Work

Geothermal fluid pump work for the forced recovery systems is largely due to the head loss through the aquifer, $h_{L,aq}$ (see Section 2.3). However, buoyancy effect due to the density difference between the production and injection well cannot be neglected for the reservoir at the depths of order of several thousand meters when the temperature difference is large. For the cold water injection case, such an effect reduces the pump work. Therefore, free flowing is also possible at an appropriately controlled flow rate and temperature difference. Another head loss, which is usually small, occurs in the well bore and surface pipelines. The flow is assumed to be laminar in the aquifer and turbulent in the well bore and

surface systems. The head produced due to the density difference between the production and injection wells, h_{by} , is

$$h_{by} = \beta \Delta T H \quad (3.1)$$

where β is the coefficient of thermal expansion of geothermal fluid, ΔT is the temperature difference between the production and injection wells and H is the depth of aquifer. The value of β for water can be expressed as a linear function of temperature.

$$\beta = (0.0642 T - 16.82) 10^{-4} \quad (3.2)$$

In the above equation, β is given in $1/K$ with T in K . Head loss in the well bores, $h_{L,W}$, can be expressed by using the flow rate(Q) and the radius of the well(r_w) assuming that the length of the well is the same as the depth of the aquifer. Pumping experience indicates that an adequate value of equivalent friction factor which considers both wells and the installed pump shaft in the production well is about 0.05[17]. Thus

$$h_{L,W} = \frac{0.05 H Q^2}{4 g \pi^2 r_w^5} \quad (3.3)$$

The head loss of surface pipelines, $h_{L,s}$ is assumed to be fixed as 15 m in this work. Then the total head loss, $h_{L,tot}$, is

$$h_{L,tot} = h_{L,aq} + h_{L,W} + h_{L,s} - h_{by} \quad (3.4)$$

The pumping power is equal to $\rho_w g Q h_{L,tot} / \eta_{gp}$, where η_{gp} is the efficiency of geothermal fluid pump. For the free flowing case, the

pumping power calculated this way shows negative value. This negative pumping power actually means that the required pumping work is zero.

3.2 Power Generation

There are presently three types of systems for electricity generation from liquid dominated reservoirs, the flash steam system, the binary cycle system and the total flow system. The power generation model chosen for this study is the binary cycle system which is usually recommendable for the lower temperature reservoirs. A sub-critical Rankine cycle using isopentane as a binary fluid is an appropriate power generation model for investigating the performance of power generation from the relatively low temperature reservoir since the critical temperature of isopentane is relatively high⁶. It is well known that superheating is not effective for this type of binary fluid[4]. Figure 3.1 shows the schematic of this model. Regeneration is not assumed here. The thermodynamic cycle of this model is shown in Figure 3.2. State 1 in Figure 3.2 is assumed to be a state of turbine inlet. State 2s represents the outlet state from the reversible turbine. Due to the irreversibility of the expansion process, the actual outlet state becomes state 2.

The thermodynamic properties of isopentane are available in the literature[18]. Several important properties for power

⁶ Critical temperature of isopentane is 461.17 K.

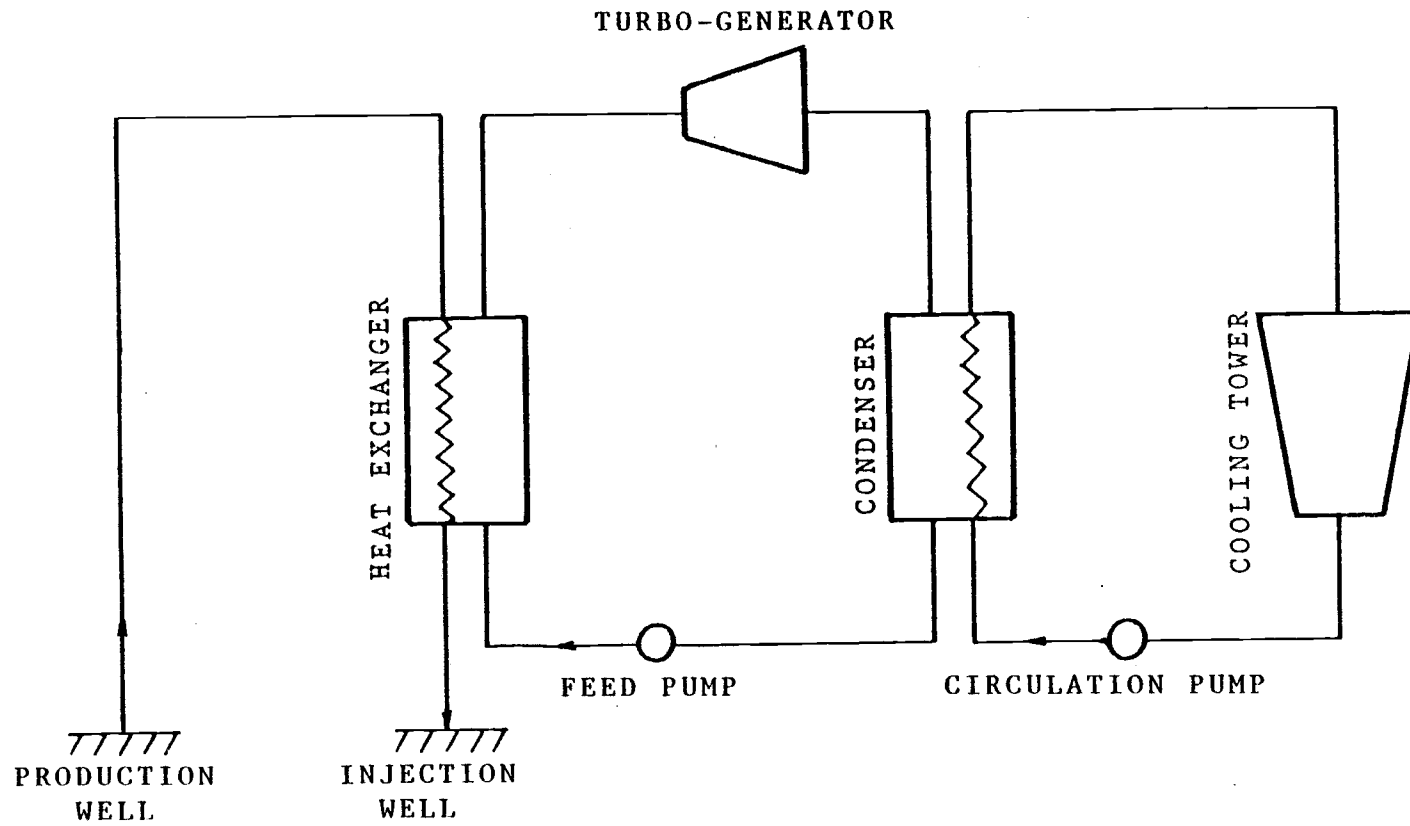


Figure 3.1. Simple schematic of binary cycle system with the energy source from the forced geothermal recovery.

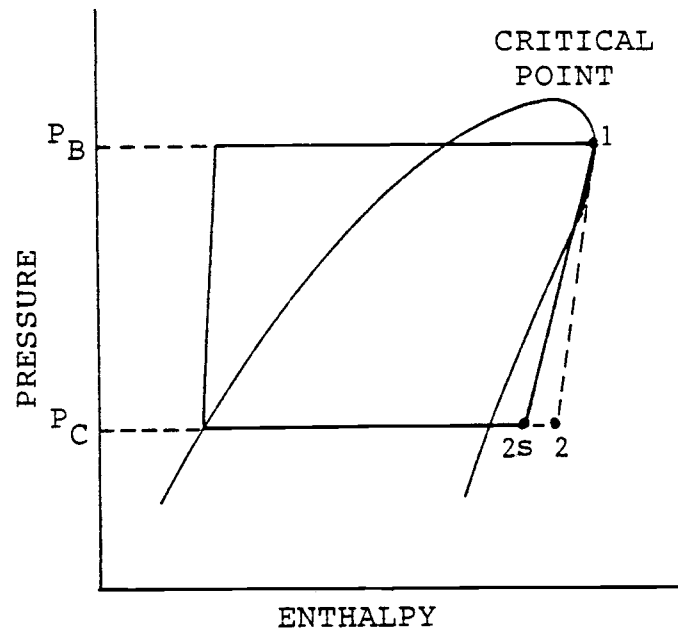


Figure 3.2. Sub-critical cycle without superheating.

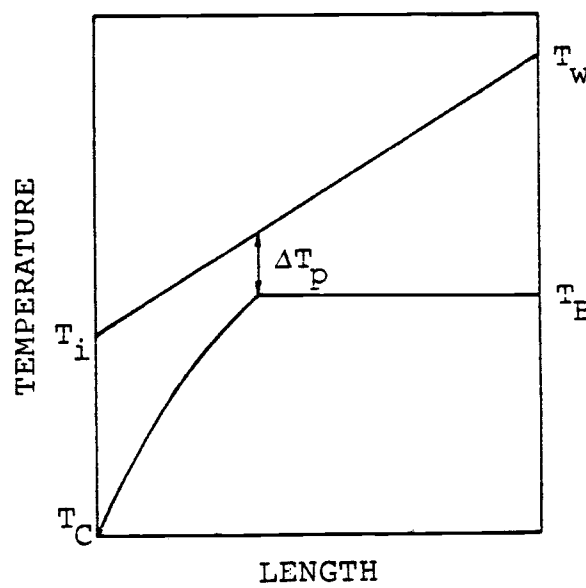


Figure 3.3. Typical temperature profile in the sub-critical heat exchanger without superheating.

generation have been developed in this work as functions of boiler temperature, T_B , with the condensing temperature fixed at 310 K. The enthalpy difference between the saturated liquid and saturated vapor, h_{fg} , is expressed as a function of T_B as:

$$h_{fg} = \left[\frac{(462 - T_B) 10^5}{1.7998} \right]^{0.3646} \quad (3.5)$$

The isentropic expansion work, $h_1 - h_{2s}$, with the back pressure corresponding to the condensing temperature, T_C , at 310 K is

$$h_1 - h_{2s} = 0.8164(T_B - 310) - 0.000187[(T_B - 382.75)^2]^{1.2838} + 11.25. \quad (3.6)$$

The pressure difference between the boiler and condenser, $p_B - p_C$, with condenser temperature at 310 K is

$$p_B - p_C = 0.1748 (T_B - 310)^{1.9519}. \quad (3.7)$$

The average specific heat of the liquid, $C_{p,av}$, given the same condenser temperature is

$$C_{p,av} = 0.00045 (T_B - 310)^{1.4175} + 2.345. \quad (3.8)$$

In the above equations, h , p , C_p and T are given in kJ/kg, kPa, kJ/kg K, K. It should be emphasized that above equations are not good for the boiler temperature near the critical temperature.

Thus it is recommended that the applications of the above equations should be restricted to the range of T_B less than 450 K. Also it should be remembered that Equation (3.6), Equation (3.7) and Equation

(3.8) are valid for the condensing temperature at 310 K. The boiler temperature (T_B) with given production and injection temperatures of geothermal fluid can be calculated by following relation:

$$\frac{T_w - T_B - \Delta T_p}{h_{fg}} = \frac{T_B - T_i + \Delta T_p}{C_{p,av}(T_B - 310)} \quad (3.9)$$

where ΔT_p is the pinch point temperature difference and T_w and T_i are the production and injection temperatures of the geothermal fluid respectively (see Figure 3.3). Equation (3.9) with Equation (3.5) and Equation (3.8) thus make it possible to find T_B . For a fixed value of ΔT_p of 8.33 K, it is found by graphical representation that Equation (3.9) yields a proper single-valued solution at T_w less than 470 K. Above this temperature, either no or a multi-valued solution results depending on the injection temperature. Thus here the application of Equation (3.9) is restricted to the range of T_w less than 470 K. The binary fluid flow rate per unit mass flow of geothermal fluid, m , is found by

$$m = \frac{(T_w - T_i)C_w}{C_{p,av}(T_B - 310) + h_{fg}} \quad (3.10)$$

where C_w is the specific heat of geothermal fluid. For the estimation of cooling tower fan work, w_{ctf} , and the circulation water pump work, w_{cirp} , the method presented by Pfeiffer[19] is adequate for this study. Assuming low head, induced draft tower, w_{ctf} and w_{cirp} are approximated as:

$$w_{ctf} = 0.1654 m_c \text{ kJ/kg geothermal fluid} \quad (3.11)$$

$$w_{cirp} = 0.0827 m_c \text{ kJ/kg geothermal fluid} \quad (3.12)$$

where m_c is the flow rate of cooling water per unit mass flow rate of geothermal fluid. The required amount of cooling water, m_c , can be calculated by

$$m_c = \frac{w_{fp} + C_w(T_w - T_i) - m(h_1 - h_{2s})\eta_T}{C_{cw}\Delta T_{cool}} \quad (3.13)$$

where C_{cw} is the specific heat of the cooling water, the value of which may be close to the specific heat of geothermal fluid, C_w and ΔT_{cool} is the temperature difference through which the water is cooled. In the above equation, w_{fp} and η_T are feed pump work per unit mass flow rate of geothermal fluid and turbine efficiency respectively. The feed pump work can be calculated using Equation (3.7). Thus

$$w_{fp} = \frac{mv_C(p_B - p_C)}{\eta_{fp}} \quad (3.14)$$

where η_{fp} is the efficiency of the feed pump and v_C is the specific volume of binary fluid at the exit of condenser.

The net power output, $POWER_{net}$, can be calculated by

$$POWER_{net} = [m(h_1 - h_{2s})\eta_T\eta_G - w_{fp} - w_{cirp} - w_{ctf}]\rho_w Q - W_{gp} \quad (3.15)$$

where $\eta_T\eta_G$ is the product of turbine and generator efficiency and W_{gp} is the pump work for the geothermal fluid circulation. Equations (3.5)~(3.15) thus make it possible to estimate the potential of power generation from the relatively low temperature water at a

given flow rate and temperature.

3.3 Space Heating

One of the most active applications of relatively low temperature geothermal energy is space heating. Depending on the reservoir temperature, direct heating or heat pumps may be used. For a specified range of reservoir temperature, a combined system of direct heating and heat pumps shows a good performance. Such a system is termed "combination" in this study. Although there are many other possible applications of geothermal heating (such as drying, cooking etc.), the investigation of heating performance is here restricted to space heating only.

3.3.1 Direct Heating

Figure 3.4 shows the simplified schematic of the direct heating model. Water is used as a loop fluid to transfer thermal energy from the geothermal fluid to the space where the heating is required. The temperature of water at the inlet of the heat exchanger is assumed to be fixed at 303.15 K. Therefore, the injection temperature of geothermal fluid (T_i) is

$$T_i = 303.15 + \Delta T_{HE} \quad (3.16)$$

where ΔT_{HE} is the temperature difference between the geothermal fluid and loop fluid in the heat exchanger, which is assumed to be constant at every section of the heat exchanger. The total heating

load, L_H , is

$$L_H = \rho_w C_w Q (T_w - T_i). \quad (3.17)$$

Direct heating is assumed to be possible for a fluid production temperature greater than 320 K. The head loss of the water is assumed to be 20 m.

3.3.2 Heat Pump

Heat pump application is assumed to be valid for the production temperature lower than 320 K. The parameter commonly used to evaluate the performance of heat pumps is the Coefficient Of Performance in Heating (COP_H) defined as:

$$\text{COP}_H = \frac{\text{Heating Output}}{\text{Electricity Input}}$$

For heat pumps, as with refrigerators and heat engines, the theoretical maximum performance is that of Carnot Cycle, $\text{COP}_{H_{CC}}$, which is expressed as:

$$\text{COP}_{H_{CC}} = \frac{T_H}{T_H - T_L}$$

where T_H is the temperature at which heating is required, and T_L is the temperature of the available low-temperature energy source. The COP_H of heat pump system in this study is approximated as 0.5 times that of Carnot Cycle between the same two temperature levels, which is typical of the performance that can be expected from an operating heat pump unless the temperature difference between two levels is very small. For very small temperature difference cases, such an

approximation shows too high of a performance. Therefore, the maximum limit of COPH is assumed to be 7. In addition to the compressor work which can be calculated with the COPH considered above, fan power is required for this model as shown in Figure 3.5. The electricity input to the fan, W_{fan} , is assumed to be 0.0421 times heating load[2]. Thus

$$W_{fan} = 0.0421 L_H \quad (3.18)$$

$$L_H = \rho_w C_w Q(T_w - T_i) + W_{comp} \quad (3.19)$$

where W_{comp} is the net electricity requirement for the compressor, which can be calculated by

$$W_{comp} = \frac{\rho_w C_w Q(T_w - T_i)}{COPH - 1}. \quad (3.20)$$

The estimation of COPH can be performed with the condenser temperature, T_{con} , and evaporator temperature, T_{evap} . The evaporator temperature should be lower than T_i by the approach temperature, ΔT_{app} (temperature difference between the geothermal fluid and refrigerant at the exit of evaporator). This leads to the estimation of COPH as:

$$COPH = \frac{1}{2} \left[\frac{T_{con}}{T_{con} - T_i + \Delta T_{app}} \right] \quad (3.21)$$

The performance of geothermal space heating with a heat pump system can be investigated with Equations (3.18) ~ (3.21).

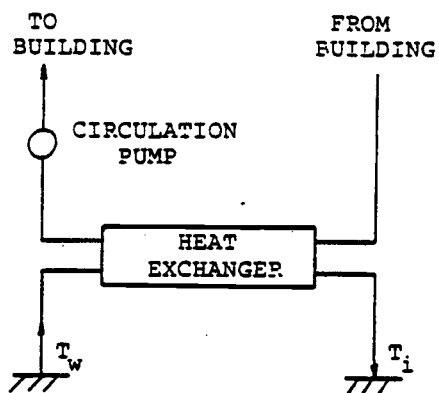


Figure 3.4. Flow diagram of direct heating system.

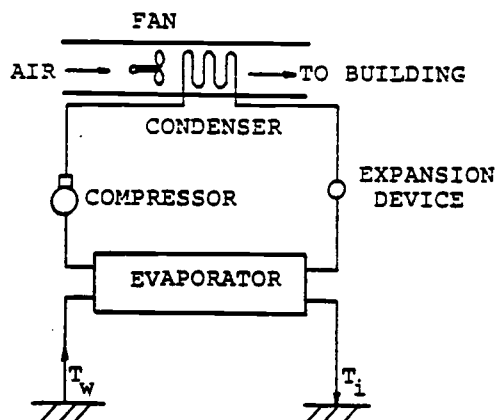


Figure 3.5. Flow diagram of heat pump system.

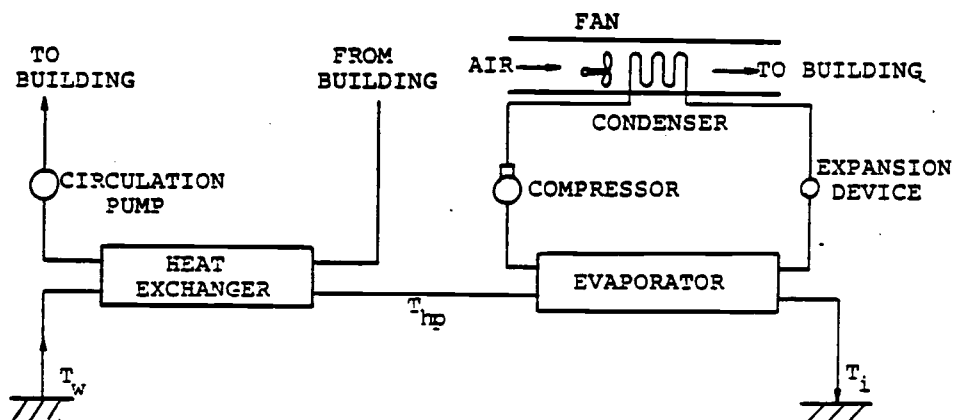


Figure 3.6. Flow diagram of combination.

3.3.3 Combination

Combination in this study refers to the series connection of direct heating and heat pump as shown in Figure 3.6. The outlet temperature of the heat exchanger, T_{hp} , which is also the inlet temperature of the evaporator is assumed as:

$$T_{hp} = 303.15 + \Delta T_{HE} \quad (3.22)$$

The direct heating model and the heat pump model of Sections 3.3.1 and 3.3.2 can be applied here for each part respectively. The fan power is assumed to be required only in the heat pump part.

$$W_{fan} = 0.0421[\rho_w C_w Q(T_{hp} - T_i) + W_{comp}] \quad (3.23)$$

The compressor work in the combination is

$$W_{comp} = \frac{\rho_w C_w Q(T_{hp} - T_i)}{COPH - 1} \quad (3.24)$$

Equation (3.19) and Equation (3.21) do not change here for the calculation of total heating and COPH. Equations (3.19), (3.21), (3.22), (3.23) and (3.24) can be used to investigate the performance of the "combination".

3.4 Performance Parameters

Geothermal energy, being thermal energy at a temperature relatively close to that of the environment, is different from conventional energy sources such as oil, natural gas, hydropower,

etc. in that its available energy⁹ is substantially lower than its energy, as commonly defined. The conventional energy sources have available energies and energy values that are almost equal.

Consequently, in order to adequately show the performance of geothermal energy systems, the effectiveness must be considered.

The effectiveness, denoted by ϵ , is defined as:

$$\epsilon = \frac{\text{increase in available energy of desired output}}{\text{decrease in available energy required}}$$

The effectiveness is a useful parameter for performance comparison because, for the evaluation of this parameter, every form of energy involved is converted to the available energy which is considered as an fair basis of energy from the viewpoint of the Second Law of Thermodynamics. Therefore, this parameter is especially useful when the involved forms of energy are not equal grade (such as geothermal energy and electricity). Thus there is a desirability to have the system operation at the maximum effectiveness by controlling the system variables under the given load conditions.

It is also noted that the imposed load condition for a given doublet greatly affects the effectiveness. In other words, as the required load increases the maximum effectiveness under the given condition decreases. This means that the small value of effectiveness may be considered as an indicator to show that the load is too high (or unfavorable) for a given well system. However, it is

⁹ Available energy is the thermodynamic property which measures the potential of a system to do work when restricted by the surroundings at temperature T_E and pressure P_E [20].

difficult to decide such a favorable or unfavorable load condition with effectiveness alone. Another useful parameter to indicate this condition has been developed in this study. This is termed the fossil fuel savings here. This concept measures how much conventional energy (assumed fossil fuel such as oil, natural gas, coal, etc.) can be saved by the operation of a given geothermal energy system. The geothermal fluid pump work in the heating system and the compressor or fan work in the heat pump system are assumed to come from the fossil fuel energy. Thus the definition of fossil fuel savings, denoted by ffs , is

$$ffs = \left(\begin{array}{l} \text{the amount of fossil fuel that is required for the} \\ \text{desired output unless geothermal energy is available} \end{array} \right) - \left(\begin{array}{l} \text{actual amount of fossil fuel that has been used in} \\ \text{the operation of geothermal energy system} \end{array} \right).$$

The amount of fossil fuel in the above equation can be expressed as a rate such that ffs can also take a rate form. It is readily seen that the fossil fuel savings can be maximum at some load condition since the geothermal fluid pump work is proportional to the square of flow rate. Such a load condition is called maximum favorable load here. Thus the load conditions which exceed that value may be considered as too high (or unfavorable) for a given well system. If such a high load is desired, another well system may be drilled to meet the load condition.

4. CONSTANT FLOW MODEL

As was illustrated in Chapter II, the thermal breakthrough time is inversely proportional to the distance between the production and injection wells. It is thus possible to maintain a constant production temperature during the entire project life time by designing the well separation appropriately. Since the production temperature is constant, the production rate is also constant to maintain a specified design load. Such a scheme is termed here the "Constant Flow Model". This chapter considers such a production scheme with the several surface applications delineated in Chapter III.

The flow rate Q and the well separation D are related by the following relation in the Constant Flow Model:

$$Q = \frac{\pi}{3} \frac{\rho_A C_A D^2 b}{\rho_w C_w t_L} \quad (4.1)$$

where t_L is the designed project life time. It should be noted that the volume of the aquifer used in this situation is equal to $\pi D^2 b/3$, which means that the energy available from the aquifer is proportional to the square of D . On the other hand, the head loss through the aquifer is only proportional to the natural logarithm of D , the effect of which is quite minimal. Therefore, the well separation should be designed to meet the specified load condition according to Equation (4.1). Consequently, it is always desirable to operate the system under the Constant Flow Model. However, another situation is possible, in which the well system already exists with small D . In

such a case, the output must be small if the operation is under the Constant Flow Model. Therefore, the flow rate should be higher than that from Equation (4.1) in order to have a moderate output in such a case. The effect of which is the continued operation after thermal breakthrough. Then the production rate must start to increase, at thermal breakthrough, in order to maintain a constant surface load since the production temperature will begin decreasing. This scheme is termed the "Increasing Flow Model" and will be discussed in Chapter V.

The main interest here is the selection of the type of system and the optimum operation of each system under the given geologic and specified load conditions. It will be shown that the optimum condition is closely related to the desired load and the geologic conditions especially when the resource temperature is relatively low. The desired load condition is somewhat arbitrary. However, certainly the output which can be expected from a given doublet must be finite. Therefore, the next interest is to find the maximum favorable load conditions.

4.1 Preliminaries

Expressions for the performance parameters, effectiveness and fossil fuel savings, must first be developed. For the expression of the effectiveness, every input or output energy must be converted to its corresponding available energy. The available energy input from the geothermal energy reservoir can be expressed as $\rho_w C_w Q[(T_o - T_E) -$

$T_E \ln(T_O/T_E)]$, where T_E is the environment temperature. It must be noted that the geothermal fluid leaving the surface system is not a useful product and is thus assumed to be discarded since the entire project is assumed to stop at the thermal breakthrough when the injected water temperature begins to affect the production temperature. The net power output(after deduction of all the auxiliary losses and geothermal fluid pump work) from the geothermal power generation system is entirely available energy. Every form of work for the heating systems are assumed to come from the electricity which will be considered to be produced from a fossil fuel. The electricity is produced with an effectiveness equal to ϵ_{pp} . A value of ϵ_{pp} of 30% will be assumed for this study[20]. As is seen in Chapter II, the geothermal fluid pump work shows unsteady behavior. Therefore, an average geothermal fluid pump work(total pump work divided by the project life time) has been calculated and used in the performance calculation. The effectiveness of the power generation is

$$\epsilon = \frac{\text{POWER}_{\text{net}}}{\rho_w C_w Q[(T_O - T_E) - T_E \ln(T_O/T_E)]} \quad (4.2)$$

The available energy output of heating system can be expressed as $L_H(1 - T_E/T_{\text{space}})$, where L_H is the total heating load and T_{space} is the required temperature of heating space. Thus the effectiveness of heating system is given by

$$\epsilon = \frac{L_H(1 - T_E/T_{\text{space}})}{\rho_w C_w Q[(T_O - T_E) - T_E \ln(T_O/T_E)] + (\Sigma \text{Work})/\epsilon_{pp}} \quad (4.3)$$

All the necessary work inputs for each heating system(see Chapter III) are denoted by ΣWork in the above equation.

The expression of another performance parameter, the fossil fuel saving, for the power generation is

$$\text{ffs} = \text{POWER}_{\text{net}} / \epsilon_{\text{pp}}. \quad (4.4)$$

It is thus seen that maximum $\text{POWER}_{\text{net}}$ results in the maximum ffs in the power generation case. By denoting the efficiency of the average fossil fuel fired boiler(for space heating) as η_{B} , the fossil fuel saving of the heating system is given by

$$\text{ffs} = L_{\text{H}} / \eta_{\text{B}} - \Sigma(\text{Work}) / \epsilon_{\text{pp}}. \quad (4.5)$$

A value of η_{B} of 75% will be assumed[20].

A computer program has been developed to calculate the performances of each system. This program uses the aquifer models of Chapter II along with performance parameter expressions for the individual system to determine overall system performance for various system and aquifer specifications and operating conditions. All of the independent parameters are specified except for the injection temperature. Then the program evaluates the system operation and calculates the performance for various injection temperatures over a specified range. The program was made in this manner because the injection temperature was considered to be major parameter in determining the best operation of the system.

One important feature of the program should be clarified. For

the power generation case, the flow rate is determined based upon the given well separation according to Equation (4.1). Then the basic pattern of aquifer resistance for each stream channel as a function of time can be established by using arbitrary resource and injection temperatures. This basic pattern of resistance can be converted to the new resistance of the new resource and injection temperature by the following relation:

$$R'(I,J) = \frac{\frac{1}{K'_i} - \frac{1}{K'_o}}{\frac{1}{K_i} - \frac{1}{K_o}} [R(I,J) - R_o] + R'_o \quad (4.6)$$

where R and K are the resistance and hydraulic conductivity of the basic pattern and R' and K' are those of the new situation. The subnotations i and o refer to the corresponding values of resource and injection temperatures respectively. The I and J in the parenthesis refer to the stream channel number and the time given in years. The use of Equation (4.6) is only possible for the case of the same geometry and flow rate with those of the basic pattern. This basic pattern greatly reduces the computing time.

However, for the heating case, computations are based on the specified load. At the specified load, the required flow rate is calculated for each injection temperature. Since different injection temperature requires different flow rate, the aquifer resistance must be evaluated for each injection temperature, which means the basic pattern is not available here. The injection temperature is varied from $T_{i,max}$ to $T_{i,min}$, in which $T_{i,max}$ is the injection

temperature of direct heating which is assumed to be fixed by Equation (3.16).

The parameters and their values used for this study are listed in Table 4.1. Under such conditions, the performances have been calculated as functions of injection temperatures. Reservoir temperature is considered as an important parameter. The intrinsic permeability also affects the results significantly. Due to the limited computer time for this research, only three values of permeabilities and corresponding results have been studied.

The thickness of aquifer also strongly affects the overall performances. However, the effects of this parameter change are similar to the effects of permeability change because both parameters are related to the only geothermal fluid pump work in the Constant Flow Model as is seen in Section 2.3. Thus the change of b value from that listed in Table 4.1 ($b = 100$ m) results in the same effects of change of k value by introducing equivalent k , k_{eq} , as following¹⁰:

$$k_{eq} = \frac{kb}{100} \left[\frac{\ln\left[\frac{1}{r_W} \left(\frac{3Q}{\pi} \frac{\rho_w C_w t_L}{100 \rho_A C_A}\right)^{\frac{1}{2}}\right]}{\ln\left[\frac{1}{r_W} \left(\frac{3Q}{\pi} \frac{\rho_w C_w t_L}{\rho_A C_A b}\right)^{\frac{1}{2}}\right]} \right] \quad (4.7)$$

$$\approx \frac{kb}{100} \quad (4.8)$$

It is not difficult to see that the right-hand side of Equation (4.7) can be approximated as Equation (4.8) since the value of the quotient

¹⁰ This relation is not valid for the Increasing Flow Model.

TABLE 4.1 THE VALUES OF PARAMETERS USED FOR THE SYSTEM PERFORMANCE CALCULATIONS

<u>PARAMETER</u>	<u>DESCRIPTION</u>	<u>VALUES</u>
<u>AQUIFER</u>		
T_o (K)	Reservoir Temperature	280 - 470
k (mD)	Intrinsic Permeability	50, 100, 200
b (m)	Thickness of Aquifer	100
ϕ	Porosity	0.2
ρ_w (kg/m ³)	Density of Geothermal Fluid	1000
C_w (J/kg K)	Heat Capacity of Geothermal Fluid	4000
$\rho_r C_r$ (J/m ³ K)	Volumetric Heat Capacity of Rock	2000000
r_w (m)	Radius of Well	0.15
η_{gp}	Efficiency of Geothermal Fluid Pump	0.75
$h_{L,s}$ (m)	Surface Head Loss of Geothermal Fluid	15
t_L (years)	System Life Time	25
<u>POWER GENERATION</u> (Isopentane Binary Cycle System, Saturated Rankine Cycle)		
T_C (K)	Condenser Temperature	310
ΔT_p (K)	Pinch Temperature	8.33
η_{fp}	Efficiency of Feed Pump	0.68
η_T	Efficiency of Turbine	0.8
T_E (K)	Environment Temperature	289

HEATING

T_E (K)	Environment Temperature	270
T_{space} (K)	Space Temperature	295

DIRECT HEATING

ΔT_{HE} (K)	Temperature Difference in the Heat Exchanger	8.33
$h_{L,lf}$ (m)	Head Loss of Loop Fluid	20
η_{lf}	Efficiency of Loop Fluid Pump	0.8

HEAT PUMP

T_{con} (K)	Condenser Temperature	322.22
ΔT_{app} (K)	Approach Temperature	8.33

of natural logarithm terms of Equation (4.7) usually falls in the range of $0.95 \sim 1.05$ for most practical variations of b .

4.2 Direct Heating

For the type of geothermal energy reservoir considered in this study, the most popular application is space heating. Direct heating is a thermodynamically very simple heating device and its heating potential from the aquifer can be fully described by Equations (3.17) and (4.1).

$$L_H = \rho_w C_w Q (T_o - T_i) \quad (3.17)$$

$$Q = \frac{\pi}{3} \frac{\rho_A C_A D^2 b}{\rho_w C_w t_L} \quad (4.1)$$

Note that the resource temperature (T_o) substitutes for the production temperature (T_w) in Equation (3.17) because the production temperature is always the same as the resource temperature in the Constant Flow Model. For a specified load, the flow rate can be obtained from Equation (3.17) and then the well separation can be calculated from Equation (4.1). Injection temperature (T_i) of geothermal fluid is assumed to be fixed by Equation (3.16).

The thermodynamic performance of direct heating is shown as a function of resource temperature in Figure 4.1. This figure shows the general tendency of the performance of direct heating. Four regions depending upon the resource temperature are also shown in this figure, Z_1 , Z_2 , Z_3 and Z_4 . The boundary of each region is not

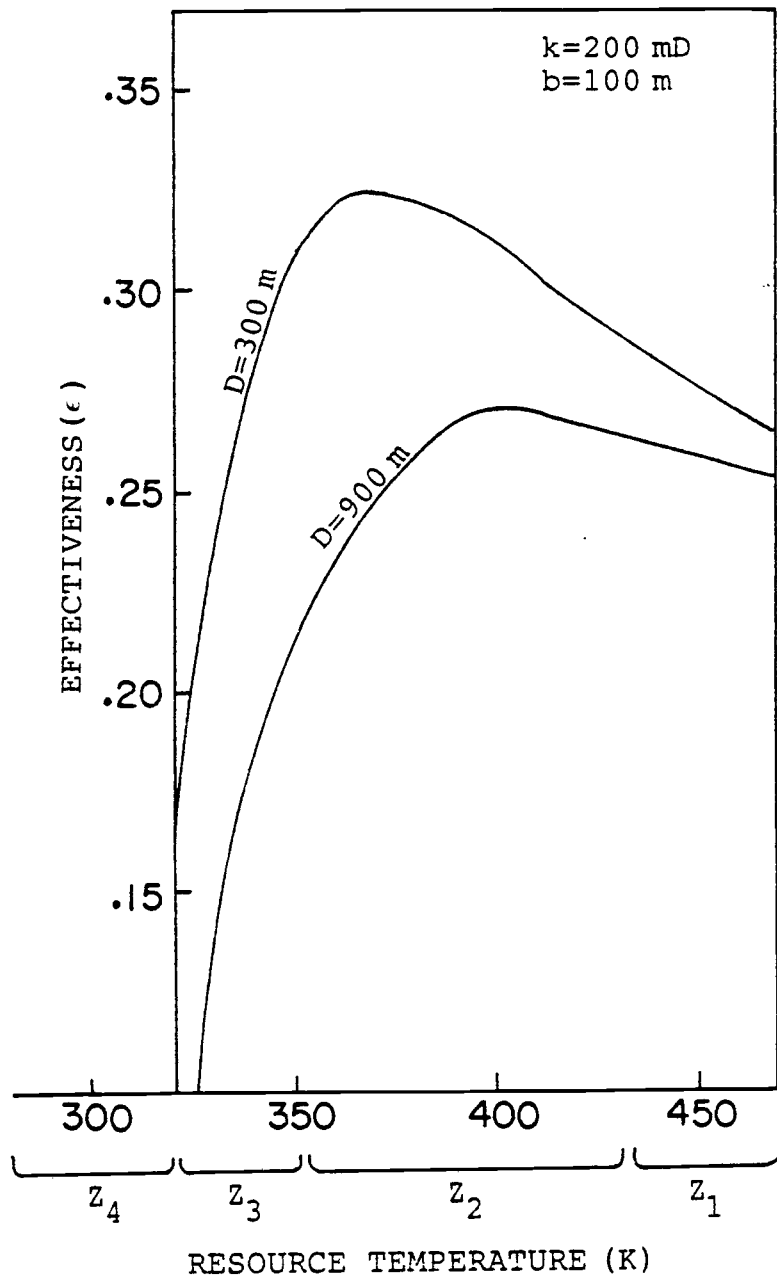


Figure 4.1. The performance of direct heating.

clearly determined yet (which will be determined later) except for region Z_4 (lower than 320 K) where the possible application is only heat pump. Good performance is seen in the middle range of resource temperature (region Z_2) in this figure. The value of effectiveness starts to decrease as the resource temperature exceeds some value due to the high irreversibilities¹¹ (losses of available energy) of heat transfer. The effectiveness is also low for the lower temperature region (region Z_3) due to the significant amount of geothermal fluid pump work compared to the total thermal energy yielded for heating.

For obtaining an improved performance, possible substitution of system for region Z_1 may be a power generation. For region Z_3 , using the combination may improve the performance. If the resource temperature is too low for direct heating (for region Z_4), the only possible system which can be applied must be a heat pump. The performance of each system thus will be investigated for the improved effectiveness.

4.3 Power Generation

Injection temperature plays an important role in the power generation performance of geothermal energy systems. As the injection temperature increases, the energy available to the surface system decreases linearly while the conversion efficiency increases as shown in Figure 4.2. The conversion efficiency, η_{power} , is defined as the

¹¹ The concept of irreversibility is explained in detail in most textbooks of thermodynamics (21,22) and will not be repeated here.

power output fraction of the energy available. These effects are combined and result in the overall performance as presented in Figure 4.3. For this case, the optimum injection temperature, $T_{i,opt}$, is about 348 K. These results are for a specific set of data as indicated. However, this example shows the general characteristics of geothermal power generation and for most practical cases the optimum injection temperature does not deviate much from the value of Figure 4.3 unless the flow rate is very high or the permeability is very low. Actually the subsurface effect is minimized (geothermal fluid pump work is very small or zero) for this high resource temperature case (region Z_1 in Figure 4.1) due to the significant buoyancy effect. Figure 4.4 shows the tendency of an increasing optimum effectiveness (at optimum injection temperature) as the resource temperature increases. This figure shows that the effectiveness is almost a linear function of the resource temperature.

It is generally believed that the power generation is more desirable than heating at high resource temperature cases. This is demonstrated thermodynamically in Figure 4.5. Power generation starts to show superior performance at the resource temperature of about 435 K. Therefore, this temperature (435 K) determines the definite boundary of the region Z_1 of Figure 4.1. The power generation is thus recommendable for the resource temperature greater than about 435 K.

The net power output from the aquifer as a function of volume flow rate of geothermal fluid is shown in Figure 4.6 for several values of resource temperature and intrinsic permeability. It is

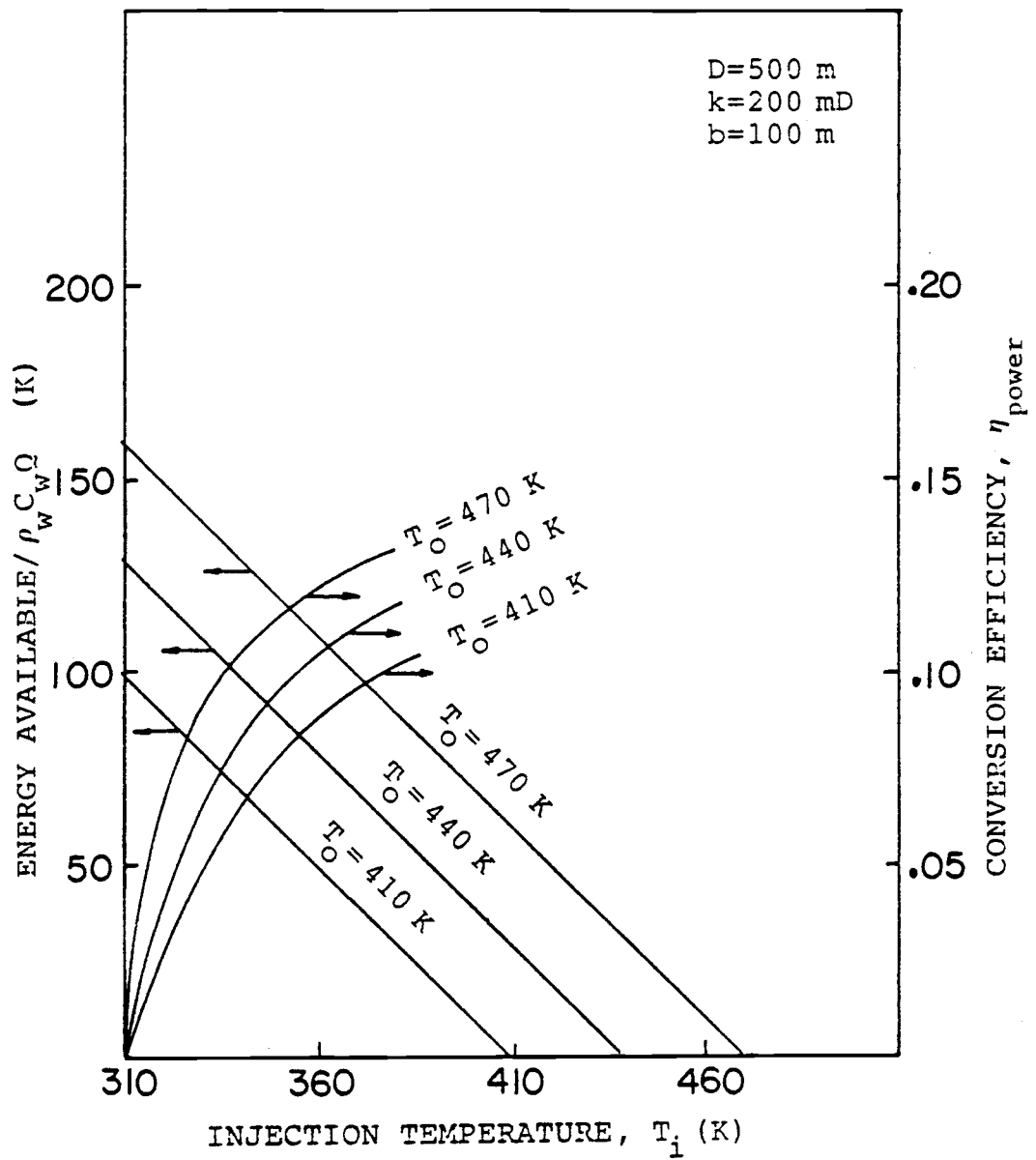


Figure 4.2. Energy available and conversion efficiency as functions of injection temperature.

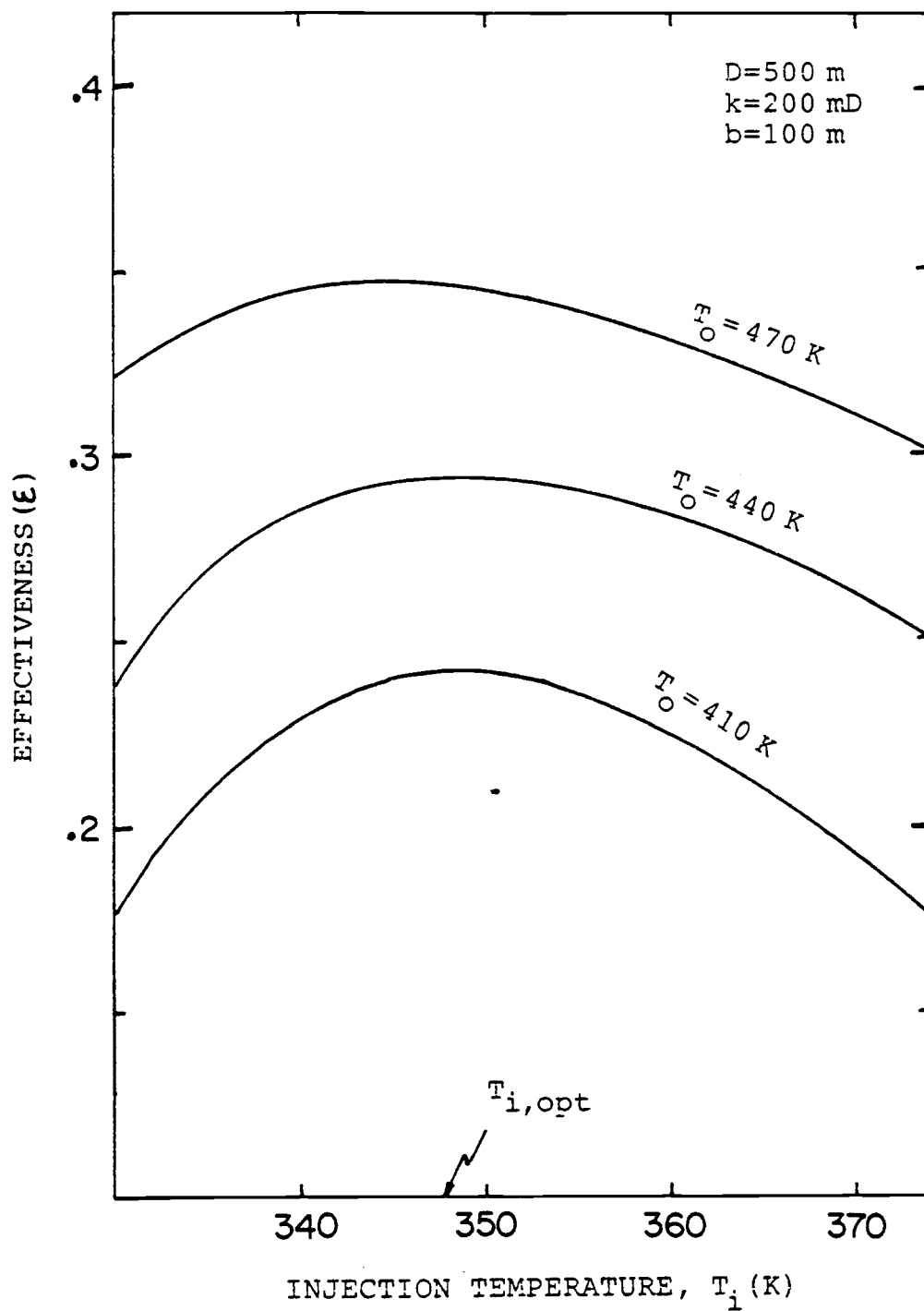


Figure 4.3. Effectiveness as a function of injection temperature in the power generation.

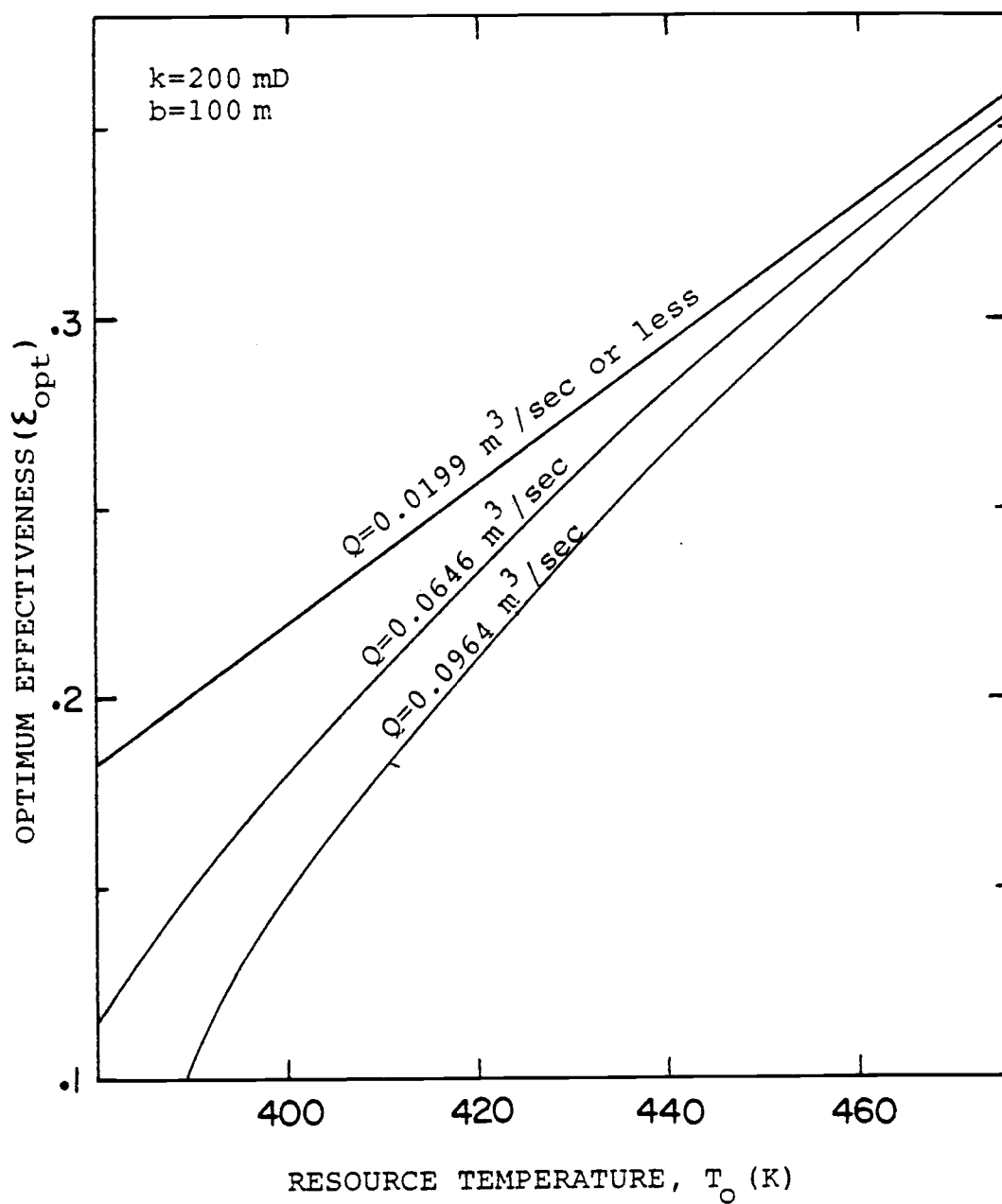


Figure 4.4. Optimum effectiveness as a function of resource temperature.

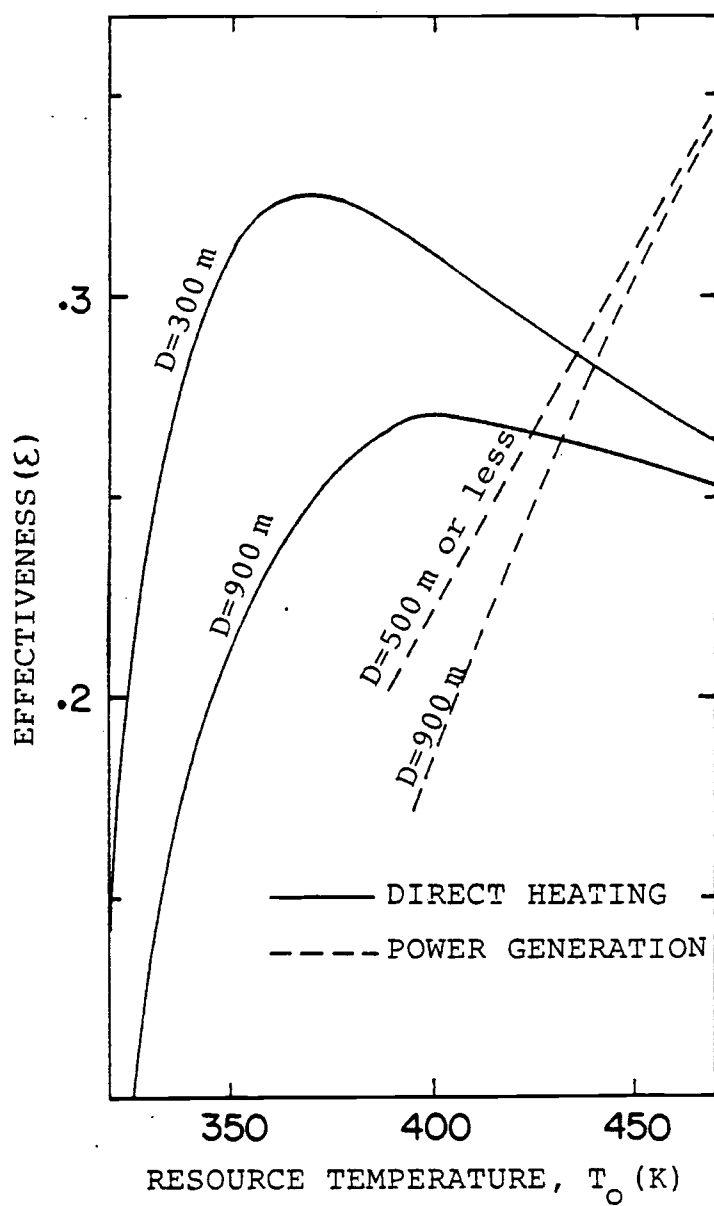


Figure 4.5. Comparison of the direct heating and power generation for a range of T_0 .

noted that the power output is almost proportional to the flow rate except for the low permeability case ($k = 50$ mD in this figure), which means that the subsurface effect is very small for this range of temperature. This figure is useful for the initial estimation of power generation potential of the aquifer. The required well separation can be readily obtained from the required flow rate of Figure 4.6 and Equation (4.1). For instance, for the net power generation of about 3000 kW from the aquifer of $T_o = 470$ K and $k = 100$ mD, the required flow rate is seen to be $0.056 \text{ m}^3/\text{sec}$ from this figure. The well separation D then can be obtained from Equation (4.1).

If the thickness of the aquifer is different from that specified in Figure 4.6, k_{eq} of Equation (4.8) must be used. For $b = 50$ m and $k = 200$ mD case, $k_{eq} = 100$ mD from Equation (4.8). Thus the corresponding curve of $k = 100$ mD in Figure 4.6 gives the necessary information for this case.

4.4 Combination

The combination can be used to improve the thermodynamic performance of heating. This is demonstrated in Figure 4.7. For the particular set of data specified, the combination at the optimum condition shows almost two times the effectiveness value of direct heating. As the injection temperature decreases the required flow rate decreases, which results in the reduced geothermal fluid pump work, while the compressor work of heat pump part increases. These two phenomena determine the optimum injection temperature.

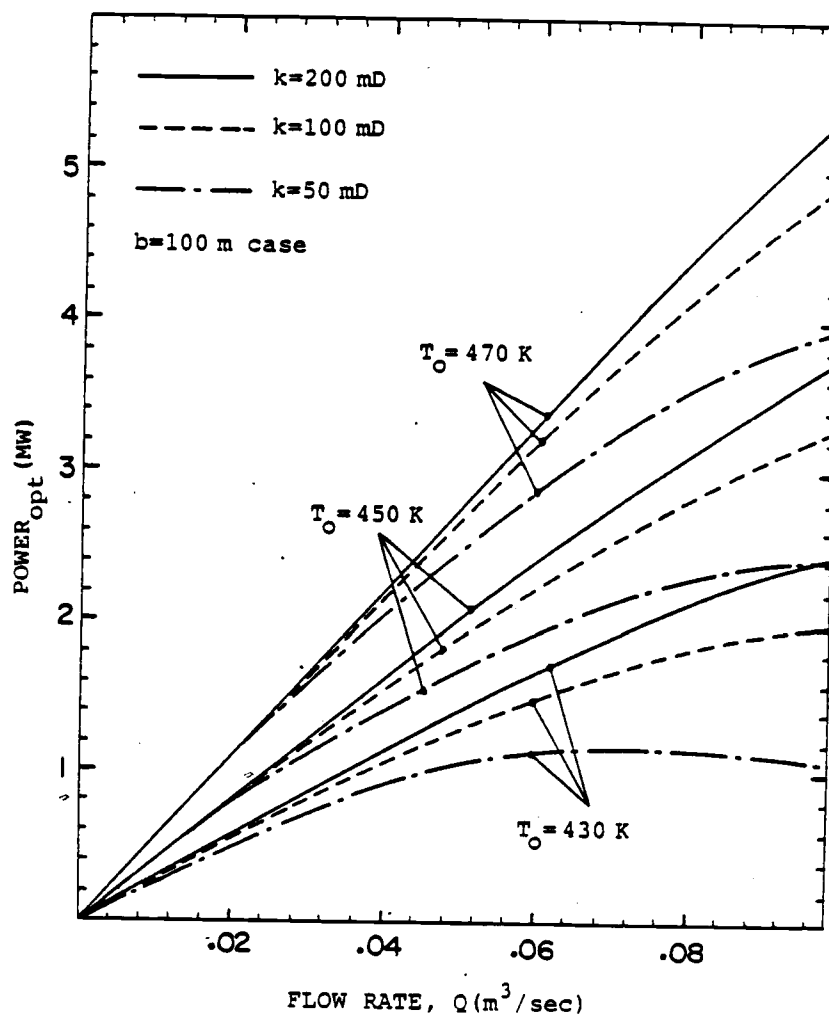


Figure 4.6. Optimum power as a function of flow rate.

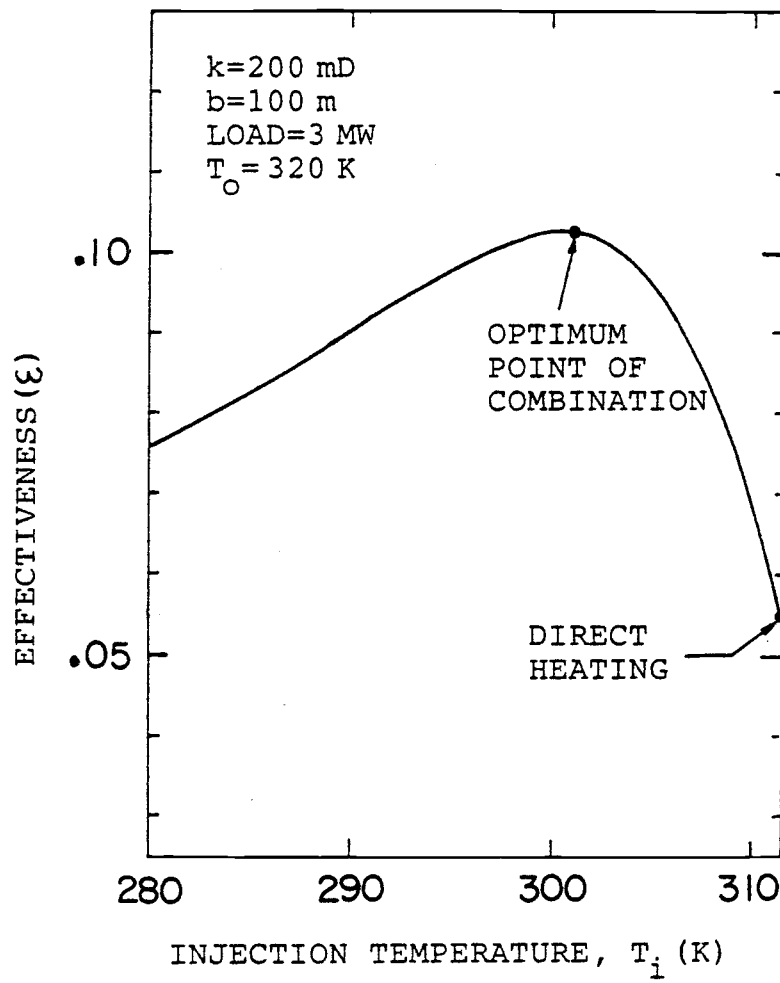


Figure 4.7. Comparison of the performances of direct heating and combination at a given load condition.

Analysis shows that the boundary of region Z_3 of Figure 4.1 cannot be simply determined by the resource temperature alone as in the power generation case. The required load condition also must be considered. The advantage of combination over the direct heating can be represented by the effectiveness ratio, ϵ_r , which is defined as:

$$\epsilon_r = \frac{\epsilon_{\text{combination}}}{\epsilon_{\text{direct heating}}} \quad (4.9)$$

Figures 4.8 through 4.10 show this parameter for three values of k (200 mD, 100 mD, 50 mD) for ranges of resource temperature and heating load. These figures can determine the boundary of region Z_3 of Figure 4.1. The value of ϵ_r close to 1 means that the combination actually does not give that much advantage over direct heating in terms of the effectiveness. Combination gives a great advantages for the lower resource temperature cases (close to 320 K which is assumed to be the lower limit temperature of direct heating) and high load cases. However, it should be remembered that even though the value of effectiveness ratio (ϵ_r) increases, the value of effectiveness (ϵ) itself decreases as the load increases.

The fossil fuel savings can be a useful parameter for determining the maximum favorable load conditions. Figure 4.11 shows how the optimum effectiveness and optimum fossil fuel savings vary for a range of heating load.¹² At a certain heating load, the fossil fuel savings show a maximum value. This load is defined as "a maximum

¹² The evaluation of fossil fuel savings is restricted to the point which yields the optimum effectiveness.

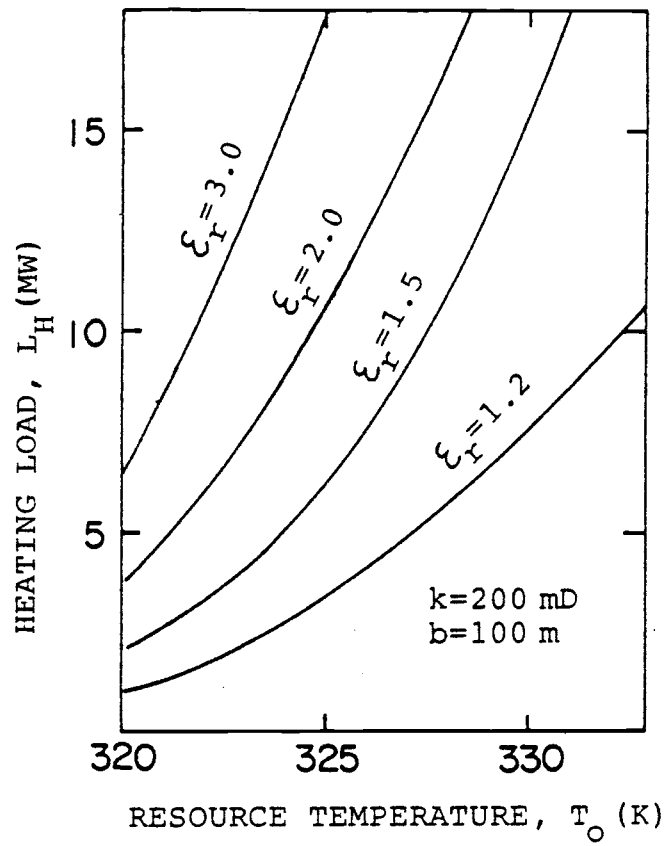


Figure 4.8. Effectiveness ratio(ϵ_r) for a range of T_O and L_H ($k = 200 \text{ mD}$ case).

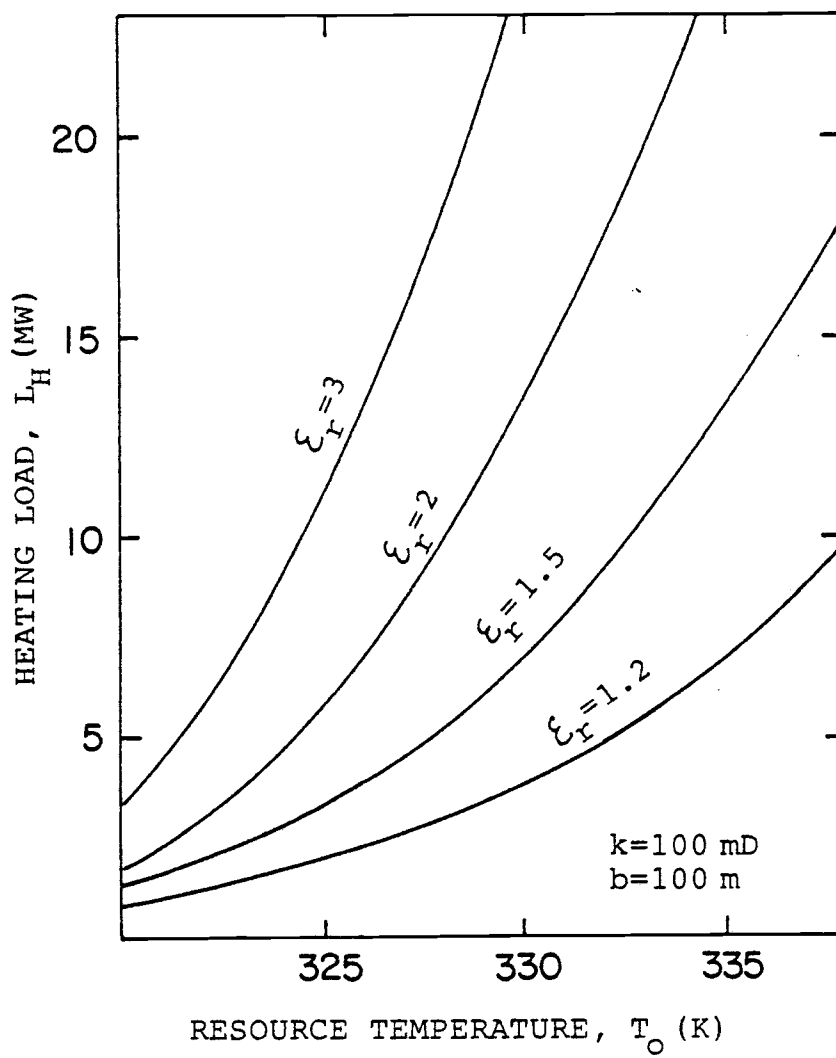


Figure 4.9. Effectiveness ratio(ϵ_r) for a range of T_O and L_H ($k=100$ mD case).

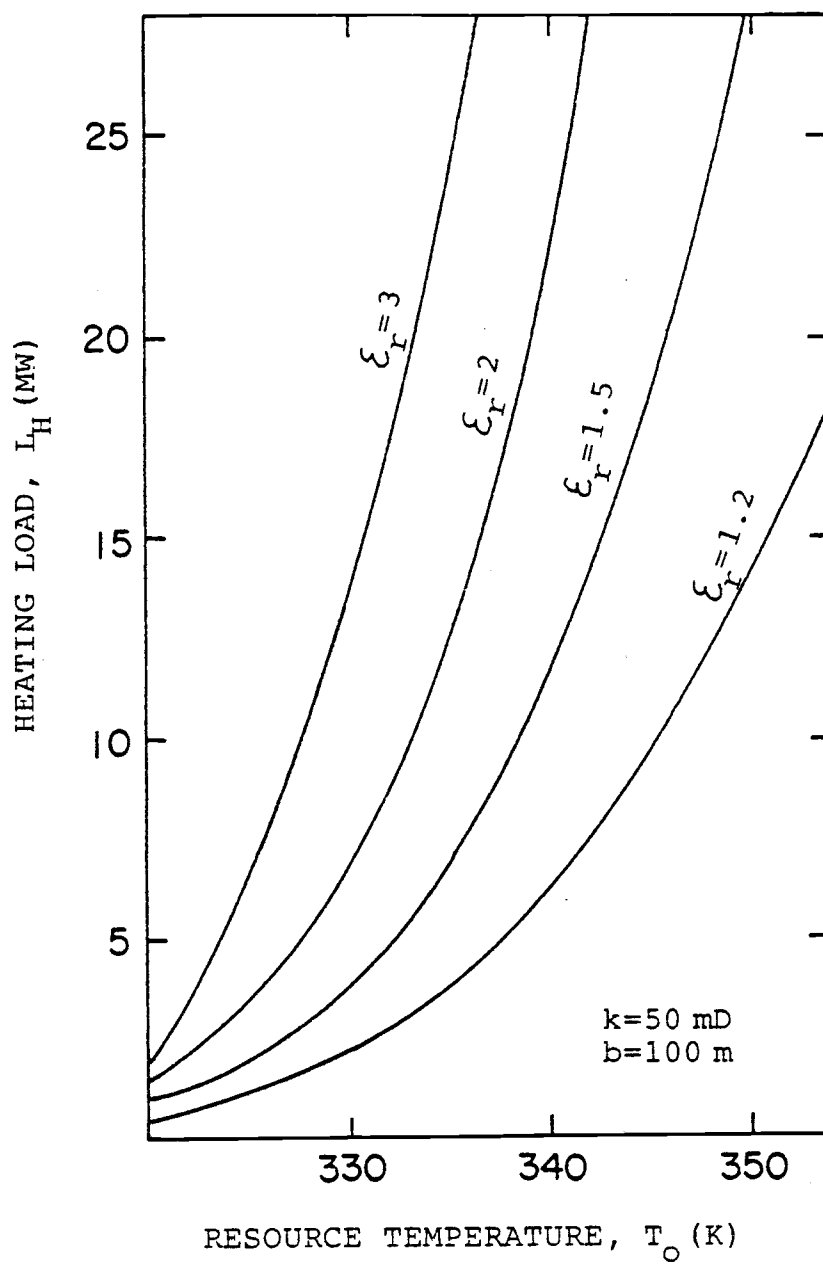


Figure 4.10. Effectiveness ratio(ϵ_r) for a range of T_O and L_H ($k = 50$ mD case),

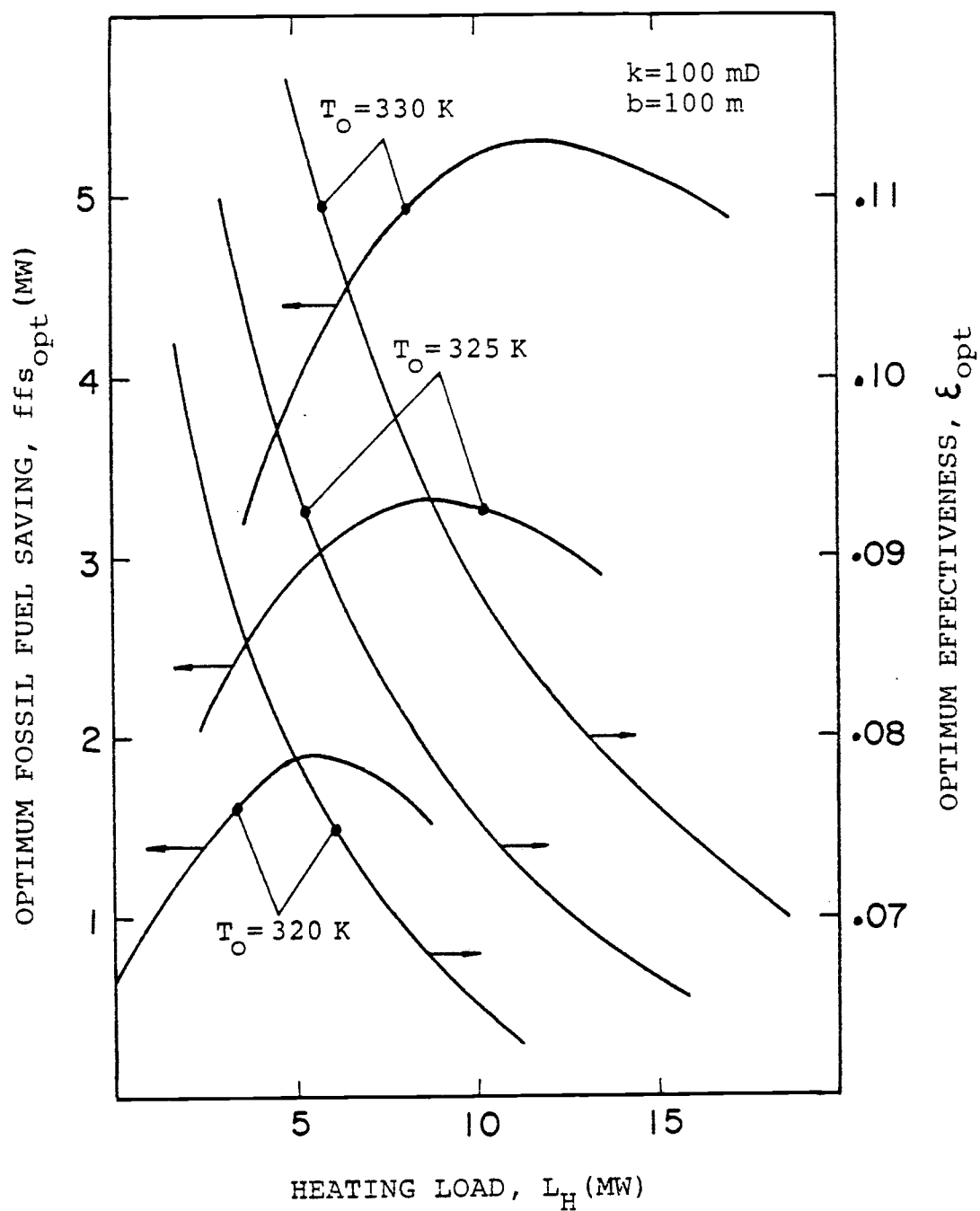


Figure 4.11. The effectiveness and fossil fuel saving for a range of L_H for a combination.

favorable load" in this study. It is thus recommended that the system load should not exceed this value per well bore pair. Figure 4.12 shows such load conditions for a range of T_o and several values of k . Figures 4.13 through 4.15 provide useful information for the initial estimation of the heating potential of aquifer at a relatively low temperature. It is noted from these figures that the required flow rates are relatively constant irrespective of resource temperatures once the load conditions are specified. This is because the differences between the resource temperature and optimum injection temperature for a specified heating load are about equal. Once the desired flow rate is known from these figures, the well separation can be calculated from Equation (4.1).

If the thickness of aquifer is different from that specified in these figures, k_{eq} evaluated from Equation (4.8) may be used. For instance, for $k = 200$ mD and $b = 50$ m case, k_{eq} from Equation (4.8) is 100 mD. Thus $k = 100$ mD curve shows the necessary information for this case.

4.5 Heat Pump System

If the resource temperature is not high enough for direct heating or combination, heat pumps must be used. Such a temperature limit is assumed to be 320 K in this study.

The role of injection temperature for the overall performance is significant in the heat pump system. Figure 4.16 shows the effect of injection temperature upon the effectiveness for a particular

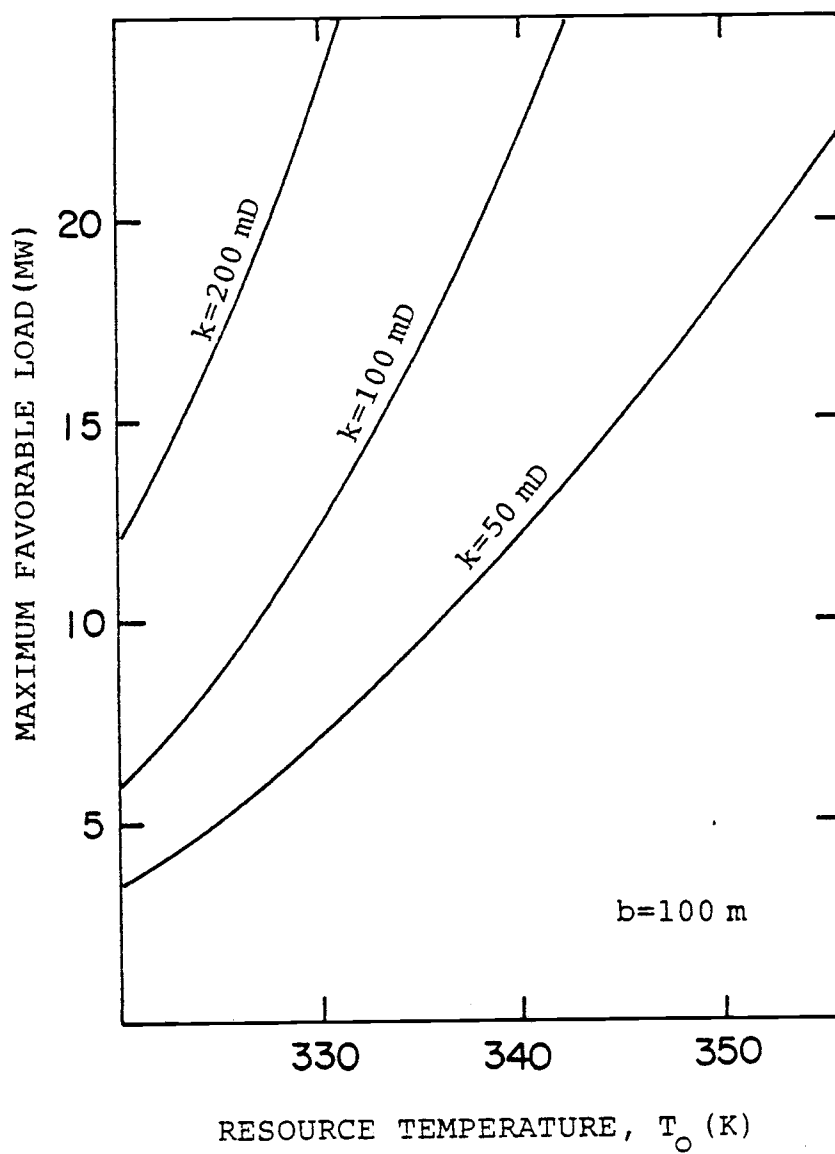


Figure 4.12. Maximum favorable load conditions for a range of T_o (combination).

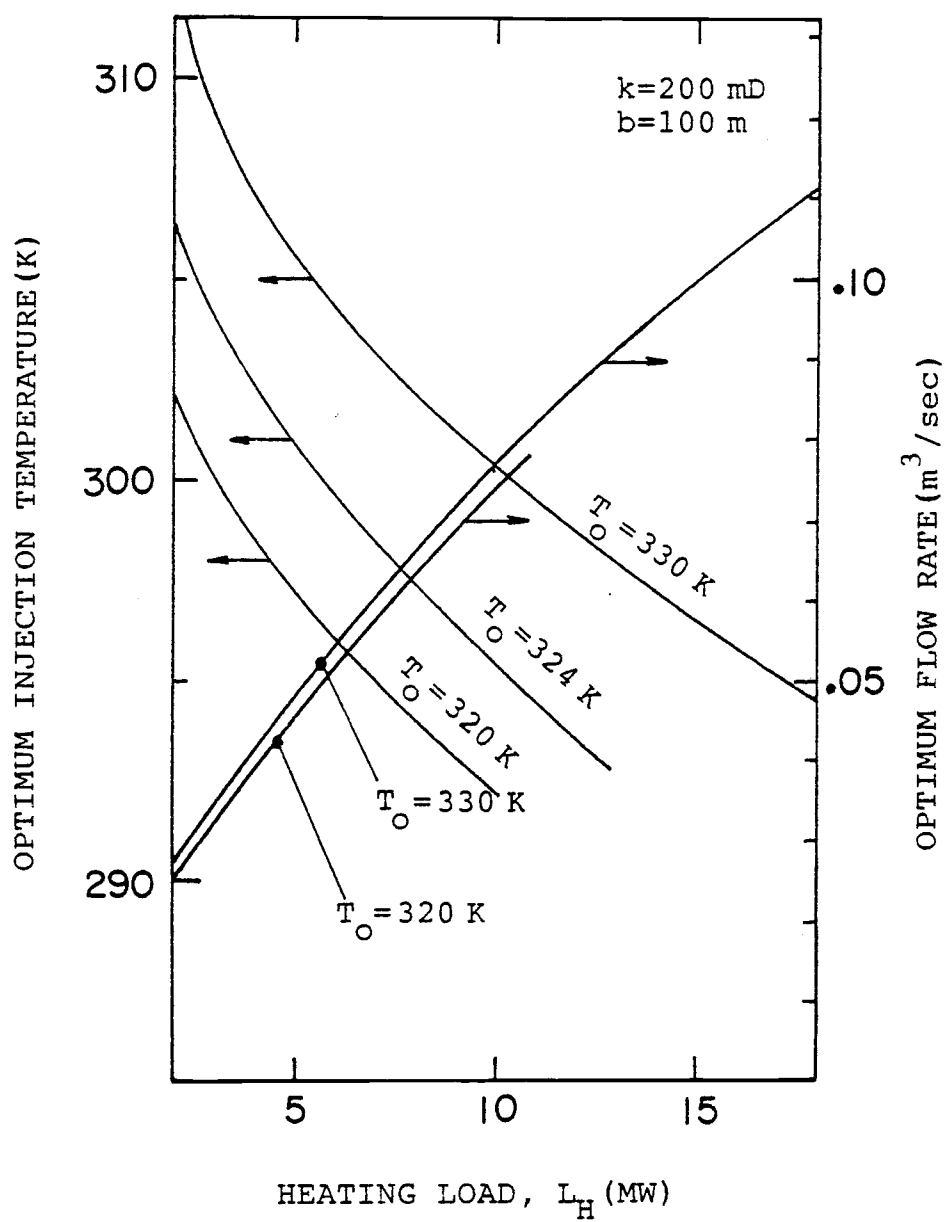


Figure 4.13. Optimum injection temperature and optimum flow rate as functions of heating load for combination ($k = 200 \text{ mD}$ case).

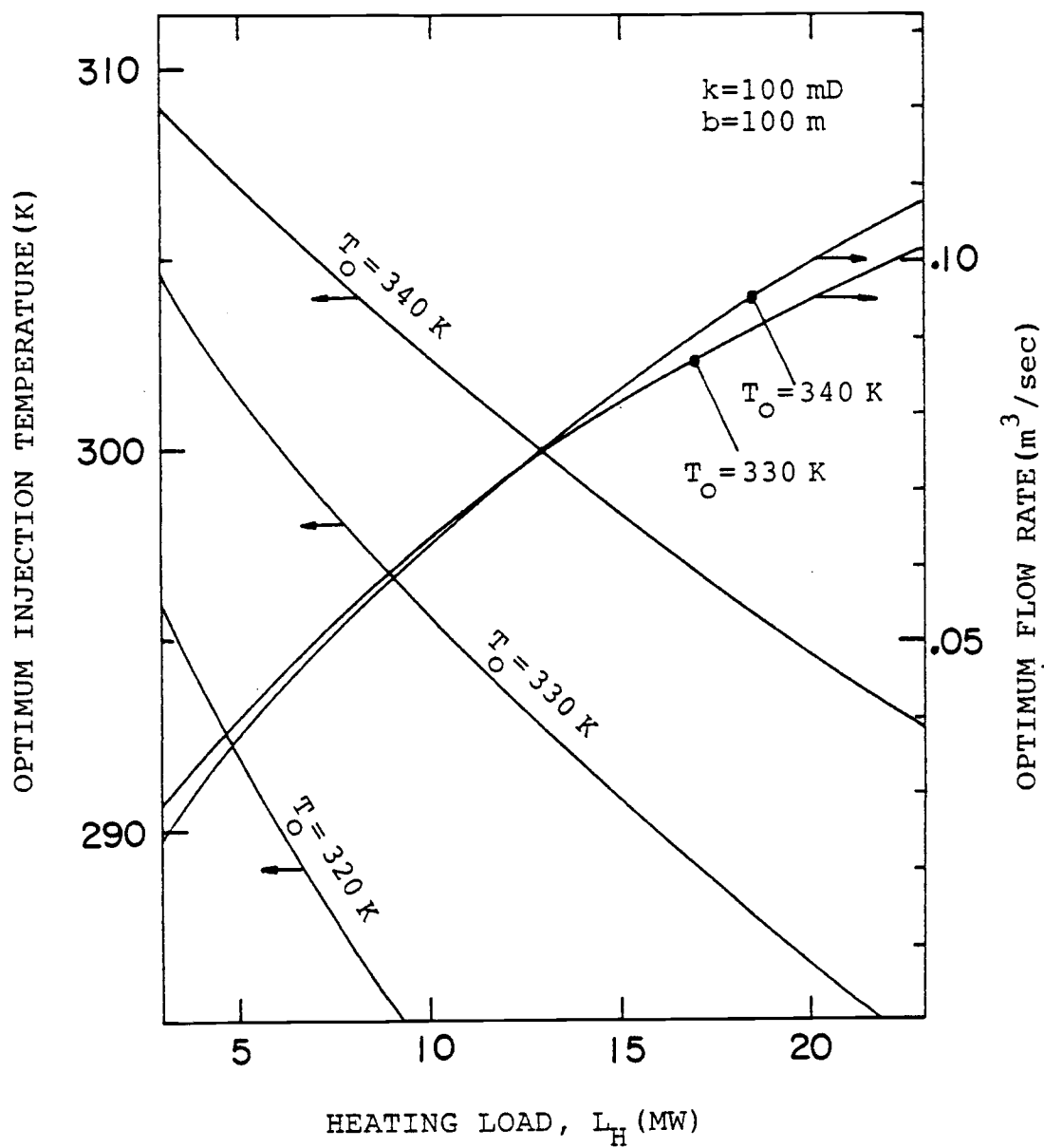


Figure 4.14. Optimum injection temperature and optimum flow rate as functions of heating load for combination ($k = 100$ mD case).

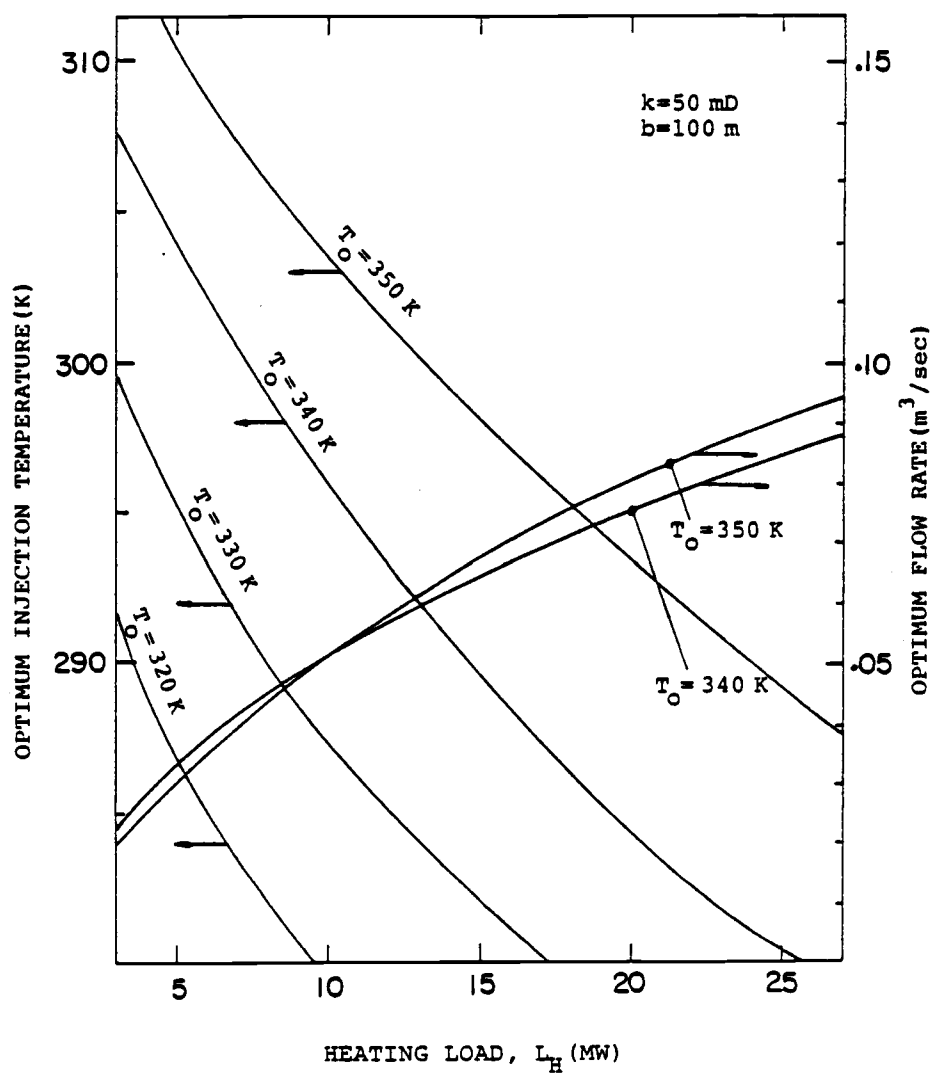


Figure 4.15. Optimum injection temperature and optimum flow rate as functions of heating load for combination ($k = 50 \text{ mD}$ case).

case specified. Here also it is noted that the value of effectiveness is very small even at the maximum case. It is thus necessary to investigate the maximum favorable load condition which maximizes the fossil fuel savings. Figure 4.17 shows such a limit of recommendable load conditions for several values of intrinsic permeability as a function of resource temperature.

Figures 4.18 through 4.20 show useful information for the initial estimation of heating potential and system design. Here also the optimum flow rate is relatively constant for a specified heating load irrespective of resource temperature since the differences between the resource temperature and optimum injection temperature for a specified heating load are about equal. The required well separation can be calculated from Equation (4.1) with the flow rate information of these figures. Here also k_{eq} can be used for the different b value cases from that specified in these figures.

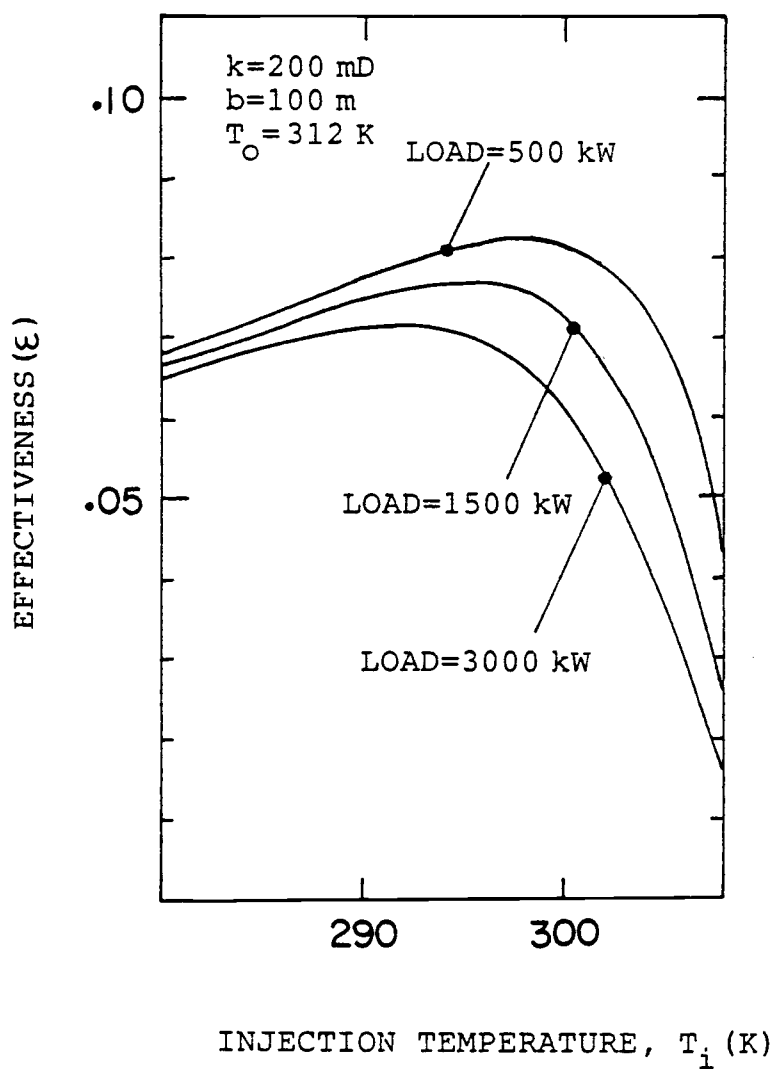


Figure 4.16. Effectiveness of heat pump system as a function of injection temperature for specified load conditions.

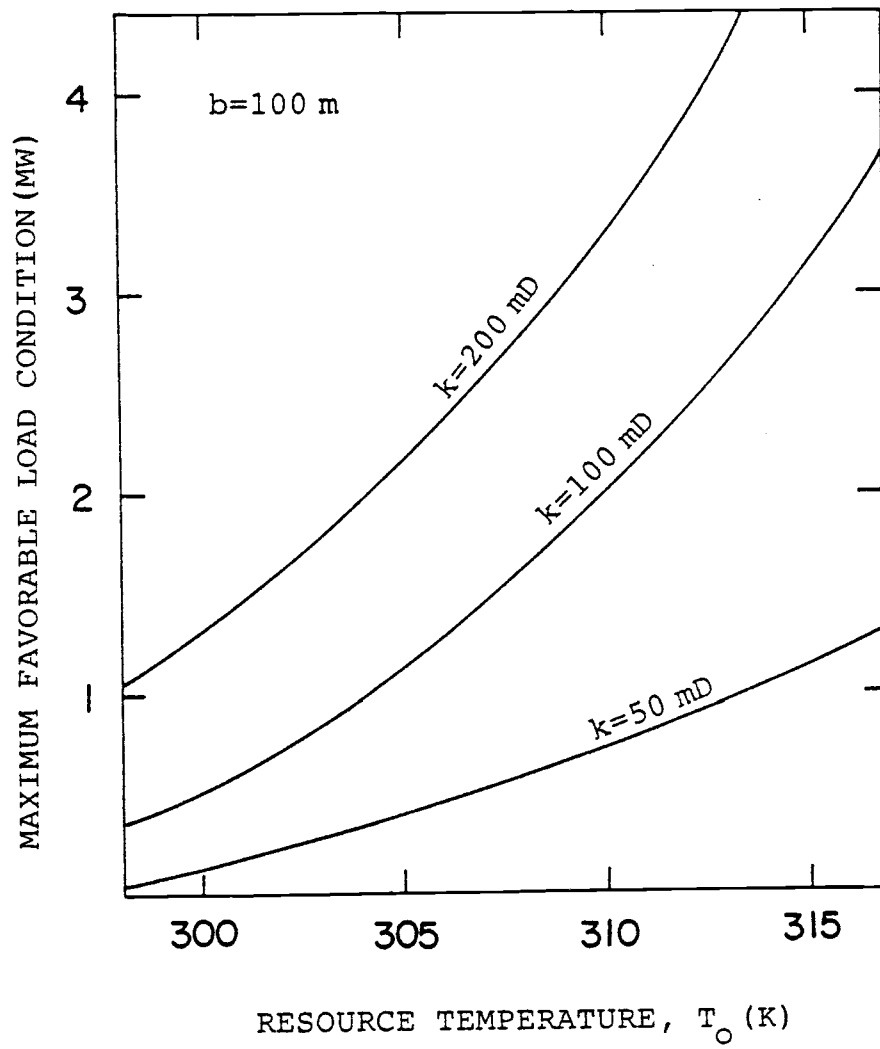


Figure 4.17. Maximum favorable load conditions for a range of T_o (heat pump).

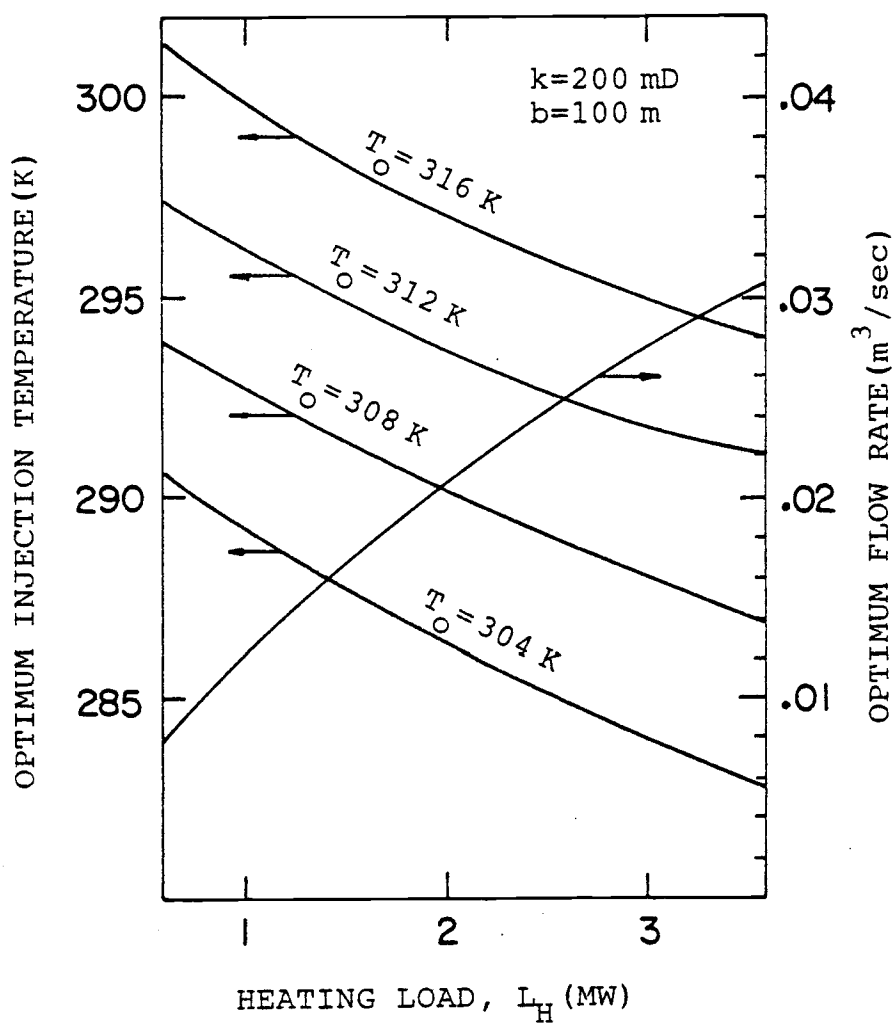


Figure 4.18. Optimum injection temperature and optimum flow rate as functions of heating load for heat pump system ($k = 200 \text{ mD}$ case).

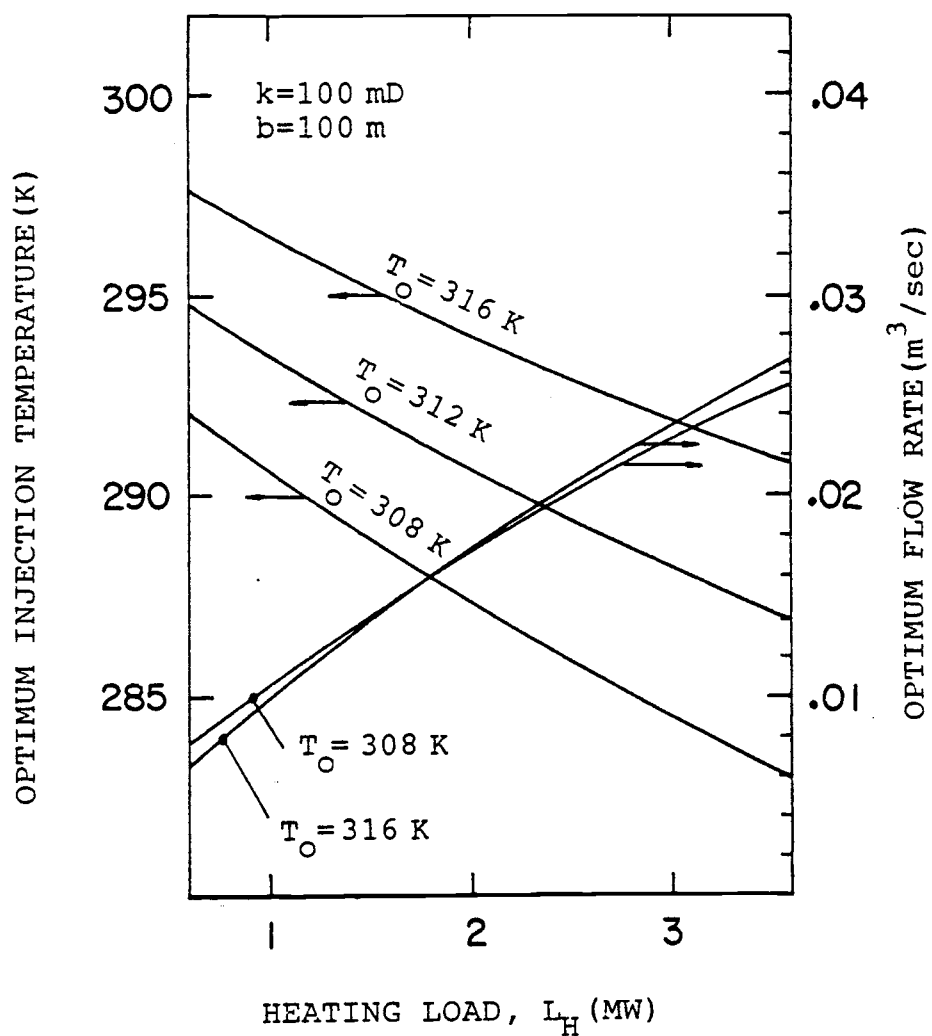


Figure 4.19. Optimum injection temperature and optimum flow rate as functions of heating load for heat pump system ($k = 100 \text{ mD}$ case).

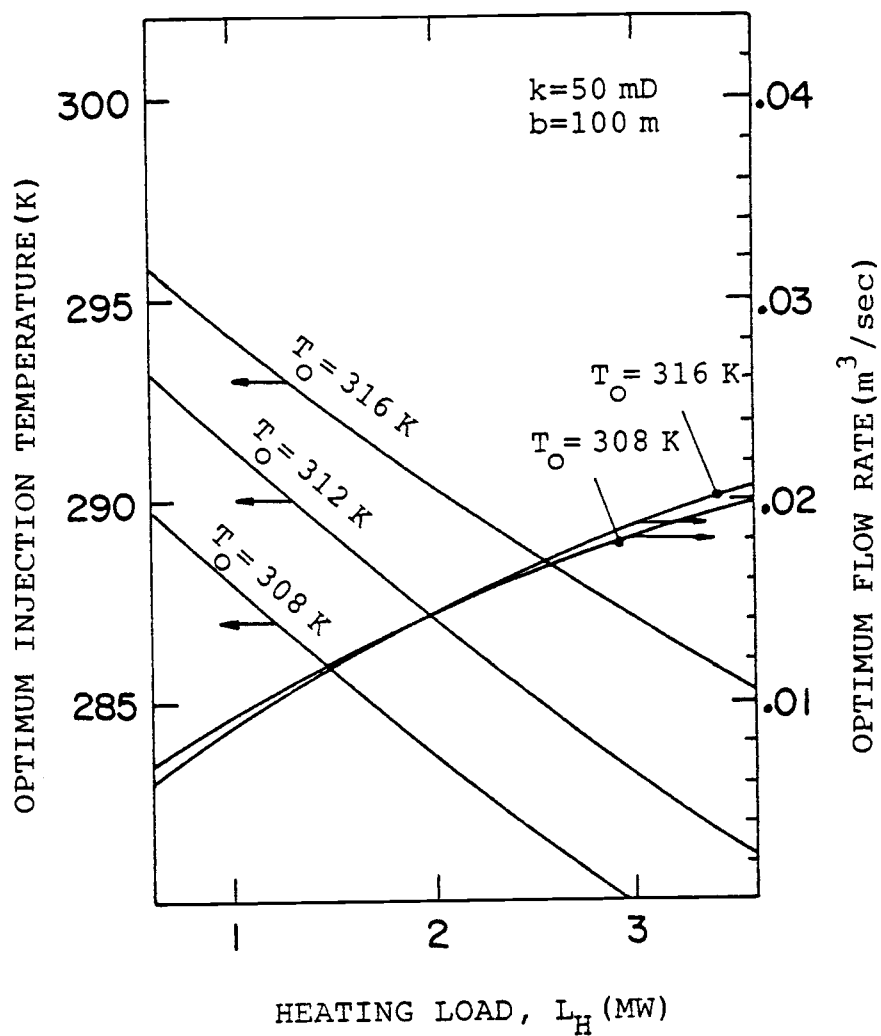


Figure 4.20. Optimum injection temperature and optimum flow rate as functions of heating load for heat pump system ($k = 50\text{ mD}$ case).

5. INCREASING FLOW MODEL

Since the production temperature drastically decreases after thermal breakthrough, it is desirable to design the system to be ended at that time. However, if the well system already exists with a small distance between the production and injection wells, the output from this system must be small if the operation stops at the thermal breakthrough. Thus the operation should be continued after thermal breakthrough for more output.

This chapter considers the case of exploiting the maximum potential from the aquifer with a fixed well separation at a relatively small distance. The production rate after thermal breakthrough is assumed to increase with a constant injection temperature to maintain a constant load. Such a scheme is termed "Increasing Flow Model" in this study. Since the surface system is under unsteady operation due to the production temperature decreasing, it is hard to predict the performance of such a system. Therefore, it is assumed that the surface system is under the steady operation by using the feed back fluid as was explained in Section 2.2.3(see Figure 2.7). The performance of such a steady operation can be safely assumed as a minimum performance that can be expected.

5.1 Preliminaries

The analysis of this chapter is based upon the same life time and the other values of parameters of Table 4.1.

The expression of the effectiveness in this model is somewhat different from that of the Constant Flow Model. It should be remembered that the injected geothermal fluid is assumed to be discarded. However, this discarded fluid starts to mix with the original resource fluid when thermal breakthrough occurs, which results in the production temperature decreasing and the flow rate increasing. Therefore, the available energy which flows through the production well bore after thermal breakthrough actually comes from two different sources, the resource and injection. The part which comes from the resource should be considered as a useful input in the expression of the effectiveness. The part from the injection only degrades the production temperature, which results in the decreased output and increased pump work. The energy extraction rate in this model is constant throughout the project life time as is evident from Equation (2.46). Therefore, the available energy extraction rate is also constant. Using the initial flow rate Q_I , the available energy extraction rate from the resource can be expressed as $\rho_w C_w Q_I [(T_o - T_E) - T_E \ln(T_o/T_E)]$. Thus for the power generation, the effectiveness is given by

$$\epsilon = \frac{\text{POWER}_{\text{net}}}{\rho_w C_w Q_I [(T_o - T_E) - T_E \ln(T_o/T_E)]} \quad (5.1)$$

and for the heating system

$$\epsilon = \frac{L_H (1 - T_E/T_{\text{space}})}{\rho_w C_w Q_I [(T_o - T_E) - T_E \ln(T_o/T_E)] + (\Sigma \text{Work})/\epsilon_{\text{pp}}} \quad (5.2)$$

Equations (4.4) and (4.5) are still valid here.

A computer program developed for this model is basically a two-dimensional search in the $Q_I - T_i$ space. The initial flow rate Q_I is varied from $Q_{I,\min}$ to $Q_{I,\max}$ in an increment of ΔQ_I . For each Q_I , the basic pattern of aquifer resistance and non-dimensional production temperature are calculated as a function of time. This temperature profile determines the flow rate Q by Equation (2.47). The injection temperature T_i is varied from $T_{i,\min}$ to $T_{i,\max}$ in an increment of ΔT_i for each Q_I . The total geothermal pump work during the project life time is computed from the basic pattern of aquifer resistance for each T_i , from which the average pump work is obtained and used for the performance calculations. The limits and increment of injection temperature are specified differently for each system (power generation, heating, combination and heat pump). The performance calculations of the surface systems are based upon the constant system inlet temperature T_s . The other parts of the program are the same as those of the Constant Flow Model.

5.2 Selection of Applicable Systems

It is shown in Chapter IV that the power generation shows better performance than heating for the high temperature region (higher than 435 K). For instance, the effectiveness of the power generation is 0.348 and the effectiveness of direct heating is only 0.266 for the resource temperature of 470 K case (see Figure 4.5). However, this is not true when the operation is continued after thermal breakthrough to exploit the maximum potential from the given well system. The

production temperature decreasing after thermal breakthrough seriously reduces the performance of the power generation.

Figure 5.1 shows the production temperature, flow rate and pump work of geothermal fluid as a function of time for the Increasing Flow Model for a set of data specified. It is shown that the production temperature starts to decrease drastically at the thermal breakthrough (about 4.8 years in this case). This results in the flow rate increasing from the initial flow rate in order to maintain a constant surface load. It is also shown that the geothermal fluid pump work is not required at an early period of project life time due to the significant buoyancy effect. Pump work is required from $t = 6$ years. From this time, the pump work increases due to the flow rate increasing. Such an increasing tendency is shown as an almost linear function of time. The flow rate and production temperature at the end of the project life time is defined as constant system flow rate, Q_s , and constant system inlet temperature, T_s , respectively (see Figures 5.1 and 2.7). The effectiveness of this system for the application of power generation during the total project life time (25 years) has been evaluated as 0.215. This is the result from the injection temperature and initial flow rate specified. A different injection temperature will result in different performance. Therefore, the optimum injection temperature will exist for each initial flow rate. Figure 5.2 shows such an optimum injection temperature and the resultant constant system inlet temperature as a function of initial flow rate Q_i for the power generation case. The net power output is

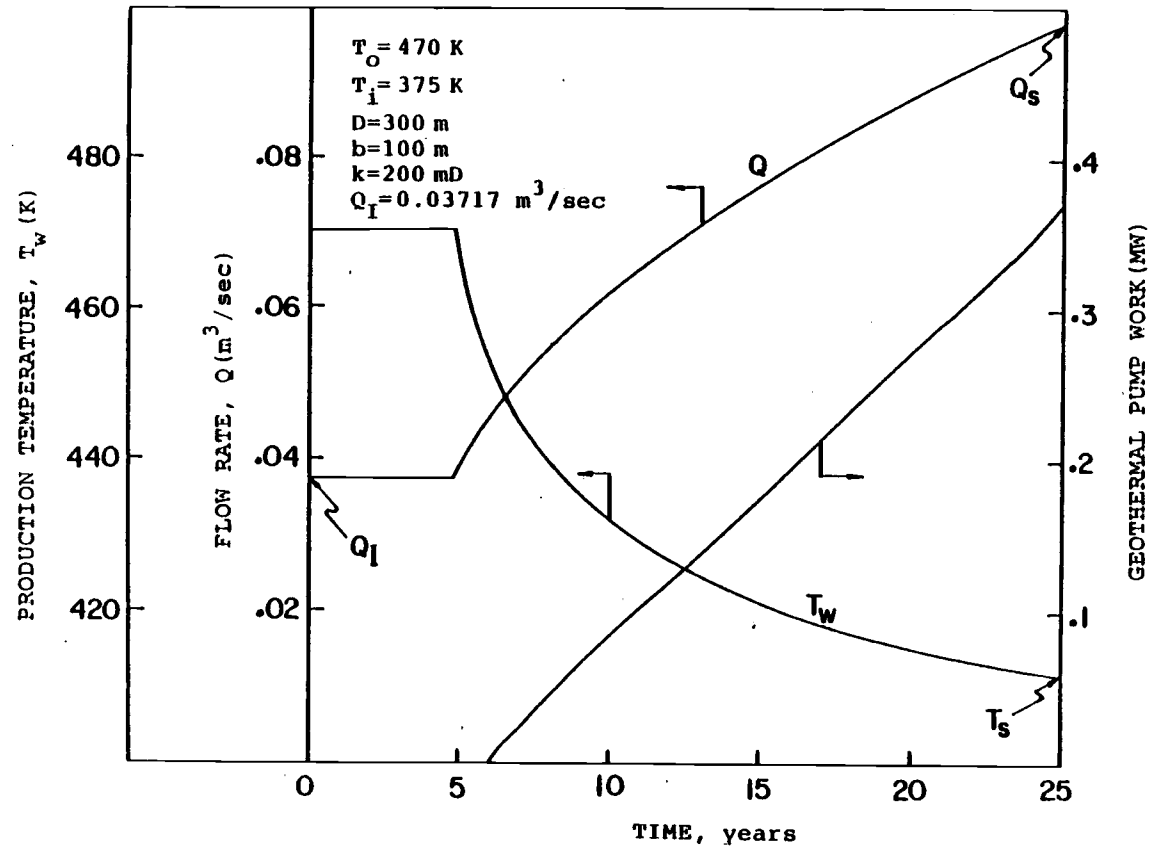


Figure 5.1. Production temperature, flow rate and pump work of geothermal fluid as a function of time for the Increasing Flow Model.

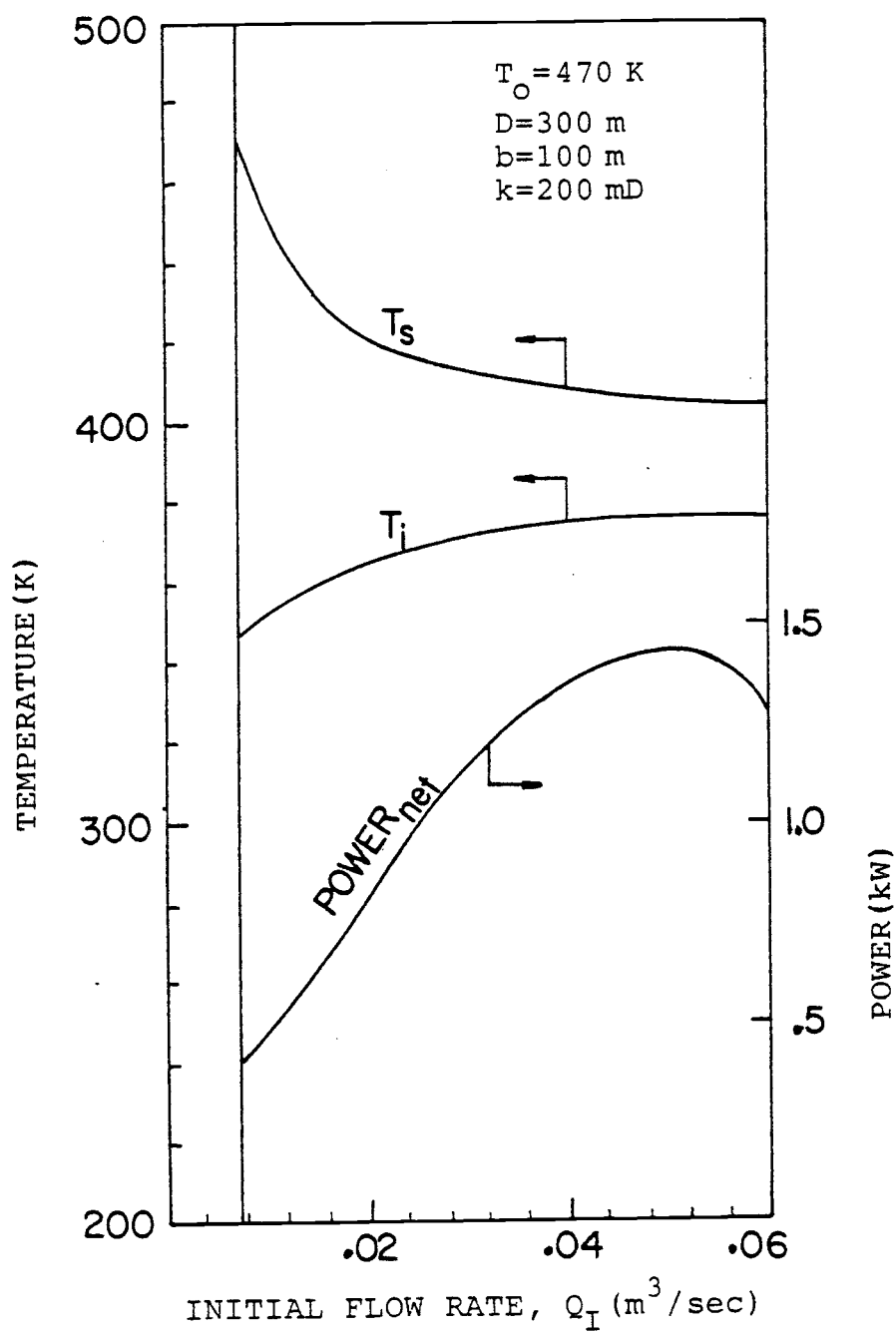


Figure 5.2. Optimum injection temperature(T_i), system inlet temperature(T_s) and net power output as functions of initial flow rate for Increasing Flow Model.

also shown. This net power should be understood as the average net power output during the project life time. It is thus considered that the following factors reduce the performance of power generation:

- 1) Injection temperature(T_i) increasing
- 2) System inlet temperature(T_s) decreasing
- 3) Geothermal fluid pump work increasing

On the other hand, the temperature decreasing effect after thermal breakthrough is not so serious for the performance of direct heating. For the direct heating system, the only factor which reduces the performance is the increasing of geothermal fluid pump work.

Figure 5.3 shows the performance comparison between the power generation and direct heating for two resource temperatures, 450 K and 470 K. It should be noted that as the initial flow rate increases from that of the Constant Flow Model(the flow rate corresponding to the vertical line denoted by CONSTANT FLOW), the performance of direct heating exceeds the performance of power generation rapidly. It is thus considered that power generation is not a good system for this production model.

The combination is also not applicable for this production model. Due to the production temperature decreasing, the combination can work only in the very narrow ranges of flow rate and injection temperature. For the visualization of the performance of combination, the performance diagram in the $Q_I - T_i$ space is useful. Figure 5.4 shows the performance diagram of the combination for the particular cases

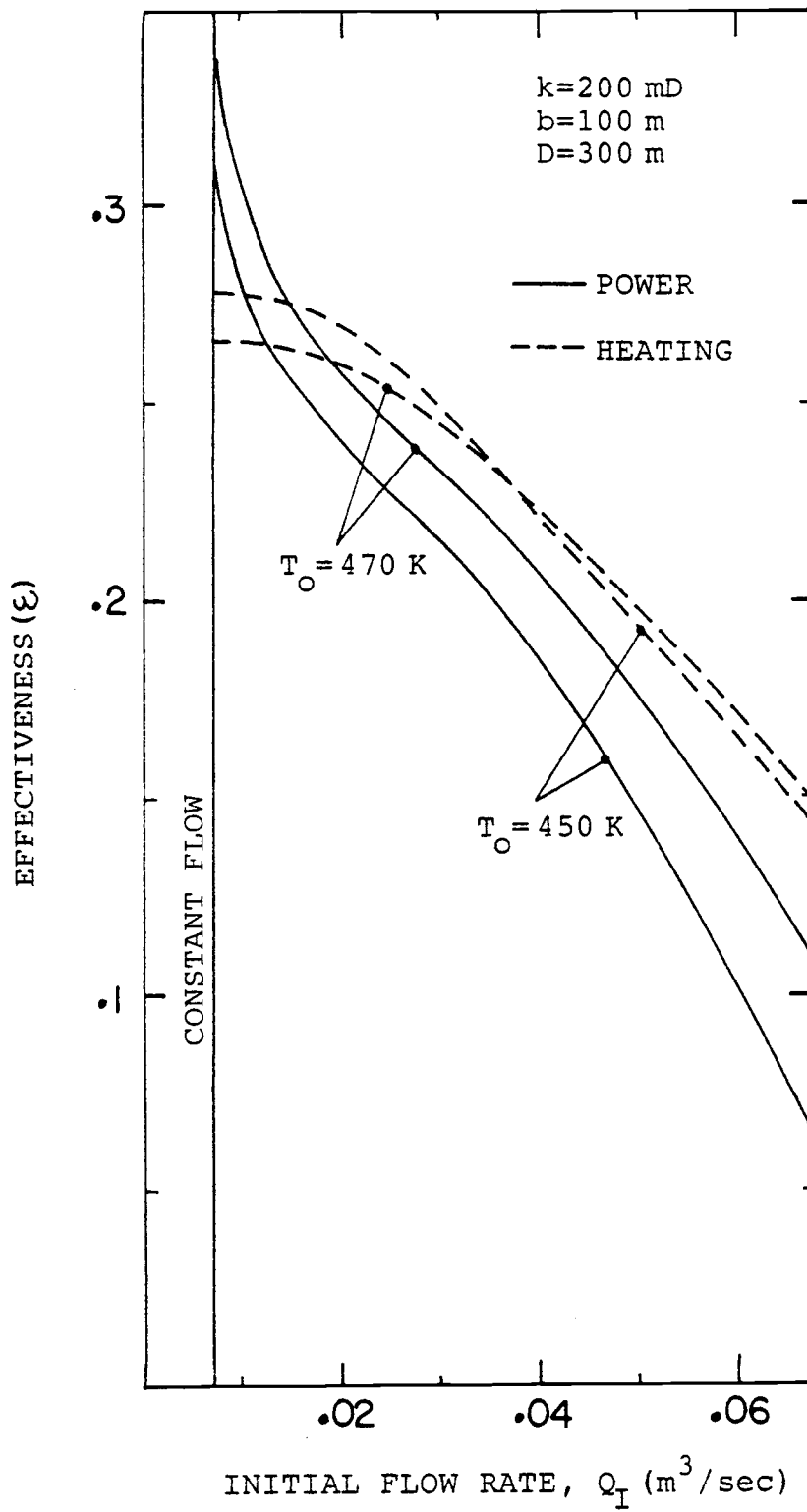


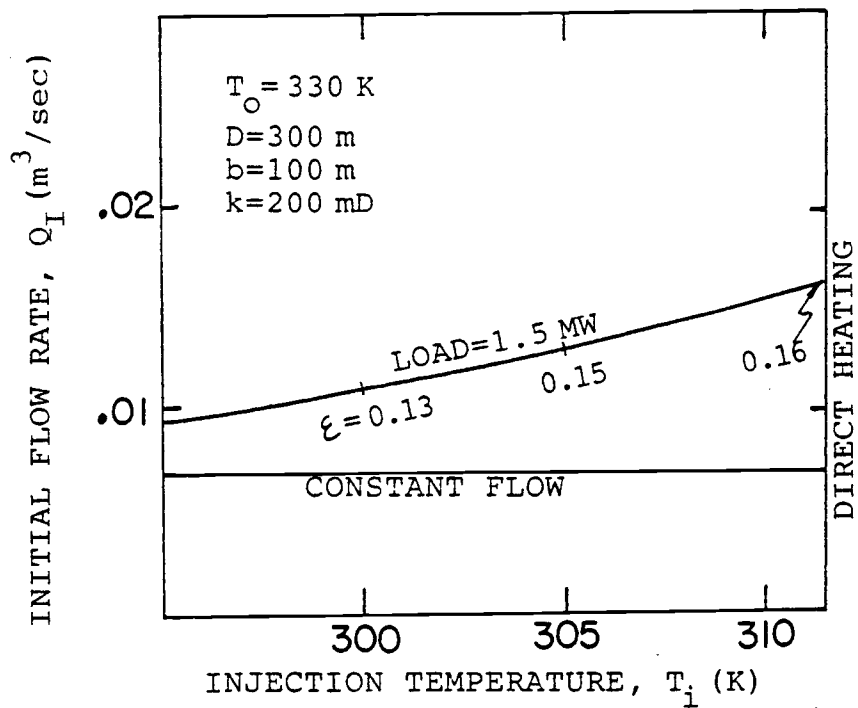
Figure 5.3. Performance comparisons of power generation and direct heating for the Increasing Flow Model.

specified. The vertical line, denoted by "DIRECT HEATING" in this figure, corresponds to the direct heating only case (no heat pump). The flow rate corresponding to the horizontal line denoted by "CONSTANT FLOW" means the flow rate which is required for the Constant Flow Model. It is shown from this figure that there are many possibilities of combining different injection temperature and flow rate to achieve a specified load. The maximum loads that can be achieved by combination are about 1.5 MW for case (A) and 6 MW for case (B). If the load conditions exceed these values, the direct heating part cannot work due to too low of a production temperature at the later part of the project life time. It is readily seen from this figure that the maximum effectiveness occurs near the direct heating lines for both cases. It is shown in Chapter IV that the combination shows a good performance for high load and low resource temperature case. However, such a high load cannot be achieved by the combination in the Increasing Flow Model. Thus the combination is also considered as an inadequate system for the production model of this chapter.

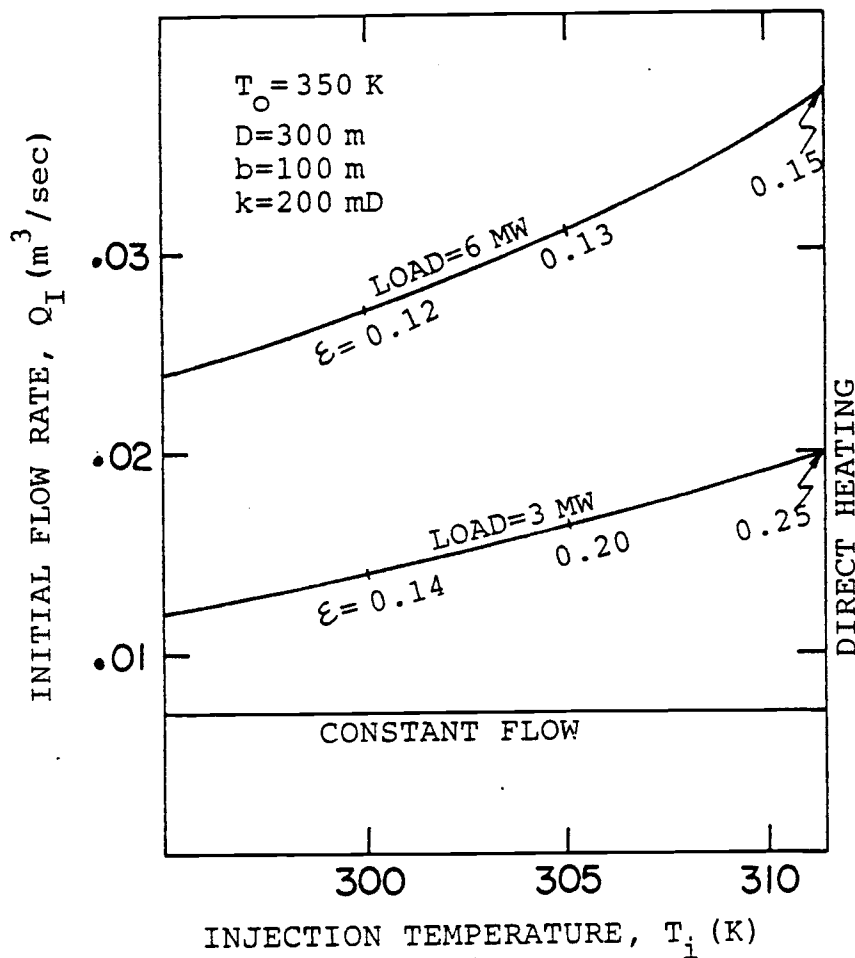
Direct heating is considered as a good system applicable for the Increasing Flow Model. If the resource temperature is too low for direct heating, the heat pump system must be considered. Thus these two systems will be considered in the following sections.

5.2.1 Direct Heating

The load is simply proportional to the flow rate for the direct



(A)



(B)

Figure 5.4. Performance diagram of combination:
 (A) $T_o = 330 \text{ K}$ case (B) $T_o = 350 \text{ K}$ case

heating because the injection temperature is constant. However, attention should be given to the geothermal fluid pump work which becomes high for the later part of the project life time due to the production temperature lowering. It is thus important to operate the system under the maximum favorable load condition which maximizes the fossil fuel savings.

Figures 5.5 and 5.6 show the load curves of direct heating system in the $Q_I - T_o$ space for two different well separation cases ($D = 300$ m and $D = 500$ m). The dotted lines are the constant load lines and the solid lines indicate the operating position for achieving the maximum favorable load. The figures in the parenthesis of the solid line are the thickness of aquifer (given in m) and the intrinsic permeability (given in mD). For instance, for $D = 300$ m, $T_o = 380$ K, $b = 50$ m and $k = 200$ mD case, such a favorable load is found to be about 10 MW from Figure 5.5. To achieve this load, the initial flow rate should be about 0.035 m³/sec. Therefore, the recommendable load conditions should not exceed this value for this case.

5.2.2 Heat Pump System

To achieve heating from the lower temperature resource (too low for direct heating), the only system which can be applied is the heat pump system. Since the injection temperature effect is shown at the production well in the Increasing Flow Model, careful control of the flow rate and injection temperature are required to accomplish a maximum performance.

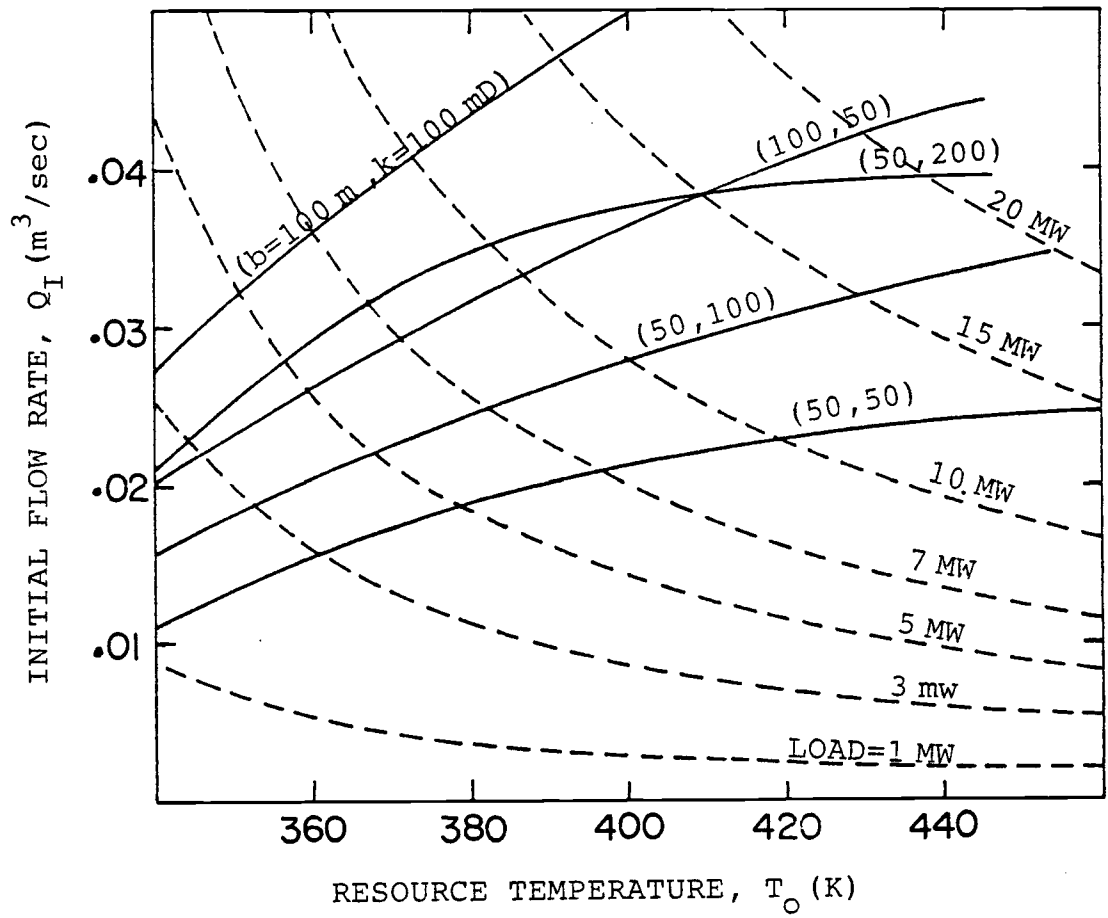


Figure 5.5. Load curve of direct heating system($D = 300 \text{ m}$ case)

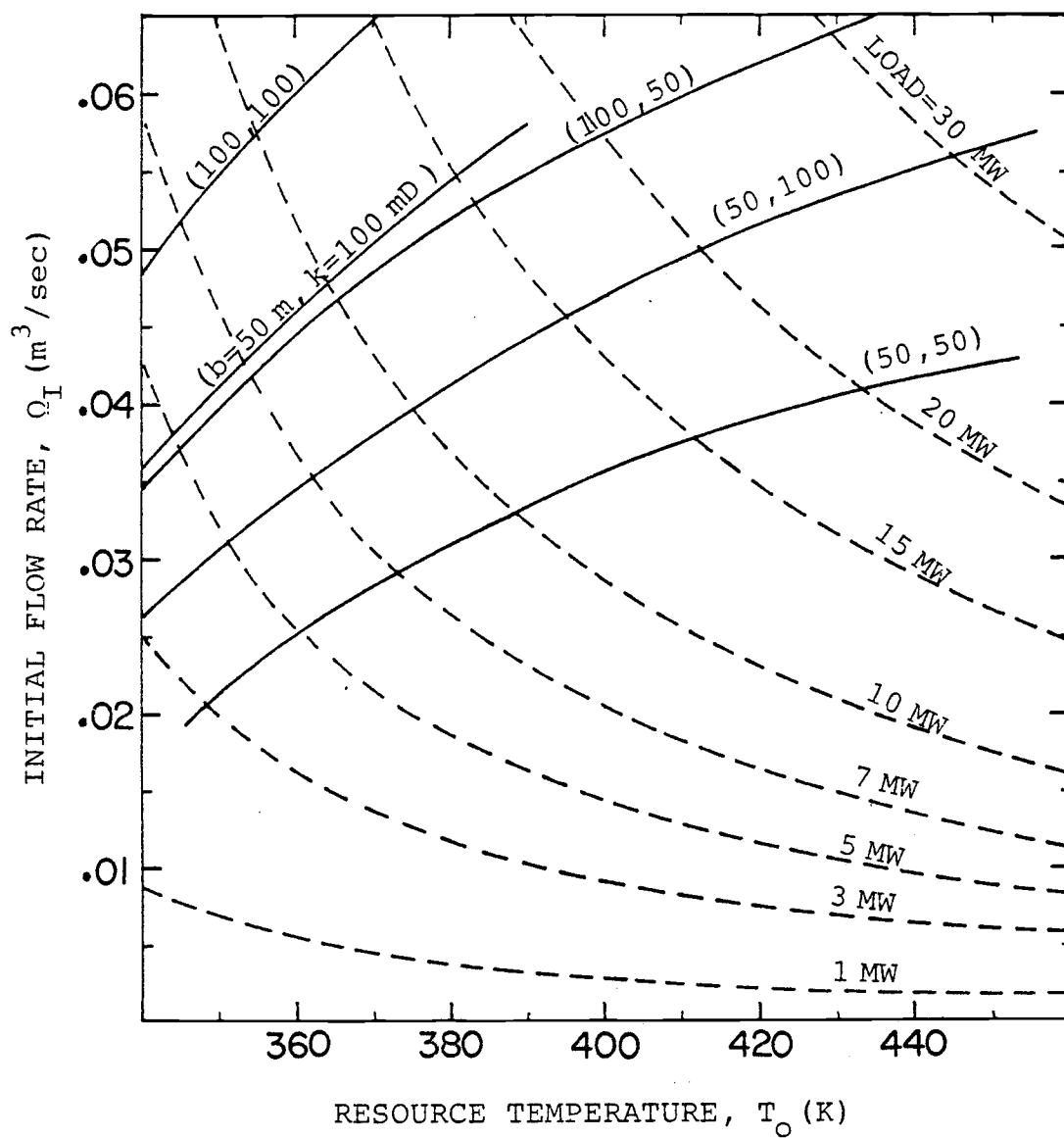


Figure 5.6. Load curve of direct heating system($D=500 \text{ m}$ case)

Figure 5.7 shows the load curves and the optimum operating lines of heat pump system in the $Q_I - T_i$ space at the particular case specified. Dotted lines are the constant load lines and the solid lines are the operating lines for achieving the maximum effectiveness. On this operating line, the maximum fossil fuel savings occur at the point denoted by ●. For $D = 300$ m, $T_o = 315$ K, $b = 100$ m and $k = 200$ mD case, such a load condition is about 2.1 MW from Figure 5.7. If the desired load is 1.5 MW, the initial flow rate and injection temperature should be $0.015 \text{ m}^3/\text{sec}$ and 295 K for accomplishing the system operation at the maximum effectiveness. The flow rate corresponding to the horizontal line denoted by CONSTANT FLOW is the one required for the Constant Flow Model. The performance diagrams for the different well separation and geologic conditions are shown in Figure 5.8. Figure 5.9 shows such diagrams for the resource temperature at 310 K.

As the geothermal fluid pump work becomes significant (low resource temperature, low intrinsic permeability and low aquifer thickness cases), the maximum favorable load point (denoted by ●) approaches the CONSTANT FLOW line, which means that the given conditions are not so adequate for the Increasing Flow Model. In other words, the Constant Flow Model may be tolerated for such cases.

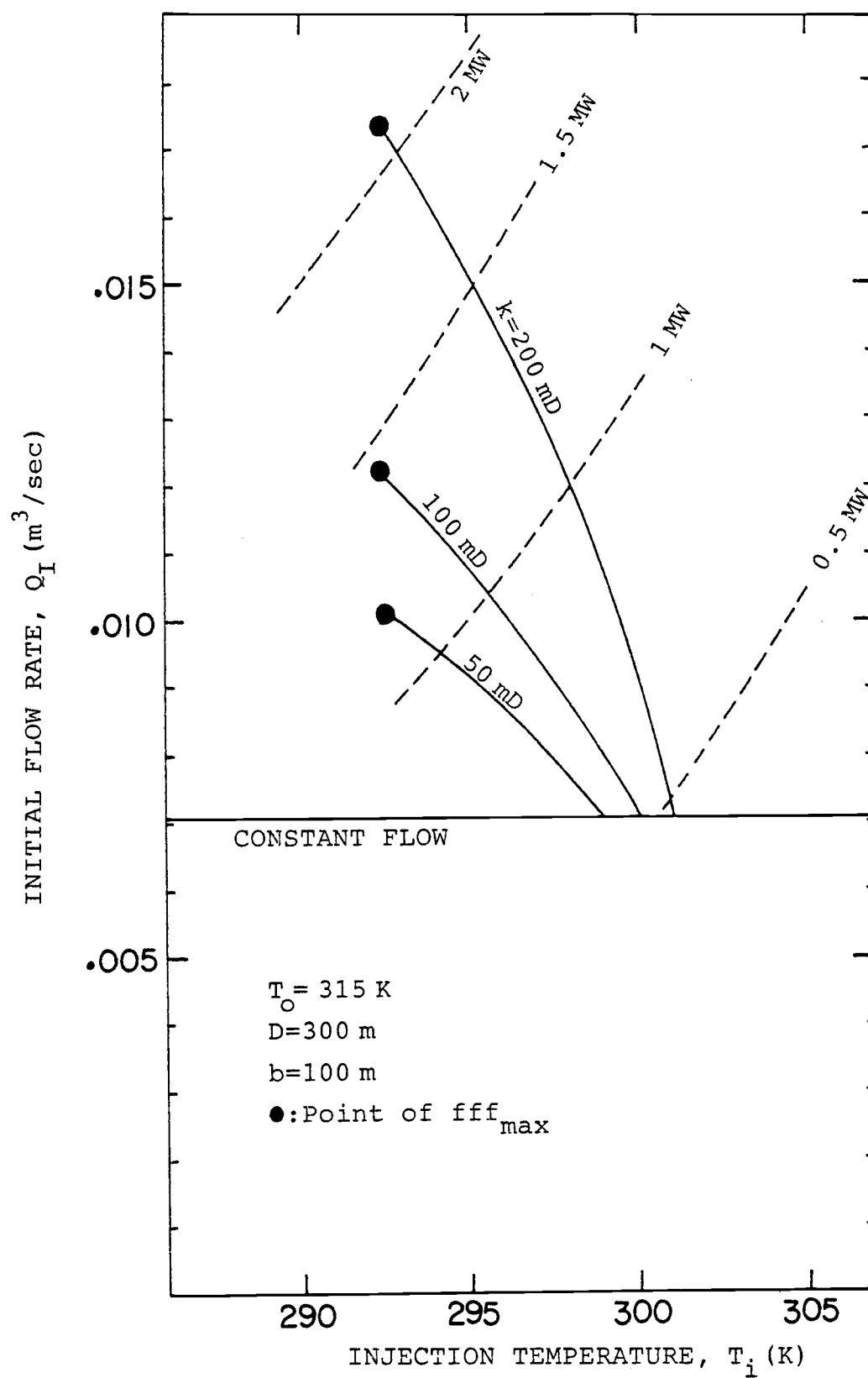


Figure 5.7. Performance diagram of heat pump.

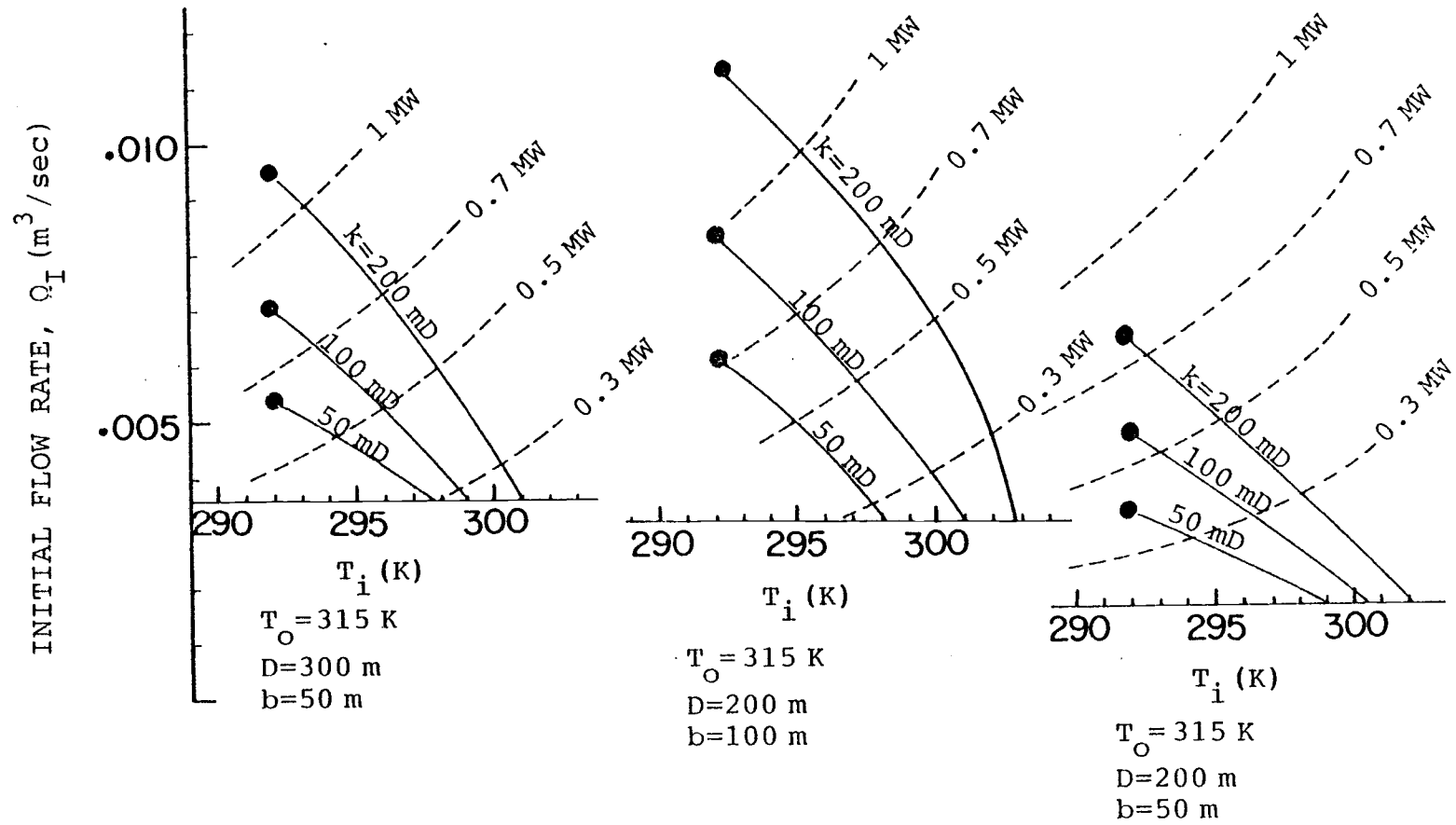


Figure 5.8. Performance diagram of heat pump ($T_o = 315$ K case).

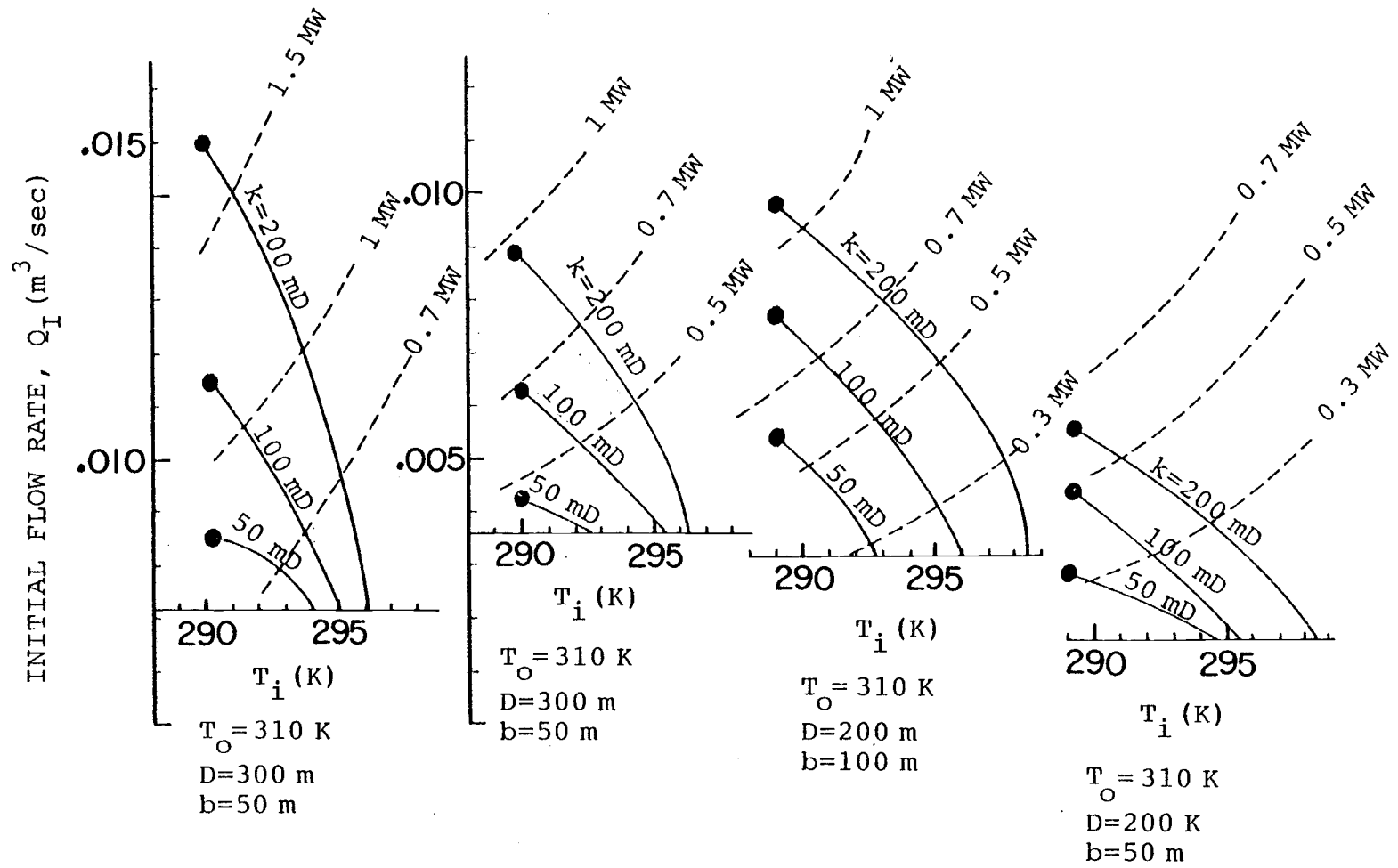


Figure 5.9. Performance diagram of heat pump($T_o = 310$ K case).

6. CONCLUSIONS AND RECOMMENDATIONS

It has been shown that for the thermodynamically desirable operation of forced geoheat recovery from hot water aquifers, attention should be given not only to the surface systems but also to the subsurface systems. The resource temperatures, load conditions, permeabilities and the thickness of the aquifers are all important parameters. The distance between the wells should be long enough to insure the constant production temperature during the designed project life time(Constant Flow Model). Injection temperature is identified as the basic parameter to be optimized.

The selection of the type of the surface application is important for the best performance. The decision regarding what the best surface application is can be made by comparison of the effectiveness of each system at the optimum operating conditions. Power generation and space heating(direct heating, combination and heat pump) have been the only candidate surface systems considered in this study. Results show that power generation can be selected based simply on the resource temperature alone. When the resource temperature is higher than about 435 K, power generation had the best performance of all systems over the range of parameters considered. However, the selection of the combination is not so simple. The load condition, the resource temperature, the permeability and the thickness of the aquifer should be all considered. Figures 4.8 through 4.10 can be used for such a decision

making. For the very low temperature resource (assumed to be lower than 320 K in this study), the only applicable system is the heat pump. These considerations automatically decide the adequate ranges of direct heating.

The optimum operation of the system as well as the selection is important. The injection temperature basically determines the optimum operation. For the power generation case, the optimum injection temperature is relatively constant at 348 K. However, for the combination and heat pump cases, the resource temperature, load condition, permeability and the thickness of aquifer must all be considered. Figures 4.13 through 4.15 show the optimum operation of the combination and Figures 4.18 through 4.20 show the optimum operation of the heat pump.

The power generation potential or the heating potential of the aquifer can be estimated from the output of such optimum operations. These estimates are useful for the initial evaluation of the geothermal well design of a doublet.

The load conditions play important roles in determining the optimum injection temperatures for combination and heat pump. The limits of favorable load conditions also have been considered for such systems.

Analyses also have been done on an existing well system with a relatively small distance between the wells. The continued operation after thermal breakthrough is desired in such a case. Careful control of flow rate and injection temperature are required. The

flow rate should increase after thermal breakthrough in order to maintain a constant surface load(Increasing Flow Model). The selection of the direct heating system has been considered as a good choice in such a case. Since the geothermal fluid pump work becomes very high at the later period of project life time, attention should be given to the limit of the favorable load conditions. For the very low temperature resource, heat pump system must be used. In such a case, the flow rate and injection temperature are equally important. The optimum operation of the heat pump system has been shown in the performance diagram of $Q_I - T_i$ space with the other parameters such as load condition, resource temperature, permeability and the thickness of the aquifer.

The well system considered in this work is the single recharging-discharging well pair, which is the most simple one in the forced geoheat recovery systems. Probably more involved well systems can be used to make better use of aquifer. One such system is the line source and line sink by infinite well array. In the actual situation, a finite number of wells can simulate such a well system. The advantage of such a well array is that the flow field generated can be approximated as a uniform flow which can simply sweep the thermal energy of the aquifer uniformly. Therefore, at the thermal breakthrough, the region of interest can be completely used unless the horizontal conduction or the buoyancy effect is significant, which results in the efficient use of the aquifer. In such a well system, the head loss through the aquifer is proportional

to the distance between the source line and sink line, the feature of which is different from that of a doublet case. Also the horizontal conduction and buoyancy effect may strongly affect the production temperature profile in such a case. Thermodynamic analysis of such a system may present interesting results and can be recommended for the future work.

BIBLIOGRAPHY

1. Kappelmeyer, O. and R. Haenel, "Geothermics with Special Reference to Application," Geoexploration Monographs, Series 1, No.4, Berlin-Stuttgart: Geopublication Associates, Gebruderborntraeger, 1974.
2. Reistad, G.M. and P. Means, Heat Pumps for Geothermal Applications: Availability and Performance, Final Report to U.S. DOE, Contract No. DE-FC07-79ID12020, May 1980.
3. Reistad, G.M., B. Yao and M. Gunderson, "A Thermodynamic Study of Heating with Geothermal Energy," ASME Journal of Engineering for Power, Vol.100, No.4, 1978.
4. Walter, R.A., Modeling of Geothermal Power Plants Using the Binary Fluid Cycle, Master Thesis, Oregon State University, 1976.
5. Steidel, R.F., Jr., Optimum Power from a Geothermal Well, Internal Report, Lawrence Livermore Laboratory, 1974.
6. Davis, S.N. and R.J.M. DeWiest, Hydrogeology, John Wiley & Sons, New York, 1966.
7. Muskat, M., The Flow of Homogeneous Fluids through Porous Media, McGraw-Hill Book Co., New York, 1937.
8. Gringarten, A.C. and J.P. Sauty, "A Theoretical Study of Heat Extraction from Aquifers with Uniform Regional Flow," J. Geophys. Res., Vol.80, No.35, pp. 4956-4962, 1975.
9. Lauwerier, H.A., "The Transport of Heat in an Oil Layer Caused by the Injection of Hot Fluid," Appl. Sci. Res., Sect.A, Vol.5, pp. 145-150, 1955.
10. Carslaw, H.S. and J.C. Jaeger, Conduction of Heat in Solids, 2nd ed., p. 396, Clarendon, Oxford, 1959.
11. Dacosta, J.A. and R.R. Bennett, "The Pattern of Flow in the Vicinity of a Recharging and Discharging Pair of Wells in an Aquifer having Areal Parallel Flow," Int. Ass. Sci. Hydrol. Publ. 52, pp. 524-536, 1960.
12. Arpaci, V.S., Conduction Heat Transfer, Addison-Wesley Co., Massachusetts, 1966.
13. Bingham, G., Fluidity and Plasticity, McGraw-Hill Book Co., New York, 1922.

14. Skibitzke, H.E., "Electronic Computers as an Aid to Analysis of Hydrologic Problems," IASH Publication, 52, 1961.
15. Stallman, R.W., "Electric Analog of Three-Dimensional Flow to Wells and its Application to Unconfined Aquifers," U.S. Geol. Survey Water-Supply Paper, 1536-H, pp. 205-242, 1963.
16. Walton W.C. and T.A. Prickett, "Hydrogeologic Electric Analog Computers," ASCE Journal of Hydraulics Division, pp. 67-91, Nov. 1963.
17. Peerless Pump Div., FMC Corp., 1200 Sycamore st., Montebello, CA 90640.
18. Starling, K.E., Fluid Thermodynamic Properties for Light Petroleum Systems, Gulf Publishing Co., Book Publishing Division, Houston, 1973.
19. Pfeiffer, E.L., "What Size Cooling Tower?," Chemical Engineering, 56, No.4, pp. 98-100, 1949.
20. Reistad, G.M., "Available Energy Conversion and Utilization in the United States," Journal of Engineering for Power, Vol.97, No.3, 1975.
21. Obert, E.F., Concepts of Thermodynamics, McGraw-Hill Book Co., New York, 1960.
22. Keenan, J.H. and G.N. Hatsopoulos, Principles of General Thermodynamics, John Wiley & Sons, New York, 1965.

APPENDICES

APPENDIX I

MAXIMUM FLOW RATE

The maximum flow rate which insures that the analyses of Chapter 2 are valid should be considered from two viewpoints, the Darcy's law viewpoint and the hydraulic fracturing viewpoint as is indicated in Chapter 2. Each viewpoint is considered below.

A. Maximum Discharge in the Range of Darcy's Law

The validity of Darcy's law falls in the region of laminar flow where the Reynolds number is less than 1. Reynolds number which is defined as Equation (2.6) is maximum at the soil surface of the well (sand face) where the water enters the aquifer and the Darcy velocity is maximum. The Darcy velocity at the sand face of well is

$$V = \frac{Q}{2r_w \pi b} . \quad (A.1)$$

Thus the following inequality is established in order to insure the total flow field in the laminar region.

$$\frac{Q \rho_w d}{2\pi r_w b \mu} < 1 \quad (A.2)$$

Therefore, the maximum flow rate, $Q_{\max,L}$, which insures the laminar flow field is

$$Q_{\max,L} = \frac{2\pi r_w b \mu}{\rho_w d} . \quad (A.3)$$

The value of average grain diameter d ranges from 0.3×10^{-4} to

2×10^{-4} m [7]. For a well radius of 0.15 m with 100 m thick aquifer at 450 K, $Q_{\max,L}$ is $0.075 \text{ m}^3/\text{sec}$ for $d = 2 \times 10^{-4}$ m.

It is noted that even if the flow rate exceeds that value, the deviation from laminar flow occurs only at the place very close to the sand face of well because the Darcy velocity is inversely proportional to the distance from the center of the well bore.

B. Hydraulic Fracturing

The water in the aquifer is at hydrostatic pressure (about 9 kPa/m of depth) which is substantially lower than the overburden compressive stress (about 23 kPa/m of depth). Hydraulic fracturing occurs when the water pressure exceeds a certain value. Such a breakdown pressure level is in the range of 0.6 to 1 times the overburden compressive stress. Maximum pressure occurs near the injection well, where the total pressure is the sum of hydrostatic pressure and the excess injection pressure. Taking the lower value of breakdown pressure level (0.6 times overburden compressive stress), the following inequality can be established in order to insure no fracturing.

$$\rho_w g H + \frac{1}{2} \frac{\mu Q}{k \pi b} \ln \frac{D}{r_w} < 1.5 \rho_w g H \quad (\text{A.4})$$

Thus the maximum flow rate, $Q_{\max,F}$, which insures no fracturing is

$$Q_{\max,F} = \frac{\rho_w g H k \pi b}{\mu \ln(D/r_w)} \quad (\text{A.5})$$

For $k = 200 \text{ mD}$, $b = 100 \text{ m}$, $D = 300 \text{ m}$, $r_w = 0.15 \text{ m}$ and $\mu = 9.4 \times 10^{-4} \text{ kg/m sec}$

(evaluated at 300 K), $Q_{\max,F} = 0.0804 \text{ m}^3/\text{sec}$ for $H = 1000 \text{ m}$ and $Q_{\max,F} = 0.1608 \text{ m}^3/\text{sec}$ for $H = 2000 \text{ m}$. $Q_{\max,F}$ can be increased about 3 times those values if μ is evaluated at 360 K. From this sample calculation, it is seen that the possibilities of fracturing are very small for the deep aquifer.

These considerations were done only near the well bore. It must be noted that these influences decrease very rapidly as the point of interest is moved from the well bore into the aquifer.

APPENDIX II

NOMENCLATURE

A	Area
A_c	Cross sectional area
a	Half distance of well separation
b	Thickness of aquifer
C	Specific heat
COPH	Coefficient of performance in heating
D	Well separation
d	Average diameter of the grain
ffs	Fossil fuel savings
H	Depth of aquifer
h	Hydraulic head
i	Unit of imaginary number
K	Hydraulic conductivity
k	Intrinsic permeability
k_{eq}	Equivalent intrinsic permeability
K_R	Thermal conductivity
L_H	Heating load
l	Length
m	Binary fluid flow rate per unit mass flow of geothermal fluid
m_c	Flow rate of cooling water per unit mass flow of geothermal fluid
N_R	Reynolds number

p	Pressure
Q	Volume flow rate of geothermal fluid
q	Volume flow rate of geothermal fluid within the stream channel
R	Aquifer resistance
r_e	Flow dimension
S	Flow channel area
S_{max}	Maximum flow channel area
S_s	Specific storage
T	Temperature
T_E	Environment temperature
T_i	Injection temperature
T_o	Resource temperature
T_w	Production temperature
T_{wD}	Non-dimensional production temperature
\hat{T}	Temperature(decreasing injection temperature case)
ΔT_p	Pinch point temperature
ΔT_{app}	Approach temperature
t	Time
t_D	Non-dimensional time
t_L	Project life time
V	Velocity
v_c	Specific volume of binary fluid at the exit of condenser
W	Work
$W(z)$	Complex potential
w	Work per unit mass flow of geothermal fluid

x	x coordinate
y	y coordinate
z	z coordinate or complex variable

Greek

α	Vertical compressibility of the granular skeleton
β	Coefficient of thermal expansion of geothermal fluid
$\hat{\beta}$	Compressibility of the fluid
ψ	Stream function
Φ	Velocity potential
ϕ	Porosity
ε	Effectiveness
ε_r	Effectiveness ratio
λ	Non-dimensional coefficient, $\rho_w C_w \rho_A C_A Q b / \rho_R C_R K_R D^2$
η	Efficiency
μ	Viscosity
ρ	Density
θ	Angle
σ_z	Vertical stress

Subscripts

A	Aquifer
aq	Aquifer
app	Approach
av	Average
B	Boiler

by	Buoyancy
C	Condenser(power system)
CC	Carnot cycle
cirp	Circulation pump
comp	Compressor
con	Condenser(heat pump)
cool	Cooling
ctf	Cooling tower fan
cw	Cooling water
D	Non-dimension
E	Environment
fg	Saturated liquid and saturated vapor
fp	Feed pump
G	Generator
gp	Geothermal fluid pump
HE	Heat exchanger
hp	Heat pump
I	Initial
i	Injection
j	Stream channel number
L	Loss
o	Resource
p	Pinch point
pp	Power plant
R	Cap rock or bed rock

r	Rock in the aquifer
s	System or isentropic process
T	Turbine
tot	Total
W	Well
w	Geothermal fluid
x	x axis component
y	y axis component
z	z axis component

APPENDIX III

LIST OF COMPUTER PROGRAM AND SAMPLE OUTPUT

A.1 Constant Flow Model(Power Generation)

```

PROGRAM POWRCF(INPUT,OUTPUT)
C*****THIS PROGRAM SIMULATES GEOTHERMAL POWER GENERATION AND SHOWS
C*****THERMODYNAMIC PERFORMANCES AS A FUNCTION OF INJECTION
C*****TEMPERATURE. PERFORMANCE PARAMETERS ARE EFFECTIVENESS AND
C*****FOSSIL FUEL SAVING.
REAL H1P,H1LW,N1LEST
DIMENSION X(50),Y(50)
COMMON R(50,100),RN(50,100),HLAQ(100),HLGP(100),CPW(100),XKO,
AXKI,RO,Q,TLY,DEPAQ,RW,PERM,HAQ,DTHETA,NTHETA,N1LY,PI,GAMAW
A,D,HLS
C*****INPUT DATA
READ*,PORSTY,RDNCW,RORCR,GAMAW,ROW,CPW,DEPAQ,HAQ
READ*,PERM
READ*,RW
READ*,TLY,DT,EFFDP,EFFI,EFFG,EFFGP,HLS,EPLANT
READ*,TENV
C*****PRINT OUT BASIC DATA
WRITE(*,699)
WRITE(*,700)
WRITE(*,701)PORSTY
WRITE(*,702)PERM
WRITE(*,703)HAQ
WRITE(*,811)DEPAQ
WRITE(*,704)RDNCW
WRITE(*,705)RORCR
WRITE(*,707)RW
WRITE(*,708)TLY
WRITE(*,709)EFFDP
WRITE(*,820)HLS
WRITE(*,710)
WRITE(*,711)
WRITE(*,712)
WRITE(*,713)DT
WRITE(*,903)EFFGP
WRITE(*,714)EFFI
WRITE(*,715)EFFG
WRITE(*,716)TENV
WRITE(*,718)EPLANT
WRITE(*,750)
C*****REQUIRED FLOW RATE
183 J=500.
IF(D.GT.1200.) THEN
  GO TO 113
ENDIF
TLS=TLY*365.*24.*3600.
RDACA=PORSTY*RDNCW*(1.-PORSTY)*RORCR
PI=4.*ATAN(1.)
Q=(RDACA*D*HAQ/(RDNCW*TLS))*PI/3.
C*****ESTABLISHMENT OF AQUIFER RESISTANCES AT SPECIFIED TEMPERATURES
C*****BY GENERATING FLOW FIELD
NTHETA=10
TD=423.
TI=340.
DIST=0./100.
XKO=GAMAW*PERM*(0.987E-15)/VISCOS(TD)
XKI=GAMAW*PERM*(0.987E-15)/VISCOS(TI)
A=0/2.
DTHETA=PI/NTHETA
THETA=DTHETA/2.
N1LY=FIX(TLY)
QAPIH=(Q*A/(PI*HAQ))*RDNCW/RDACA
DO 51 I=1,NTHETA
  VDS=0.
  X(I)=0/2.-RW*COS(THETA)
  Y(I)=RW*SIN(THETA)
  THETA=THETA+DTHETA
  XTH=X(I)
  YTH=Y(I)
  RO=2.*ALOG(D/RW)/(XKO*HAQ*DTHETA)
  NCOUNT=1
  TIMEY=0.
  R1=RO
  TY1=0.
40 VXTH=VX(XTH,TH,A)*QAPIH
  VYTH=VY(XTH,TH,A)*QAPIH

```

```

VTH=SQRT(VXT1**2+VYTH**2)
L1=SQRT((XTH+A)**2+YTH**2)
IF(L1.LT.DIST*3.14E4
DTS=DIST/(VT1*10.)
ELSE
DTS=DIST/VTH
ENDIF
DTY=DTS/31536000.
XTHM=XTH+VXT1*DTS/2.
YTHM=YTH+VYTH*DTS/2.
VXTHM=VX(XTHM,YTHM,A)*Q4*IH
VYTHM=VY(XTHM,YTHM,A)*Q4*IH
VTHM=SQRT(VXTHM**2+VYTHM**2)
XTHF=XTH+VXT1*M*DTS
YTHF=YTH+VYTH*M*DTS
XTHM=XTH+VXT1*M*DTS/2.
YTHM=YTH+VYTH*M*DTS/2.
XTH=XTHF
YTH=YTHF
VXM=VX(XTHM,YTHM,A)*(Q4/(PI*HAQ*PORSTY))
VYM=VY(XTHM,YTHM,A)*(Q4/(PI*HAQ*PORSTY))
VM=SQRT(VXM**2+VYM**2)
DS=VTHM*DTS
VDS=VDS+VM*DS
TIMEY=TIMEY+DTY
RESIST=RO*2.*PI*PORSTY*(1.-XKI/XKO)*VDS/(Q*DTHEF1*XKI)
NY=IFIX(TIMEY)
IF(NY.GE.NCOUNT)THEN
DO 52 K=NCOUNT,NY
R(I,K)=R1+(RESIST-R1)*(FLOAT(K)-TY1)/(TIMEY-TY1)
CONTINUE
R1=RESIST
TY1=TIMEY
NCOUNT=NY+1
ENDIF
IF(TIMEY.GT.FL1)THEN
GO TO 51
ENDIF
L=SQRT((XTH+A)**2+YTH**2)
IF(L.LT.DIST*3.14E4)THEN
DO 53 KK=NCOUNT,NTRY
R(I,KK)=RO*XKO/XKI
CONTINUE
ELSE
GO TO 40
ENDIF
51 CONTINUE
C*****POWER GENERATION
WRITE(*,821)Q
WRITE(*,822)Q
WRITE(*,201)
WRITE(*,202)
WRITE(*,203)
TO=400.
14 AAQ=(PI*O*O*234CA*HAQ/3.)*(TO-TENV-TENV*ALOG(TO/TENV))
WRITE(*,988)T3
TI=338.
C*****BOILER TEMPERATURE FINDER
12 TB=310.5
HFGIP=((462.-T3)*100000./1.7998)**0.3646)*1000.
CPA VIP=(0.00045*((T3-310.)**1.4175)+2.345)*1000.
DIFF=(TO-TB-DTP)/HFGIP-(TB-DTP-TI)/(CPA VIP*(TB-310.))
DIFF1=DIFF
TB1=TB
TB=311.
11 IF(TB.GT.TO)THEN
GO TO 13
ENDIF
HFGIP=((462.-T3)*100000./1.7998)**0.3646)*1000.
CPA VIP=(0.00045*((T3-310.)**1.4175)+2.345)*1000.
DIFF=(TO-TB-DTP)/HFGIP-(TB-DTP-TI)/(CPA VIP*(TB-310.))
IF 40 DIFF.LT.0.1 THEN
TB=TB1+ABS(DIFF1)/(ABS(DIFF1)+ABS(DIFF))
ELSE
TB1=TB
DIFF1=DIFF
TB=TB+2.

```

```

GO TO 11
ENDIF
C***** CROSS POWER JET AND LOSSES
CPA VIP = (0.00045 * ((TB-310.) ** 1.4175) + 2.3+5) * 1000.
MFGIP = (((1+62-T3) * 100000 / (1-7998) ** 0.36+6) * 1000.
MIP = (TO-TI) * CPW / (CPA VIP * (TB-310.) + MFGIP)
PBPCIP = 0.1745 * ((TB-310.) ** 1.9519) * 1000.
WFDP = (MIP * 0.3016547 * PBPCIP / EFFDPI * ROW * 3
H12SIP = (0.8164 * (TB-310.) - 0.000187 * (((TB-382.75) ** 2) ** 1.2838)
+ 11.25) * 1000.
SELECT = MIP * H12SIP * EFFI * EFFG * ROW * Q
MCLM = ((WFDP / (ROW * Q)) + CPW * (TO-TI) - MIP * H12SIP * EFFI) / (4180. * 8.33)
MCIRP = 82.7 * MCLM * ROW * 3
MCLTF = 155.4 * MCLM * ROW * Q
CALL GFPM(TO,TI,GPWAV)
NELECT = SELECT * FDFP - MCIRP - MCLTF - GPWAV
AOUT = NELECT * 3.6 * 1000
EPOWER = AOUT / 440
FFSP = NELECT / EPLANT
WRITE(*,204) TI, NELECT, EPOWER, FFSP, GPWAV
C***** ASSIGNING DIFFERENT INJECTION TEMPERATURE
TI = TI + 2.
IF (TI .LE. 370.) THEN
GO TO 12
ENDIF
C***** ASSIGNING DIFFERENT PRODUCTION TEMPERATURE
IS
TO = TO + 10.
IF (TO .LE. 470.) THEN
GO TO 14
ENDIF
C***** ASSIGNING DIFFERENT WELL SEPARATION
D = D + 200.
GO TO 183
599 FORMAT(11, #3 BASIC DATA)
700 FORMAT(20, #20 IFR)
701 FORMAT(20, #20 JRSITY OF AQUIFER, 26X, F12.2)
702 FORMAT(20, #20 INTRINSIC PERMEABILITY, 23X, F12.2, #40)
703 FORMAT(20, #20 THICKNESS OF AQUIFER, 25X, F12.2, #40)
811 FORMAT(20, #20 DEPTH OF AQUIFER, 29X, F12.2, #40)
704 FORMAT(20, #20 HEAT CAPACITY OF WATER, 23X, F12.2, #40)
705 FORMAT(20, #20 HEAT CAPACITY OF ROCK, 24X, F12.2, #40)
707 FORMAT(20, #20 RADIUS OF WELL, 31X, F12.2, #40)
708 FORMAT(20, #20 SYSTEM LIFE TIME, 29X, F12.2, #40)
709 FORMAT(20, #20 EFFICIENCY OF GEOTHERMAL FLUID PUMP, 10X, F12.2)
710 FORMAT(20, #20 POWER GENERATION)
711 FORMAT(20, #20 ISO-PENTANE BINARY CYCLE (SATURATED RANKINE CYCLE) #)
712 FORMAT(20, #20 CONDENSER TEMPERATURE, 29X, #310.00 (#)
713 FORMAT(20, #20 PINCH TEMPERATURE, 28X, F12.2, #40)
903 FORMAT(20, #20 EFFICIENCY OF FEED PUMP, 22X, F12.2)
714 FORMAT(20, #20 EFFICIENCY OF TURBINE, 24X, F12.2)
715 FORMAT(20, #20 EFFICIENCY OF GENERATOR, 22X, F12.2)
750 FORMAT(20, #20 POWER GENERATION)
716 FORMAT(20, #20 ENVIRONMENT TEMPERATURE, 22X, F12.2, #40)
821 FORMAT(20, #20 WELL SEPARATION, #, F8.2, #40)
822 FORMAT(20, #20 FLOW RATE, #, F8.4, #40)
823 FORMAT(20, #20 SURFACE HEAD LOSS OF GEOTHERMAL FLUID, #, 8X, F12.2, #40)
728 FORMAT(20, #20 AVERAGE EFFECTIVENESS OF FOSSIL FUEL POWER PLANT, #,
AF9.2)
201 FORMAT(20, #20 PRODUCTION, 5X, # INJECTION, 5X, # ELECTRICITY, 5X, # EFFECT
IVENESS, 5X, # FOSSIL FUEL, 5X, # GEOTHERMAL PUMP)
202 FORMAT(20, #20 IE4, 18X, # TEMP, 12X, # NET, 29X, # SAVING, 8X,
A # WORK, AVERAGE)
203 FORMAT(20, #20 (K), 12X, # (K), 18X, # (J/SEC), 27X, # (J/SEC), 11X,
A # (J/SEC) #)
204 FORMAT(20, #20, 14X, #8.2, 7X, E11.4, 6X, #8.4, 9X, E11.4, 7X, E11.4)
908 FORMAT(20, #20, F8.2)
113 STOP
END

```

```

C*****DEFINITION OF SUBROUTINE GFPM
SUBROUTINE GFPM(TO,PI,GPWAV)
COMMON R(50,100),RN(50,100),HLAQ(100),HLGP(100),GPM(100),XKD,XKT,
ARO,Q,TLY,EFFGP,DEPAQ,RN,PERM,HAQ,OTHEA,NTHETA,NFLY,PI,GAMAW
A,D,HL
XKON=GAMAW*PERM*(0.987E-15)/VISCOS(TO)
XKIN=GAMAW*PERM*(0.987E-15)/VISCOS(TI)
RON=2.*ALOG(D/R1)/(XKON*HAQ*OTHEA)

DO 101 I=1,NTHETA
DO 102 J=1,NFLY
RN(I,J)=(1./XKIN-1./XKON)*(R(I,J)-RO)/(1./XKI-1./XKO+RON)
102 CONTINUE
101 CONTINUE
C*****HEAD LOSS IN THE AQUIFER
HLAQ=Q*ALOG(D/R1)/(XKON*HAQ*PI)
DO 103 J=1,NFLY
RTOTIN=0.
DO 104 I=1,NTHETA
RTOTIN=RTOTIN+1./RN(I,J)
104 CONTINUE
RTOT=1./(RTOTIN*2.)
HLAQ(J)=RTOT*Q
103 CONTINUE
C*****HEAD LOSS IN THE WELLS, HEAD LOSS IN THE SURFACE SYSTEMS AND
C*****HEAD GAIN DUE TO BUOYANCY EFFECT
HLWELL=0.05*Q*Q/Q/(4.*9.81*PI*PI*(RW**5))
HGB=((0.06*2*(TO+TI)/2.-16.82/10000.)*(TO-TI)*DEPAQ
DO 105 J=1,NFLY
HLGP(J)=HLAQ(J)+HLWELL+HLS-HGB
IF (HLGP(J).LT.0.) THEN
HLGP(J)=0.
ENDIF
105 CONTINUE
HLGPO=HLAQ+HLWELL+HLS-HGB
IF (HLGPO.LT.0.) THEN
HLGPO=0.
ENDIF
GPMIN=GAMAW*2*HLGPO/EFFGP
DO 106 J=1,NFLY
GPM(J)=GAMAW*2*HLGP(J)/EFFGP
106 CONTINUE
GPMAX=GPM(NFLY)
C*****CALCULATION OF TOTAL GEOTHERMAL FLUID PUMP WORK BY TRAPEZOIDAL
C*****RULE
GPWTOT=0.
NFI=NFLY-1
DO 107 J=1,NFI
GPWTOT=GPWTOT+GPM(J)
107 CONTINUE
GPWTOT=GPWTOT*31536000.+(GPMIN+GPMAX)*31536000./2.
GPMAX=GPWTOT/(NFI*31536000.)
RETURN
END

C*****DEFINITION OF FUNCTION VISCOS
FUNCTION VISCOS(T)
VISCOS=SQRT((T-281.585)**2+8078.4)
VISCOS=((VISCOS+T-281.585)*2.1482-120.)*18.
VISCOS=1./VISCOS
RETURN
END

C*****DEFINITION OF FUNCTION VX
FUNCTION VX(X,Y,A)
VX=(X**2-Y**2-A**2)/(X**2-Y**2-A**2+4.*(X**2)*(Y**2))
RETURN
END

C*****DEFINITION OF FUNCTION VY
FUNCTION VY(X,Y,A)
VY=2.*X*Y/(X**2-Y**2-A**2+4.*(X**2)*(Y**2))
RETURN
END

```

A.2 Sample Computer Output of Constant Flow Model(Power Generation)

BASIC DATA	
AQUIFER	
POROSITY OF AQUIFER	.20
INTRINSIC PERMEABILITY	100.00 MD
THICKNESS OF AQUIFER	100.00 M
DEPTH OF AQUIFER	2000.00 M
HEAT CAPACITY OF WATER	4000000.00 J/M**3 K
HEAT CAPACITY OF ROCK	2000000.00 J/M**3 K
RADIUS OF WELL	.15 M
SYSTEM LIFE TIME	25.00 YEARS
EFFICIENCY OF GEOTHERMAL FLUID PUMP	.75
SURFACE HEAD LOSS OF GEOTHERMAL FLUID	15.00 M
POWER GENERATION	
ISO-PENTANE BINARY CYCLE(SATURATED RANKINE CYCLE)	
CONDENSER TEMPERATURE	310.00 K
PINCH TEMPERATURE	8.33 K
EFFICIENCY OF FEED PUMP	.68
EFFICIENCY OF TURBINE	.80
EFFICIENCY OF GENERATOR	.90
ENVIRONMENT TEMPERATURE	289.00 K
AVERAGE EFFECTIVENESS OF FOSSIL FUEL POWER PLANT	.30

POWER GENERATION

WELL SEPARATION 500.00 M

FLOW RATE .0199 M**3/SEC

PRODUCTION TEMP (K)	INJECTION TEMP (K)	ELECTRICITY NET (J/SEC)	EFFECTIVENESS	FOSSIL FUEL SAVING (J/SEC)	GEO THERMAL PUMP WORK, AVERAGE (J/SEC)
400.00	330.00	.1930E+06	.1425	.6461E+06	.2659E+05
	332.00	.2110E+06	.1550	.7061E+06	.2617E+05
	334.00	.2266E+06	.1666	.7554E+06	.2581E+05
	336.00	.2471E+06	.1817	.8236E+06	.2551E+05
	338.00	.2563E+06	.1884	.8542E+06	.2526E+05
	340.00	.2632E+06	.1936	.8774E+06	.2506E+05
	342.00	.2682E+06	.1972	.8941E+06	.2490E+05
	344.00	.2775E+06	.2041	.9250E+06	.2479E+05
	346.00	.2786E+06	.2049	.9288E+06	.2473E+05
	348.00	.2783E+06	.2046	.9275E+06	.2470E+05
	350.00	.2765E+06	.2033	.9216E+06	.2471E+05
	352.00	.2734E+06	.2011	.9115E+06	.2476E+05
	354.00	.2692E+06	.1979	.8973E+06	.2485E+05
	356.00	.2630E+06	.1940	.8794E+06	.2497E+05
	358.00	.2530E+06	.1866	.8461E+06	.2513E+05
	360.00	.2467E+06	.1814	.8225E+06	.2532E+05
	362.00	.2387E+06	.1756	.7958E+06	.2554E+05
	364.00	.2299E+06	.1690	.7662E+06	.2579E+05
	366.00	.2202E+06	.1619	.7339E+06	.2607E+05
	368.00	.2073E+06	.1524	.6910E+06	.2638E+05
	370.00	.1964E+06	.1444	.6545E+06	.2672E+05
410.00	330.00	.2581E+06	.1625	.8605E+06	.2041E+05
	332.00	.2893E+06	.1821	.9642E+06	.2000E+05
	334.00	.3061E+06	.1927	.1020E+07	.1964E+05
	336.00	.3190E+06	.2014	.1066E+07	.1934E+05
	338.00	.3392E+06	.2136	.1131E+07	.1909E+05
	340.00	.3474E+06	.2188	.1150E+07	.1889E+05
	342.00	.3534E+06	.2229	.1170E+07	.1873E+05
	344.00	.3575E+06	.2251	.1192E+07	.1862E+05
	346.00	.3662E+06	.2306	.1221E+07	.1855E+05
	348.00	.3665E+06	.2308	.1222E+07	.1853E+05
	350.00	.3654E+06	.2301	.1210E+07	.1854E+05
	352.00	.3630E+06	.2286	.1210E+07	.1859E+05

B.1 Constant Flow Model(Heating)

```

PROGRAM HEATF(INPUT,OUTPUT)
C*****THIS PROGRAM CALCULATES THE HEATING PERFORMANCES OF GEOTHERMAL
C*****DIRECT HEATING, COMBINATION OF DIRECT HEATING AND HEAT PUMP
C*****AND HEAT PUMP ONLY CASES AT A SPECIFIED LOAD AS A FUNCTION
C*****OF INJECTION TEMPERATURE. PERFORMANCE PARAMETERS ARE
C*****EFFECTIVENESS AND FOSSIL FUEL SAVING.
REAL LOAD1,LOAD
COMMON X(50),Y(50),R(50,100),HLAQ(100),HLGP(100),GPM(100),Q,TLY,
ATLS,EFFSP,DEPAQ,RM,PERM,HAQ,PI,GAMAH,D,HLS,RDWH,RDACA,PORSTY
C*****INPUT DATA
READ*,PORSTY,RDWH,RORCR,GAMAH,DEPAQ,HAQ
READ*,PERM
READ*,RM,TLY
READ*,DTA,DTH,EFFSP,EFFDWP,EPLANT,HLBH,HLS
READ*,TENV,TSPACE,TCONH,TOUTDH
READ*,EFFB
C*****WRITE BASIC DATA
WRITE(*,699)
WRITE(*,700)
WRITE(*,701)PORSTY
WRITE(*,702)PERM
WRITE(*,703)HAQ
WRITE(*,704)DEPAQ
WRITE(*,705)RDWH
WRITE(*,706)RORCR
WRITE(*,707)RM
WRITE(*,708)TLY
WRITE(*,709)EFFSP
WRITE(*,710)HLS
WRITE(*,711)
WRITE(*,712)DTH
WRITE(*,713)EFFDWP
WRITE(*,714)HLBH
WRITE(*,715)TOUTDH
WRITE(*,716)DTA
WRITE(*,717)TCONH
WRITE(*,718)EPLANT
WRITE(*,719)TENV
WRITE(*,720)TSPACE
WRITE(*,682)EFFB
PI=4.*ATAN(1)
ROACA=PORSTY*(RDWH+(1.-PORSTY)*RORCR)
TLS=TLY*365.*24.*3500.
C*****DECISION MAKING OF TEMPERATURE INCREASE AND HIGHEST TEMPERATURE
C*****FOR COMBINATION
IF(PERM.LT.30.)THEN
  DTDC=10.
  TOLC=380.
ELSE IF(PERM.LT.60.)THEN
  DTDC=10.
  TOLC=360.
ELSE IF(PERM.LT.110.)THEN
  DTDC=5.
  TOLC=340.
ELSE
  DTDC=3.
  TOLC=330.
ENDIF
C*****AQUIFER TEMPERATURE
TD=320.
385 IF(TD.GT.478.)THEN
  GO TO 306
ENDIF
WRITE(*,200)
WRITE(*,201)TD
WRITE(*,202)
WRITE(*,203)
WRITE(*,204)
C*****LOAD CONDITIONS DEPENDING ON AQUIFER TEMPERATURE
LOAD1=(TD-310.)*200000.
LOAD=LOAD1
503 IF(LOAD.GT.LOAD1*.1)THEN
  GO TO 304
ENDIF

```

```

C*****DIRECT HEATING
TI=TOUTDH+DTHE
C*****FLOW RATE, WELL SEPARATION AND AVAILABILITY OF AQUIFER FOR
C*****GIVEN CONDITIONS
Q=LOAD/(ROWCW*(TO-TI))
D=SQRT(ROWCW*2*TLS*3./((RDACA*HAQ*PI))
AAQ=(PI*D*D*RDACA*HAQ/3.)*(TO-TENV-TENV*ALOG(TO/TENV))
C*****PERFORMANCE CALCULATIONS
CALL GFPH(TO,TI,GPWAV)
DMPW=GAMAW*Q*MLDH/EFFDW
AQUT=LOAD*TLS*(1.-TENV/TSPACE)
AIN=AAQ+(GPWAV+DMPW)*TLS/EPLANT
E=AQUT/AIN
FFS=LOAD/EFFB-(GPWAV+DMPW)/EPLANT
WRITE(*,205)LOAD,TI,Q,D,E,FFS,GPWAV
IF(TO-TOLOLT)THEN
GO TO 382
ENDIF
C*****COMBINATION OF DIRECT HEATING AND HEAT PUMP
TI=306.
301 IF(TI.LT.280.)THEN
GO TO 302
ENDIF
C*****HEAT PUMP COPH
COPH=TCONHP/(2.*(TCONHP-TI+DTA))
IF(COPH.GT.7.)THEN
COPH=7.
ENDIF
C*****FLOW RATE, WELL SEPARATION AND AQUIFER AVAILABILITY FO GIVEN
C*****CONDITIONS
Q=LOAD/(ROWCW*(TO-TI)+ROWCW*(TOUTDH+DTHE-TI)/(COPH-1.))
D=SQRT(ROWCW*2*TLS*3./((RDACA*HAQ*PI))
AAQ=(PI*D*D*RDACA*HAQ/3.)*(TO-TENV-TENV*ALOG(TO/TENV))
C*****PERFORMANCE CALCULATIONS
CALL GFPH(TO,TI,GPWAV)
MCONP=ROWCW*2*(TOUTDH+DTHE-TI)/(COPH-1.)
LOADHP=ROWCW*2*(TOUTDH+DTHE-TI)+MCONP
WFAN=0.0421*LOADHP
DMPW=GAMAW*Q*MLDH/EFFDW
AQUT=LOAD*TLS*(1.-TENV/TSPACE)
AIN=AAQ+(GPWAV+DMPW+WFAN+MCONP)*TLS/EPLANT
E=AQUT/AIN
FFS=LOAD/EFFB-(GPWAV+DMPW+WFAN+MCONP)/EPLANT
WRITE(*,206)TI,Q,D,E,FFS,GPWAV
C*****ASSIGNING DIFFERENT INJECTION TEMPERATURE FOR HEAT PUMP
TI=TI-4.
GO TO 301
C*****ASSIGNING DIFFERENT LOAD
302 LOAD=LOAD+LOAD1
GO TO 303
C*****ASSIGNING DIFFERENT AQUIFER TEMPERATURE
304 IF(TO.LT.TOLC)THEN
TO=TO+DTDC
ELSE
TO=TO+20.
ENDIF
GO TO 305
C*****HEAT PUMP ONLY
306 WRITE(*,901)
C*****AQUIFER TEMPERATURE
TO=316.
311 IF(TO.LT.300.)THEN
GO TO 312
ENDIF
WRITE(*,201)Q
WRITE(*,202)
WRITE(*,203)
WRITE(*,204)
C*****SPECIFYING LOAD
LOAD1=1000000.
LOAD=LOAD1
309 IF(LOAD.GT.LOAD1*4.)THEN
GO TO 310
ENDIF
WRITE(*,902)LOAD
TI=TO-4.
307 IF(TI.LT.280.)THEN

```



```

GO TO 308
ENDIF
COPH=TCUNHP/(2.*(TCUNHP-TI+DTA))
IF(COPH.GT.7.) THEN
COPH=7.
ENDIF
C***** FLOW RATE, WELL SEPARATION AND AVAILABILITY OF AQUIFER FOR
C***** GIVEN CONDITIONS
Q=LOAD*(COPH-1.)/(ROKCH*(TO-TI)*COPH)
D=SQRT(ROKCH*Q*TLS*3.7/(ROACA*HAQ*PI))
HAQ=(PI*D*D*ROKCH*HAQ/3.7*(TO-TENV-TENV*ALOG(TO/TENV)))
C***** PERFORMANCE CALCULATIONS
CALL GEPW(TO,TI,GPAV)
WCOMP=ROKCH*2*(TO-TI)/(COPH-1.)
WFAN=0.8421*LOAD
AQUT=LOAD*TLS*(1.-TENV/TSPACE)
AIN=AAQ*(GPAV+WCOMP+WFAN)*TLS/EPLANT
E=AQUT/AIN
FFS=LOAD/EFFB-(GPAV+WCOMP+WFAN)/EPLANT
WRITE(2,206)TI,2,D,E,FFS,GPAV
C***** ASSIGNING DIFFERENT INJECTION TEMPERATURE
TI=TI-4.
GO TO 307
C***** ASSIGNING DIFFERENT LOAD
306 LOAD=LOAD+LOADI
GO TO 309
C***** ASSIGNING DIFFERENT AQUIFER TEMPERATURE
310 TO=TO-4.
GO TO 311
699 FORMAT(12,8BASIC DATA)
700 FORMAT(20,8AQUIFER)
701 FORMAT(20,8PERMEABILITY OF AQUIFER,26X,F12.2)
702 FORMAT(2,8INTRINSIC PERMEABILITY,23X,F12.2,840)
703 FORMAT(2,8THICKNESS OF AQUIFER,25X,F12.2,8M)
811 FORMAT(2,8DEPTH OF AQUIFER,29X,F12.2,8M)
704 FORMAT(2,8HEAT CAPACITY OF WATER,23X,F12.2,8J/M**3 K)
705 FORMAT(2,8HEAT CAPACITY OF ROCK,24X,F12.2,8J/M**3 K)
707 FORMAT(2,8RADIUS OF WELL,31X,F12.2,8M)
708 FORMAT(2,8SYSTEM LIFE TIME,29X,F12.2,8YEARS)
709 FORMAT(2,8EFFICIENCY OF GEOTHERMAL FLUID PUMP,18X,F12.2)
710 FORMAT(2,8SURFACE HEAD LOSS OF GEOTHERMAL FLUID,8X,F12.2,8M)
717 FORMAT(28,8HEATING)
718 FORMAT(28,8TEMPERATURE DIFFERENCE IN THE HEAT EXCHANGER,6X,
AF7.2,8K)
719 FORMAT(2,8EFFICIENCY OF DOMESTIC WATER PUMP,18X,F7.2)
720 FORMAT(2,8HEAD LOSS OF DOMESTIC WATER,23X,F7.2,8M)
812 FORMAT(2,8OUTLET TEMPERATURE OF DOMESTIC WATER,9X,F12.2,8K)
723 FORMAT(20,8HEAT PUMP)
724 FORMAT(20,8ROACH TEMPERATURE,30X,F7.2,8K)
725 FORMAT(2,8CONDENSER TEMPERATURE,29X,F7.2,8K)
728 FORMAT(28,8AVERAGE EFFECTIVENESS OF FOSSIL FUEL POWER PLANT,
AF9.2)
722 FORMAT(2,8ENVIRONMENT TEMPERATURE,27X,F7.2,8K)
721 FORMAT(2,8SPACE TEMPERATURE,33X,F7.2,8K)
200 FORMAT(12,8DIRECT HEATING AND COMBINATION OF DIRECT HEATING AND
AHEAT PUMP)
201 FORMAT(20,8PRODUCTION TEMPERATURE,8F8.2,8K)
202 FORMAT(20,8HEATING LOAD,4X,8INJECTION,4X,8FLOW RATE,7X,8WELL,
8FX,8EFFECTIVENESS,8X,8FOSSIL FUEL,8X,8GEOTHERMAL PUMP)
203 FORMAT(2,818X,8TEMP,28X,8SEPARATION,23X,8SAVING,8X,
8WORK,8AVERAGE)
204 FORMAT(2,8(J/SEC),10X,8(K),7X,8(M**3/SEC),6X,8(M),27X,8(J/
ASEC),11X,8(J/SEC))
205 FORMAT(2,8E11,4X,8F8.2,6X,8F8.4,6X,8F8.2,6X,8F8.4,7X,8E11.4,7X,
8E11.4,8**0M)
206 FORMAT(2,815X,8F8.2,6X,8F8.4,6X,8F8.2,6X,8F8.4,7X,8E11.4,7X,8E11.4)
901 FORMAT(22,8HEAT PUMP JNCT)
902 FORMAT(2,8E11.4)
682 FORMAT(2,8EFFICIENCY OF FOSSIL FUEL BOILER FOR HEATING,8F12.2)
312 STOP
END

```

```

C***** DEFINITION OF SUBROUTINE GPPW
SUBROUTINE GPPW(IJ,IT,3*HAY)
COMMON X(50),Y(50),R(50,100),HLAQ(100),HIGP(100),GPW(100),Q,TLY,
ATLS,EFFGP,DEPAQ,RW,PERM,HAQ,PI,GAMAW,D,HLS,ROMCA,ROACA,PORSTY
NTHTA=18
C***** ESTABLISHMENT OF AQUIFER RESISTANCES AT SPECIFIED TEMPERATURES
C***** BY GENERATING FLOW FIELD
DIST=D/18.
XKO=GAMAW*PERM*(1.987E-15)/VISCOS(TO)
XKI=GAMAW*PERM*(0.987E-15)/VISCOS(TI)
A=D/2.
DTHTA=PI/NTHTA
THETA=DTHTA/2.
NTLY=IFIX(TLY)
QAPIH=(Q*A/(PI*HAQ))*ROMCH/ROACA
DO 51 I=1,NTHTA
VDS=0.
X(I)=D/2.-RW*COS(THETA)
Y(I)=RW*SIN(THETA)
THETA=THETA+DTHTA
XTH=X(I)
YTH=Y(I)
RO=2.*ALOG(D/RW)/(XKO*HAQ*DTHTA)
NCOUNT=1
TIMEY=0.
R1=RO
TY1=0.
40 VXTH=VX(XTH,YTH,A)*QAPIH
VYTH=VY(XTH,YTH,A)*QAPIH
VTH=SQRT(VXTH**2+VYTH**2)
L1=SQRT((XTH+A)**2+YTH**2)
IF(L1.LT.DIST*3.) THEN
DTS=DIST/(VTH*10.)
ELSE
DTS=DIST/VTH
ENDIF
DTY=DTS/31536000.
XTHM=XTH+VXTH*DTS/2.
YTHM=YTH+VYTH*DTS/2.
VXTHM=VX(XTHM,YTHM,A)*QAPIH
VYTHM=VY(XTHM,YTHM,A)*QAPIH
VTHM=SQRT(VXTHM**2+VYTHM**2)
XTHF=XTH+VXTHM*DTS
YTHF=YTH+VYTHM*DTS
XTHM=XTH+VXTHM*DTS/2.
YTHM=YTH+VYTHM*DTS/2.
XTH=XTHF
YTH=YTHF
VXM=VX(XTHM,YTHM,A)*(1.-XKI/XKO)
VYM=VY(XTHM,YTHM,A)*(1.-XKI/XKO)
VM=SQRT(VXM**2+VYM**2)
DS=VTHM*DTS
VDS=VDS+VM*DS
TIMEY=TIMEY+DTY
RESIST=RO+2.*PI*PORSTY*(1.-XKI/XKO)*VDS/(Q*DTHTA*XKI)
NY=IFIX(TIMEY)
IF(NY.GE.NCOUNT) THEN
DO 52 K=NCOUNT,NY
R(I,K)=R1+(RESIST-R1)*(FLOAT(K)-TY1)/(TIMEY-TY1)
52 CONTINUE
R1=RESIST
TY1=TIMEY
NCOUNT=NY+1
ENDIF
IF(TIMEY.GT.TLY) THEN
GO TO 51
ENDIF
L=SQRT((XTH+A)**2+YTH**2)
IF(L.LT.DIST*0.2) THEN
DO 53 KK=NCOUNT,NTLY
R(I,KK)=RO*XKO/XKI
53 CONTINUE
ELSE
GO TO 40
ENDIF

```

```

51 CONTINUE
C***** HEAD LOSS IN THE AQUIFER
HLAQ=Q*ALOG(I/RW)/(XK0*HAQ*PI)
DO 103 J=1,NTRY
  RTOTIN=0
  DO 104 I=1,NTHETA
    RTOTIN=RTOTIN+1./R(I,J)
  104 CONTINUE
  RTOT=1./(RTOTIN*2.)
  HLAQ(J)=RTOT*Q
103 CONTINUE
C***** HEAD LOSS IN THE WELLS, HEAD LOSS IN THE SURFACE SYSTEMS AND
C***** HEAD GAIN DUE TO BOUYANCY EFFECT
HLWELL=0.85*DEPAQ*Q*Q/(4.*9.81*PI*PI*(RW**5))
HGB=((0.0642*(T0+TI)/2.-16.82)/10000.)*(T0-TI)*DEPAQ
DO 105 J=1,NTRY
  HLGP(J)=HLAQ(J)+HLWELL+4LS-HGB
  IF(HLGP(J).LT.0.) THEN
    HLGP(J)=0.
  ENDIF
105 CONTINUE
HLGPD=HLAQ+HLWELL+4LS-HGB
IF(HLGPD.LT.0.) THEN
  HLGPD=0.
ENDIF
GPMIN=GAMAW*Q*HLGPD/EFFGP
DO 106 J=1,NTRY
  GPW(J)=GAMAW*Q*HLGP(J)/EFFGP
106 CONTINUE
GPMAX=GPW(NTRY)
C***** CALCULATION OF TOTAL GEOTHERMAL FLUID PUMP WORK BY TRAPEZOIDAL
C***** RULE
GPWTOT=0.
NTR=NTRY-1
DO 107 J=1,NTR
  GPWTOT=GPWTOT+GPW(J)
107 CONTINUE
GPWTOT=GPWTOT*31536000.+(GPMIN+GPMAX)*31536000./2.
GPMWV=GPWTOT/(NTRY*31536000.)
RETURN
END

C***** DEFINITION OF FUNCTION VISCOS
FUNCTION VISCOS(T)
VISCOS=SQRT((T-281.585)**2+8078.4)
VISCOS=((VISCOS+T-281.585)*2.1482-120.)*10.
VISCOS=1./VISCOS
RETURN
END

C***** DEFINITION OF FUNCTION VX
FUNCTION VX(X,Y,A)
VX=(X**2-Y**2-A**2)/((X**2+Y**2-A**2)**2+4.)*(X**2)*(Y**2)
RETURN
END

C***** DEFINITION OF FUNCTION VY
FUNCTION VY(X,Y,A)
VY=2.*X*Y/((X**2+Y**2-A**2)**2+4.)*(X**2)*(Y**2)
RETURN
END

```

B.2 Sample Computer Output of Constant Flow Model(Heating)

BASIC DATA

AQUIFER

POROSITY OF AQUIFER	.20
INTRINSIC PERMEABILITY	100.00 MD
THICKNESS OF AQUIFER	100.00 M
DEPTH OF AQUIFER	2000.00 M
HEAT CAPACITY OF WATER	4000000.00 J/M**3 K
HEAT CAPACITY OF ROCK	2000000.00 J/M**3 K
RADIUS OF WELL	.15 M
SYSTEM LIFE TIME	25.00 YEARS
EFFICIENCY OF GEOTHERMAL FLUID PUMP	.75
SURFACE HEAD LOSS OF GEOTHERMAL FLUID	15.00 M

HEATING

TEMPERATURE DIFFERENCE IN THE HEAT EXCHANGER	0.33 K
EFFICIENCY OF DOMESTIC WATER PUMP	.80
HEAD LOSS OF DOMESTIC WATER	20.00 M
OUTLET TEMPERATURE OF DOMESTIC WATER	303.15 K

HEAT PUMP

APPROACH TEMPERATURE	0.33 K
CONDENSER TEMPERATURE	322.22 K
AVERAGE EFFECTIVENESS OF FOSSIL FUEL POWER PLANT	.30
ENVIRONMENT TEMPERATURE	270.00 K
SPACE TEMPERATURE	295.00 K
EFFICIENCY OF FOSSIL FUEL BOILER FOR HEATING	.75

DIRECT HEATING AND COMBINATION OF DIRECT HEATING AND HEAT PUMP

PRODUCTION TEMPERATURE 320.00 K

HEATING LOAD (J/SEC)	INJECTION TEMP (K)	FLOW RATE (M**3/SEC)	WELL SEPARATION (M)	EFFECTIVENESS	FOSSIL FUEL SAVING (J/SEC)	GEO THERMAL PUMP WORK, AVERAGE (J/SEC)
.2000E+07	311.40	.0507	850.12	.0458	-.0039E+05	.0097E+06 ***DH
	306.00	.0334	647.05	.0839	.1196E+07	.2651E+06
	302.00	.0249	559.90	.0954	.1301E+07	.1913E+06
	298.00	.0197	496.87	.0972	.1247E+07	.9649E+05
	294.00	.0161	448.94	.0941	.1130E+07	.6632E+05
	290.00	.0134	418.54	.0890	.9050E+06	.4810E+05
	286.00	.0114	378.74	.0835	.8257E+06	.3638E+05
	282.00	.0099	351.72	.0781	.6587E+06	.2847E+05
.4000E+07	311.40	.1174	1213.97	.0294	-.0062E+07	.3398E+07 ***DH
	306.00	.0667	915.07	.0569	.4757E+06	.1105E+07
	302.00	.0499	791.29	.0738	.1512E+07	.6299E+05
	298.00	.0393	702.68	.0809	.1795E+07	.4028E+06
	294.00	.0321	634.89	.0838	.1777E+07	.2776E+06
	290.00	.0269	580.59	.0815	.1616E+07	.2024E+06

HEAT PUMP ONLY

PRODUCTION TEMPERATURE 316.00 K

HEATING LOAD (J/SEC)	INJECTION TEMP (K)	FLOW RATE (M**3/SEC)	WELL SEPARATION (M)	EFFECTIVENESS	FOSSIL FUEL SAVING (J/SEC)	GEO THERMAL PUMP WORK, AVERAGE (J/SEC)
.1000E+07	312.00	.0536	819.88	.0229	-.1607E+07	.6973E+06
	308.00	.0268	579.74	.0539	.1300E+06	.1736E+06
	304.00	.0174	467.26	.0717	.3965E+06	.7417E+05
	300.00	.0127	398.60	.0782	.4275E+06	.4084E+05
	296.00	.0098	351.01	.0788	.3960E+06	.2466E+05
	292.00	.0079	315.33	.0767	.3403E+06	.1653E+05
	288.00	.0066	287.13	.0735	.2735E+06	.1179E+05
	284.00	.0056	264.02	.0700	.2007E+06	.8744E+04
.2000E+07	312.00	.1071	1159.48	.0136	-.0265E+07	.2910E+07
	308.00	.0536	819.88	.0387	-.9634E+06	.7191E+06
	304.00	.0348	660.81	.0586	.2653E+06	.3066E+06
	300.00	.0253	563.71	.0691	.5693E+06	.1658E+06
	296.00	.0196	496.41	.0728	.6152E+06	.1023E+06
	292.00	.0158	445.94	.0728	.5613E+06	.6885E+05
	288.00	.0131	406.07	.0789	.4613E+06	.4921E+05
	284.00	.0111	373.88	.0682	.3370E+06	.3682E+05
	280.00	.0095	345.82	.0651	.1989E+06	.2868E+05

C.1 Increasing Flow Model(Power and Heating)

```

PROGRAM GEO(INPUT,OUTPUT)
C THIS PROGRAM SIMULATES THE OPERATIONS OF GEOTHERMAL ENERGY SYSTEMS
C WITH FORCED RECOVERY FROM AQUIFERS. WELL SEPARATION OF A DOUBLET
C IS LIMITED AND PRODUCTION MODEL IS AN INCREASING FLOW RATE MODEL
C WITH A CONSTANT INJECTION TEMPERATURE AFTER THERMAL BREAK-
C THROUGH. THE PERFORMANCES OF POWER GENERATION, HEATING AND
C HEAT PUMP ARE ALL CONSIDERED FOR A GIVEN AQUIFER TEMPERATURE AS
C FUNCTIONS OF INITIAL FLOW RATE AND INJECTION TEMPERATURE.
REAL MIP,MCLW,NELECT
COMMON X(50),Y(50),R(20,50),RN(20,50),HLAQ(50),IGD(50),
AHLWELL(50),HLGP(50),GPH(50),XKO,XKI,PO,QI,TLY,NTLY,EFFGP,DEPAQ,
ARM,PERM,HAQ,PI,GAMAH,D,HLS,GPMIN,GPMAX,GPAV,TO,TI,ROACA,ROWCH,
ARORCR,XKR,TWDD(50),NTHETA,PORSTY,DTHETA
C*****DATA INPUT
READ*,PORSTY,XKR,ROWCH,ARORCR,GAMAH,ROW,CPM,DEPAQ
READ*,D,HAQ,PERM,RW
READ*,TLY,DTP,EFFDP,EFFI,EFFG,EFFGP,HLS,DTA,DTHE,EFFDWP,HLDM
READ*,TSPACE,TDONHP,TDUTDH,TENVV,TENVH
READ*,NTHETA
READ*,EFFB,EPLANT
PI=4.*ATAN(1.)
ROACA=PORSTY*ROWCH*(1.-PORSTY)*ARORCR
C*****PRINT OUT BASIC DATA
WRITE(*,699)
WRITE(*,700)
WRITE(*,701)PORSTY
WRITE(*,702)PERM
WRITE(*,703)HAQ
WRITE(*,811)DEPAQ
WRITE(*,704)ROWCH
WRITE(*,705)ARORCR
WRITE(*,707)RW
WRITE(*,708)TLY
WRITE(*,709)EFFB
WRITE(*,820)HLS
WRITE(*,710)
WRITE(*,711)
WRITE(*,712)
WRITE(*,713)DT
WRITE(*,903)EFFDP
WRITE(*,714)EFFI
WRITE(*,715)EFFG
WRITE(*,201)TENVV
WRITE(*,717)
WRITE(*,718)DTHE
WRITE(*,719)EFFDWP
WRITE(*,720)HLDM
WRITE(*,812)TDUTDH
WRITE(*,721)TSPACE
WRITE(*,201)TENVH
WRITE(*,723)
WRITE(*,724)DTA
WRITE(*,725)TDONHP
WRITE(*,721)TSPACE
WRITE(*,201)TENVH
WRITE(*,683)EPLANT
WRITE(*,682)EFFB
TLS=TLY*31536000.
QI=(ROACA*D*D*HAQ/(ROWCH*TLS))*PI/3.
116 CALL AQUIFR
QS=QI/(1.-TWDD(NTLY))
IF(QS.GT.D.2)TLEN
GO TO 115
ENDIF
WRITE(*,202)QI
DO 203 I=1,NTLY
WRITE(*,204)I,TWDD(I)
203 CONTINUE
C*****POWER GENERATION
WRITE(*,710)
TO=410.
DO 100 NTO=1,3
TO=TO+20.
WRITE(*,696)D,QI,QS,TO
WRITE(*,695)

```

```

WRITE(*,694)
TI=335.
DO 120 NTI=1,13
  TI=TI+5.
  TS=TO-(TO-TI)*TWDD(NTLY)
  IF((TS-TI).LT.10.)THEN
    GO TO 120
  ENDIF
C*****BOILER TEMPERATURE FINDER
  TB=310.5
  HFGIP=((462.-TB)*100000./1.7998)**0.3646)*1000.
  CPAVIP=(0.00045*((TB-310.)*1.4175)+2.345)*1000.
  DIFF=(TS-TB-DTP)/HFGIP-(TB+DTP-TI)/(CPAVIP*(TB-310.))
  DIFF1=DIFF
  TB1=TB
  TB=311.
11 IF(TB.GT.TS)THEN
  GO TO 120
ENDIF
HFGIP=((462.-TB)*100000./1.7998)**0.3646)*1000.
CPAVIP=(0.00045*((TB-310.)*1.4175)+2.345)*1000.
DIFF=(TS-TB-DTP)/HFGIP-(TB+DTP-TI)/(CPAVIP*(TB-310.))
IF(DIFF.LT.0.)THEN
  TB=TB1+48S(DIFF1)/(ABS(DIFF1)+ABS(DIFF))
ELSE
  TB1=TB
  DIFF1=DIFF
  TB=TB+2.
  GO TO 11
ENDIF
C*****GROSS POWER OUT AND LOSSES
CPAVIP=(0.00045*((TB-310.)*1.4175)+2.345)*1000.
HFGIP=((462.-TB)*100000./1.7998)**0.3646)*1000.
MIP=(TS-TI)*CP/(CPAVIP*(TB-310.))+HFGIP
PBPCIP=0.1745*((TB-310.)*1.9519)*1000.
WFDP=(MIP*0.0016547*PBPCIP/EFB)*ROW*QS
H12SIP=(0.8164*(TB-310.)-0.000187*((TB-382.75)**2)**1.2838)
  A+11.25)*1000.
GELECT=MIP*H12SIP*EFFT*EFFG*ROW*QS
MCLW=((WFDP/(ROW*QS))+G*W*(TS-TI)-MIP*H12SIP*EFFT)/(4180.*8.33)
MCIRP=A2.7*MCLW*ROW*QS
MCLTF=165.4*MCLW*ROW*QS
CALL GFPW
NELECT=GELECT-WFDP-MCIRP-MCLTF-GPWAV
E=NELECT/(ROW*QI*(TO-TENVP-TENVP*ALOG(TO/TENVP)))
FFS=NELECT/EPLANT
WRITE(*,692)TI,TS,NELECT,GPWMIN,GPWMAX,GPWAV,E,FFS
120 CONTINUE
100 CONTINUE
C*****HEATING AND HEAT PUMP
WRITE(*,717)
TO=328.
DO 121 NTO=1,9
  IF(TO.GE.350.)THEN
    DTO=20.
  ELSE
    DTO=10.
  ENDIF
  TO=TO+DTO
  WRITE(*,696)D,DT,QS,TO
  WRITE(*,695)
  WRITE(*,694)
C*****DIRECT HEATING
  TI=311.48
  TS=TO-(TO-TI)*TWDD(NTLY)
  IF((TS-TI).LT.320.)THEN
    GO TO 121
  ENDIF
  CALL GFPW
  HTLOAD=ROW*QI*(TO-TI)
  DWPW=GAMAW*QS*4LOH/EFBWP
  FFS=HTLOAD/EFB-(GPWAV+DWPW)/EPLANT
  AIN=ROW*QI*(TO-TENVH-TENVH*ALOG(TO/TENVH))+GPWAV+DWPW)/EPLANT
  AOUT=HTLOAD*(1.-TENVH/TSPACE)
  E=AOUT/AIN
  WRITE(*,692)TI,TS,HTLOAD,GPWMIN,GPWMAX,GPWAV,E,FFS
C*****COMBINATION OF HEATING AND HEAT PUMP

```

```

IF (TO.GT.400.) THEN
  GO TO 121
ENDIF
TI=312.
DO 123 NTI=1,10
  TI=TI-3.
  TS=TO-(TO-TI)*TWDD(NTLY)
  IF (TS.LT.320.) THEN
    GO TO 121
  ENDIF
  CALL GFWW
  COPH=TCONHP/(2.*(TCONHP-TI+DTA))
  IF (COPH.GT.7.) THEN
    COPH=7.
  ENDIF
  WCOMP=ROWCH*QS*(TOUTDH-TI+DTHE)/(COPH-1.)
  HTLDHP=ROWCH*QS*(TOUTDH-TI+DTHE)+WCOMP
  HTLDHP=ROWCH*QS*(TS-DTHE-TOUTDH)
  HTTOT=HTLDHP+HTLDH
  WFAN=0.0421*HTLDHP
  FFS=HTTOT/EEFB-(GPWAV+DWPW+WFAN+WCOMP)/EPLANT
  AIN=ROWCH*QI*(TO-TENVH-TENVH*ALOG(TO/TENVH))+(GPWAV+DWPW+WFAN+
  WCOMP)/EPLANT
  AOUT=HTTOT*(1.-TENVH/TS*ACE)
  E=AOUT/AIN
  WRITE(*,692) TI,TS,HTTOT,GPWMIN,GPWMAX,GPWAV,E,FFS
123 CONTINUE
121 CONTINUE
C***** HEAT PUMP ONLY
WRITE(*,723)
TO=325.
DO 124 NT0=1,5
  TO=TO-5.
  WRITE(*,696) O,QI,QS,TO
  WRITE(*,695)
  WRITE(*,694)
  TI=TO-3.
  DO 125 NTI=1,12
    TI=TI-3.
    TS=TO-(TO-TI)*TWDD(NTLY)
    CALL GFWW
    COPH=TCONHP/(2.*(TCONHP-TI+DTA))
    IF (COPH.GT.7.) THEN
      COPH=7.
    ENDIF
    WCOMP=ROWCH*QS*(TS-TI)/(COPH-1.)
    HTLDHP=ROWCH*QS*(TS-TI)+WCOMP
    WFAN=0.0421*HTLDHP
    FFS=HTLDHP/EEFB-(GPWAV+WCOMP+WFAN)/EPLANT
    AIN=ROWCH*QI*(TO-TENVH-TENVH*ALOG(TO/TENVH))+(GPWAV+WCOMP+WFAN)/
    EPLANT
    AOUT=HTLDHP*(1.-TENVH/TS*ACE)
    E=AOUT/AIN
    WRITE(*,692) TI,TS,HTLDHP,GPWMIN,GPWMAX,GPWAV,E,FFS
126 CONTINUE
124 CONTINUE
QI=QI+0.005
GO TO 116
699 FORMAT(11X,'BASIC DATA')
700 FORMAT(10X,'AQUIFER')
701 FORMAT(10X,'POROSITY OF AQUIFER',26X,F12.2)
702 FORMAT(10X,'INTRINSIC PERMEABILITY',23X,F12.2,' MD')
703 FORMAT(10X,'THICKNESS OF AQUIFER',25X,F12.2,' M')
811 FORMAT(10X,'DEPTH OF AQUIFER',29X,F12.2,' M')
704 FORMAT(10X,'HEAT CAPACITY OF WATER',23X,F12.2,' J/M**3 K')
705 FORMAT(10X,'HEAT CAPACITY OF ROCK',24X,F12.2,' J/M**3 K')
707 FORMAT(10X,'RADIUS OF WELL',31X,F12.2,' M')
708 FORMAT(10X,'SYSTEM LIFE TIME',29X,F12.2,' YEARS')
709 FORMAT(10X,'EFFICIENCY OF GEOTHERMAL FLUID PUMP',10X,F12.2)
710 FORMAT(10X,'POWER GENERATION')
711 FORMAT(10X,'ISO-PENTANE BINARY CYCLE (SATURATED RANKINE CYCLE)')
712 FORMAT(10X,'CONDENSER TEMPERATURE',29X,' 310.00 (K)')
713 FORMAT(10X,'PINCH TEMPERATURE',28X,F12.2,' K')
903 FORMAT(10X,'EFFICIENCY OF FEED PUMP',22X,F12.2)
714 FORMAT(10X,'EFFICIENCY OF TURBINE',24X,F12.2)
715 FORMAT(10X,'EFFICIENCY OF GENERATOR',22X,F12.2)
717 FORMAT(10X,'HEATING')

```



```

718 FORMAT(#0#,#TEMPERATURE DIFFERENCE IN THE HEAT EXCHANGER#,6X,
      AF7.2,# K#)
719 FORMAT(# #,#EFFICIENCY OF DOMESTIC WATER PUMP#,18X,F7.2)
720 FORMAT(# #,#HEAD LOSS OF DOMESTIC WATER#,23X,F7.2,# M#)
812 FORMAT(# #,#OUTLET TEMPERATURE OF DOMESTIC WATER#,9X,F12.2,# K#)
723 FORMAT(#0#,#HEAT PUMP#)
724 FORMAT(#0#,#APPROACH TEMPERATURE#,30X,F7.2,# K#)
725 FORMAT(# #,#CONDENSER TEMPERATURE#,29X,F7.2,# K#)
721 FORMAT(# #,#SPACE TEMPERATURE#,33X,F7.2,# K#)
820 FORMAT(# #,#SURFACE HEAD LOSS OF GEOTHERMAL FLUID#,8X,F12.2,# M#)
697 FORMAT(#1#,#POWER GENERATION#)
696 FORMAT(#1#,#HEATING AND HEAT PUMP#)
584 FORMAT(#1#,#HEAT PUMP ONLY#)
683 FORMAT(#0#,#AVERAGE EFFECTIVENESS OF FOSSIL FUEL POWER PLANT#,
      AF9.2)
682 FORMAT(# #,#EFFICIENCY OF FOSSIL FUEL BOILER FOR HEATING #,F12.2)
701 FORMAT(# #,#ENVIRONMENT TEMPERATURE#,27X,F7.2,# K#)
202 FORMAT(#1#,#X,#YEAR#,7X,#TWD#,7X,#QI = #,F9.5,# M**3/SEC#)
204 FORMAT(# #,#X,I2,5X,F6.3)
696 FORMAT(#0#,#D-#,F7.2,# #,5X,#QI-#,F7.5,# M**3/SEC#,5X,#QS-#,
      AF7.5,# M**3/SEC#,5X,#TD-#,F7.2,# K#)
695 FORMAT(#0#,#X,#T#,9X,#TS#,10X,#LOAD#,11X,#GPMIN#,10X,#GPMAX#,
      A11X,#GPMWAV#,10X,#E#,11X,#FFS#)
694 FORMAT(# #,#X,#(K)#,8X,#(K)#,8X,#(J/SEC)#,9X,#(J/SEC)#,9X,
      A11J/SEC#,10X,#(J/SEC)#,18X,#(J/SEC)#)
692 FORMAT(# #,#F8.2,3X,F8.2,5X,E11.4,5X,E11.4,5X,E11.4,5X,E11.4,4X,
      AF7.4,4X,E11.4)
115 STOP
      END

```

```

SUBROUTINE AQUIFR
THIS SUBROUTINE PERFORMS THE CALCULATIONS OF NON-DIMENSIONAL
PRODUCTION TEMPERATURE AND BASIC PATTERN OF AQUIFER
RESISTANCES BY GENERATING FLOW FIELD.
COMMON X(50),Y(50),R(20,50),RN(20,50),HLAG(50),HGB(50),
AHLWELL(50),HLGP(50),GPW(50),XKO,XKI,RO,QI,TLY,NILY,EFFCP,DEPAQ,
ARM,PERM,HAQ,PI,GAMMA,D,HLS,GPWMIN,GPWMAX,GPWAV,T0,TI,ROACA,ROWCW,
APORCR,XKR,TWDD(50),NTHETA,PORSTY,DTHETA
DIST=D/20.
T01=400.
TI1=300.
XKO=GAMMA*PERM*(0.987E-15)/VISCOS(T01)
XKI=GAMMA*PERM*(0.987-15)/VISCOS(TI1)
ROACA=PORSTY*ROWCW*(1.-PORSTY)*RORCR
A=D/2.
DTHETA=PI/NTHETA
THETA=DTHETA/2.
NILE=FIXITLY
DTDI=ROWCW*QI*31536000./((ROACA*D*D*HAQ)
RMDAI=ROWCW*ROACA*HAQ*QI/(XKR*RORCR*D*D)
RMDAAV=RMDAI
TDI=0.
C*****CALCULATION OF NON-DIMENSIONAL TEMPERATURE
NILEY=NILE+20
DO 10 I=1,NILEY
TDI=TDI+DTDI
IF(TDI.GT.PI/3.) THEN
NI=I
GO TO 120
ELSE
TWDD(I)=0.
ENDIF
10 CONTINUE
GO TO 150
120 TDAV=TDI
CALL TEMP(RMDAAV,TDAV,TWD)
TDAV=(1./((1.-TWD)+1.)*(TDI-PI/3.)/2.+PI/3.
RMDAAV=RMDAI*TDAV/TDI
130 TWDD=TWDD
CALL TEMP(RMDAAV,TDAV,TWD)
TDAV=(1./((1.-TWD)+1.)*(TDI-PI/3.)/2.+PI/3.
EPSLON=TWDD/TWDD-1.
IF(EPSLON.GT.0.0001) THEN
GO TO 130
ENDIF
TWDD(NI)=TWDD
NII=NI+1
IF(NII.GT.NILEY) THEN
GO TO 150
ENDIF
DO 20 J=NII,NILEY
TDI=TDI+DTDI
TDAVI=TDAV
TDAV=TDAVI+DTDI/(1.-TWD)
TWDD=TWDD
CALL TEMP(RMDAAV,TDAV,TWD)
TDAV=TDAVI+(1./((1.-TWD)+1.)/(1.-TWD))*DTDI/2.
RMDAAV=RMDAI*TDAV/TDI
140 TWDD=TWDD
CALL TEMP(RMDAAV,TDAV,TWD)
TDAV=TDAVI+(1./((1.-TWD)+1.)/(1.-TWD))*DTDI/2.
RMDAAV=RMDAI*TDAV/TDI
EPSLON=TWDD/TWDD-1.
IF(EPSLON.GT.0.0001) THEN
GO TO 140
ENDIF
TWDD(J)=TWDD
20 CONTINUE
C*****CALCULATION OF NON-STEADY RESISTANCES
150 RD=2.*ALOG(D/RW)/(XKO*HAQ*DTHETA)
DO 30 I=1,NTHETA
VDS=0.
X(I)=D/2.-RW*COS(THETA)
Y(I)=RW*SIN(THETA)
THETA=THETA+DTHETA

```

```

XTH=X(I)
YTH=Y(I)
Q=QI
TIMEY=0.
NCOUNT=1
R1=90
TY1=0.
40 VXT=XTH*(XTH+4)*Q*(Q*(PI*HAQ1))*ROWCW/ROACA
VYTH=VYTH*(XTH+4)*Q*(Q*(PI*HAQ1))*ROWCW/ROACA
VTH=SQRT(VXT**2+VYTH**2)
L1=SQRT((XTH+4)**2+YTH**2)
IF(L1.LT.DIST*3.)THEN
DTS=DIST/(VT*10.)
ELSE
DTS=DIST/VTH
ENDIF
DTY=DTS/31536000.
XTHM=XTH+VXT*DTY/2.
YTHM=YTH+VYTH*DTY/2.
TIMEYM=TIMEY+DTY/2.
NY=IFIX(TIMEYM)
NYY=NYY+1
IF(NY.EQ.0)THEN
QNY=QI
ELSE
QNY=QI/(1.-TWDD(NY))
ENDIF
QNYQ=QI/(1.-TWDD(NYY))
Q=QNY+(QNYQ-QNY)*(TIMEYM-FLOAT(NY))
VXTM=XTH*(XTHM+4)*Q*(Q*(PI*HAQ1))*ROWCW/ROACA
VYTHM=VYTH*(XTHM+4)*Q*(Q*(PI*HAQ1))*ROWCW/ROACA
VTHM=SQRT(VXTM**2+VYTHM**2)
XTHF=XTH+VXTM*DTS
YTHF=YTH+VYTHM*DTS
XTHM=XTH+VXTM*DTS/2.
YTHM=YTH+VYTHM*DTS/2.
XTH=XTHF
YTH=YTHF
VXMI=XTH*(XTHM+4)*Q*(Q*(PI*HAQ1)*PORSTY)
VYMI=VYTH*(XTHM+4)*Q*(Q*(PI*HAQ1)*PORSTY)
VMI=SQRT(VXMI**2+VYMI**2)
DS=VTHM*DTS
VDS=VDS+VMI*DS
TIMEY=TIMEY+DTY
NY=IFIX(TIMEY)
NYY=NYY+1
IF(NY.EQ.0)THEN
QNY=QI
ELSE
QNY=QI/(1.-TWDD(NY))
ENDIF
QNYQ=QI/(1.-TWDD(NYY))
Q=QNY+(QNYQ-QNY)*(TIMEY-FLOAT(NY))
RESIST=RO+2.*PI*PORSTY*(1.-XKI/XKO)*VDS/(QI*DTHEA*XKI)
IF(NY.GE.NCOUNT)THEN
DO 50 K=NCOUNT,NY
R(I,K)=R1*(RESIST-R1)*(FLOAT(K)-TY1)/(TIMEY-TY1)
50 CONTINUE
R1=RESIST
TY1=TIMEY
NCOUNT=NY+1
ENDIF
IF(TIMEY.GT.TLY)THEN
GO TO 30
ENDIF
L=SQRT((XTH+4)**2+YTH**2)
IF(L.LT.DIST*0.2)THEN
DO 60 KK=NCOUNT,NTRY
R(I,KK)=RO*XKO/XKI
60 CONTINUE
ELSE
GO TO 40
ENDIF
30 CONTINUE
RETURN
END

```

```

SUBROUTINE GFP4
COMMON X(50),Y(50),R(20,50),RN(20,50),HLAQ(50),HGB(50),
AHLWELL(50),HLGPI(50),GPW(50),XKO,XKI,RO,QI,TLY,NTLY,EFFGP,DEPAQ,
ARW,PERM,HAQ,SI,GAMAW,D,ILS,GPWHIN,GPWMAX,GPWAV,TO,TI,ROACA,ROWCH,
ARORCR,XKR,TWDD(50),NTHETA,PORSTY,DTHETA
XKON=GAMAW*PERM*(0.987E-15)/VISCOS(TO)
XKIN=GAMAW*PERM*(0.987E-15)/VISCOS(TI)
RON=2.*ALOG(D/RW)/(XKON*HAQ*DTHETA)
DO 101 I=1,NTLY
DO 102 J=1,NTLY
RN(I,J)=(1./XKIN-1./XKON)*(R(I,J)-RO)/(1./XKI-1./XKO)+RON
102 CONTINUE
101 CONTINUE
C*****HEAD LOSS IN THE AQUIFER
DO 103 J=1,NTLY
RTOTIN=0.
DO 104 I=1,NTHETA
RTOTIN=RTOTIN+1./RN(I,J)
104 CONTINUE
RTOT=1./(RTOTIN*2.)
HLAQ(J)=RTOT*QI/(1.-TWDD(J))
103 CONTINUE
C*****HEAD LOSS IN THE WELLS. HEAD LOSS IN THE SURFACE SYSTEMS AND
C*****HEAD GAIN DUE TO BOUYANCY EFFECT
HLAQO=QI*ALOG(D/RW)/(XKON*HAQ*PI)
DO 105 J=1,NTLY
Q=QI/(1.-TWDD(J))
HLWELL(J)=0.05*DEPAQ*Q*Q/(4.*9.81*PI*PI*(RW**5))
TW=(TO-(TO-TI)*TWDD(J))
HGB(J)=((0.0642*(TW+TI)/2.-16.82)/10000.)*(TW-TI)*DEPAQ
HLGP(J)=HLAQ(J)+HLWELL(J)+HLS-HGB(J)
IF (HLGP(J).LT.0.) THEN
HLGP(J)=0.
ENDIF
GPW(J)=GAMAW*Q*HLGP(J)/EFFGP
105 CONTINUE
HLWELLO=0.05*DEPAQ*QI*QI/(4.*9.81*PI*PI*(RW**5))
HGBO=((0.0642*(TO+TI)/2.-16.82)/10000.)*(TO-TI)*DEPAQ
HLGPO=HLAQO+HLWELLO+HLS-HGBO
IF (HLGPO.LT.0.) THEN
HLGPO=0.
ENDIF
GPWHIN=GAMAW*QI*HLGPO/EFFGP
GPWMAX=GPW(NTLY)
C*****TOTAL GEOTHERMAL PUMP WORK CALCULATION
GPWTOT=0.
NTL=NTLY-1
DO 107 J=1,NTL
GPWTOT=GPWTOT+GPW(J)
107 CONTINUE
GPWTOT=GPWTOT*31536000.+(GPWHIN+GPWMAX)*31536000./2.
GPWAV=GPWTOT/(NTLY*31536000.)
RETURN
END

```

```

SUBROUTINE TEMP(RMDA,TD,TWD)
PI=3.141592653589793
IF(RMDA.GT.10000.)THEN
  NANGL=60
ELSE IF(RMDA.GT.500.)THEN
  NANGL=40
ELSE
  NANGL=20
ENDIF
DANGL=PI/NANGL
ANGL=0.
SUMERC=0.
ERC=0.
DO 11 I=1,NANGL
  ANGL=ANGL+DANGL
  IF(I.EQ.NANGL)THEN
    FTH=PI/3.
  ELSE
    FTH=FTHETA(ANGL)
  ENDIF
  IF(FTH.GE.TD)THEN
    ERC=0.
  ELSE
    ARG=FTH/SQRT(RMDA*((TD-FTH)))
    IF(ARG.GT.25.)THEN
      ERC=0.
    ELSE
      ERC=ERFC(ARG)
    ENDIF
  ENDIF
  SUMERC=SUMERC+ERC
11 CONTINUE
SUMERC=SUMERC-(ERC*.5)
TWD=SUMERC/NANGL
RETURN
END

```

```

FUNCTION FTHETA(A)
PI=3.141592653589793
FTHETA=PI-COS(A)/(SIN(A**3.)*(PI-A+SIN(A)*COS(A))+PI
RETURN
END

```

```

FUNCTION VISCOS(T)
VISCOS=SQRT((T-281.585)*2.0078.4)
VISCOS=((VISCOS+T-281.585)*2.1482-120.)*10.
VISCOS=1./VISCOS
RETURN
END

```

```

FUNCTION VX(X,Y,A)
VX=(X**2-Y**2-A**2)/((X**2-Y**2-A**2)**2+4.*(X**2)*(Y**2))
RETURN
END

```

```

FUNCTION VY(X,Y,A)
VY=2.*X*Y/((X**2-Y**2-A**2)**2+4.*(X**2)*(Y**2))
RETURN
END

```

C.2 Sample Computer Output of Increasing Flow Model(Power and Heating)

<u>BASIC DATA</u>	
<u>AQUIFER</u>	
POROSITY OF AQUIFER	.20
INTRINSIC PERMEABILITY	100.00 MD
THICKNESS OF AQUIFER	100.00 M
DEPTH OF AQUIFER	2000.00 M
HEAT CAPACITY OF WATER	4000000.00 J/M**3 K
HEAT CAPACITY OF ROCK	2000000.00 J/M**3 K
RADIUS OF WELL	.15 M
SYSTEM LIFE TIME	25.00 YEARS
EFFICIENCY OF GEOTHERMAL FLUID PUMP	.75
SURFACE HEAD LOSS OF GEOTHERMAL FLUID	15.00 M
<u>POWER GENERATION</u>	
ISO-PENTANE BINARY CYCLE(SATURATED RANKINE CYCLE)	
CONDENSER TEMPERATURE	310.00 K
PINCH TEMPERATURE	8.33 K
EFFICIENCY OF FEED PUMP	.68
EFFICIENCY OF TURBINE	.80
EFFICIENCY OF GENERATOR	.90
ENVIRONMENT TEMPERATURE	289.00 K
<u>HEATING</u>	
TEMPERATURE DIFFERENCE IN THE HEAT EXCHANGER	8.33 K
EFFICIENCY OF DOMESTIC WATER PUMP	.80
HEAD LOSS OF DOMESTIC WATER	20.00 M
OUTLET TEMPERATURE OF DOMESTIC WATER	303.15 K
SPACE TEMPERATURE	295.00 K
ENVIRONMENT TEMPERATURE	270.00 K
<u>HEAT PUMP</u>	
APPROACH TEMPERATURE	8.33 K
CONDENSER TEMPERATURE	322.22 K
SPACE TEMPERATURE	295.00 K
ENVIRONMENT TEMPERATURE	270.00 K
AVERAGE EFFECTIVENESS OF FOSSIL FUEL POWER PLANT	.30
EFFICIENCY OF FOSSIL FUEL BOILER FOR HEATING	.75

YEAR TWO QI = .01717 M**3/SEC

1	0.000
2	0.000
3	0.000
4	0.000
5	0.000
6	0.000
7	0.000
8	0.000
9	0.000
10	0.000
11	.042
12	.106
13	.153
14	.195
15	.229
16	.251
17	.253
18	.299
19	.322
20	.341
21	.351
22	.370
23	.387
24	.397
25	.404

POWER GENERATION

D= 300.00 M QI= .01717 M**3/SEC QS= .02881 M**3/SEC TO= 430.00 K

TI (K)	TS (K)	LOAD (J/SEC)	GPMIN (J/SEC)	GPMAX (J/SEC)	GPAV (J/SEC)	E	FFS (J/SEC)
340.00	393.65	.1309E+06	0.	.7283E+05	.2347E+05	.1841	.1103E+07
345.00	395.67	.13640E+06	0.	.6848E+05	.2203E+05	.2025	.1213E+07
350.00	397.69	.13849E+06	0.	.6476E+05	.2084E+05	.2142	.1283E+07
355.00	399.71	.13957E+06	0.	.6158E+05	.1989E+05	.2202	.1319E+07
360.00	401.73	.13980E+06	0.	.5889E+05	.1918E+05	.2214	.1327E+07
365.00	403.75	.14087E+06	0.	.5664E+05	.1880E+05	.2163	.1296E+07
370.00	405.77	.13742E+06	0.	.5478E+05	.1868E+05	.2104	.1261E+07
375.00	407.79	.13591E+06	0.	.5329E+05	.1882E+05	.1998	.1197E+07
380.00	409.81	.13365E+06	0.	.5212E+05	.1914E+05	.1872	.1122E+07
385.00	411.83	.13105E+06	.1574E+04	.5125E+05	.1968E+05	.1728	.1035E+07
390.00	413.84	.12816E+06	.3334E+04	.5067E+05	.2039E+05	.1567	.9386E+06
395.00	415.86	.12439E+06	.5269E+04	.5034E+05	.2125E+05	.1390	.8329E+06
400.00	417.88	.12156E+06	.7220E+04	.5026E+05	.2227E+05	.1200	.7186E+06

HEATING

D= 300.00 M QI= .01717 M**3/SEC QS= .02881 M**3/SEC TO= 330.00 K							
TI (K)	TS (K)	LOAD (J/SEC)	GPMIN (J/SEC)	GPMAX (J/SEC)	GPAV (J/SEC)	E	FFS (J/SEC)
311.48	322.52	.1272E+07	.4786E+05	.1728E+06	.9289E+05	.1471	.1363E+07
309.00	321.52	.1430E+07	.4752E+05	.1787E+06	.9549E+05	.1333	.1439E+07
306.00	320.51	.1702E+07	.4712E+05	.1866E+06	.9896E+05	.1288	.1513E+07

D= 300.00 M QI= .01717 M**3/SEC QS= .02881 M**3/SEC TO= 340.00 K							
TI (K)	TS (K)	LOAD (J/SEC)	GPMIN (J/SEC)	GPMAX (J/SEC)	GPAV (J/SEC)	E	FFS (J/SEC)
311.48	328.48	.1999E+07	.3923E+05	.1650E+06	.8643E+05	.1368	.2300E+07
309.00	327.48	.2177E+07	.3889E+05	.1709E+06	.8900E+05	.1743	.2377E+07
306.00	326.27	.2449E+07	.3849E+05	.1786E+06	.9244E+05	.1540	.2451E+07
303.00	325.06	.2743E+07	.3813E+05	.1872E+06	.9628E+05	.1356	.2476E+07
300.00	323.84	.3057E+07	.3778E+05	.1967E+06	.1006E+06	.1204	.2457E+07
297.00	322.63	.3393E+07	.3747E+05	.2073E+06	.1054E+06	.1070	.2390E+07
294.00	321.42	.3751E+07	.3718E+05	.2191E+06	.1108E+06	.0979	.2272E+07
291.00	320.21	.4134E+07	.3692E+05	.2324E+06	.1169E+06	.0880	.2100E+07

D= 300.00 M QI= .01717 M**3/SEC QS= .02881 M**3/SEC TO= 350.00 K							
TI (K)	TS (K)	LOAD (J/SEC)	GPMIN (J/SEC)	GPMAX (J/SEC)	GPAV (J/SEC)	E	FFS (J/SEC)
311.48	334.44	.2646E+07	.3171E+05	.1540E+06	.8058E+05	.2301	.3236E+07
309.00	333.44	.2864E+07	.3136E+05	.1638E+06	.8313E+05	.2042	.3312E+07
306.00	332.23	.3136E+07	.3097E+05	.1715E+06	.8654E+05	.1799	.3386E+07
303.00	331.02	.3439E+07	.3060E+05	.1801E+06	.9036E+05	.1576	.3411E+07
300.00	329.81	.3744E+07	.3026E+05	.1895E+06	.9463E+05	.1390	.3392E+07
297.00	328.59	.4079E+07	.2994E+05	.2000E+06	.9943E+05	.1237	.3326E+07
294.00	327.38	.4438E+07	.2965E+05	.2114E+06	.1044E+06	.1109	.3208E+07
291.00	326.17	.4821E+07	.2939E+05	.2249E+06	.1109E+06	.1003	.3036E+07
288.00	324.96	.5230E+07	.2915E+05	.2398E+06	.1178E+06	.0914	.2884E+07
285.00	323.75	.5668E+07	.2894E+05	.2567E+06	.1257E+06	.0833	.2588E+07
282.00	322.54	.6136E+07	.2875E+05	.2759E+06	.1344E+06	.0774	.2142E+07

HEAT PUMP

D= 300.00 M QI= .01717 M**3/SEC QS= .02431 M**3/SEC TO= 320.00 K

TI (K)	TS (K)	LOAD (J/SEC)	GPMIN (J/SEC)	GPMAX (J/SEC)	GPMAY (J/SEC)	E	FFS (J/SEC)
314.00	317.58	.4808E+06	.5852E+05	.1759E+06	.9777E+05	.0450	.1875E+05
311.00	316.37	.7212E+06	.5808E+05	.1628E+06	.1007E+06	.0574	.1812E+06
308.00	315.15	.9617E+06	.5767E+05	.1903E+06	.1040E+06	.0666	.3426E+06
305.00	313.94	.1225E+07	.5729E+05	.1956E+06	.1077E+06	.0710	.4546E+06
302.00	312.73	.1503E+07	.5693E+05	.2078E+06	.1118E+06	.0726	.5325E+06
299.00	311.52	.1794E+07	.5659E+05	.2179E+06	.1163E+06	.0726	.5812E+06
296.00	310.31	.2099E+07	.5629E+05	.2292E+06	.1215E+06	.0716	.5986E+06
293.00	309.10	.2418E+07	.5600E+05	.2417E+06	.1272E+06	.0700	.5822E+06
290.00	307.88	.2754E+07	.5575E+05	.2558E+06	.1337E+06	.0681	.5293E+06
287.00	306.67	.3107E+07	.5552E+05	.2717E+06	.1410E+06	.0660	.4388E+06
284.00	305.46	.3478E+07	.5532E+05	.2896E+06	.1494E+06	.0638	.3014E+06
281.00	304.25	.3869E+07	.5514E+05	.3102E+06	.1590E+06	.0616	.1191E+06

D= 300.00 M QI= .01717 M**3/SEC QS= .02431 M**3/SEC TO= 315.00 K

TI (K)	TS (K)	LOAD (J/SEC)	GPMIN (J/SEC)	GPMAX (J/SEC)	GPMAY (J/SEC)	E	FFS (J/SEC)
309.00	312.53	.4808E+06	.6382E+05	.1928E+06	.1071E+06	.0460	-.1219E+05
306.00	311.37	.7294E+06	.6343E+05	.2009E+06	.1106E+06	.0576	.1309E+06
303.00	310.15	.9943E+06	.6306E+05	.2099E+06	.1146E+06	.0638	.2374E+06
300.00	308.94	.1271E+07	.6272E+05	.2198E+06	.1191E+06	.0669	.3163E+06
297.00	307.73	.1562E+07	.6240E+05	.2308E+06	.1248E+06	.0679	.3656E+06
294.00	306.52	.1866E+07	.6211E+05	.2430E+06	.1296E+06	.0677	.3830E+06
291.00	305.31	.2185E+07	.6185E+05	.2567E+06	.1359E+06	.0666	.3659E+06
288.00	304.10	.2520E+07	.6161E+05	.2720E+06	.1430E+06	.0651	.3114E+06
285.00	302.88	.2873E+07	.6140E+05	.2894E+06	.1510E+06	.0633	.2165E+06
282.00	301.67	.3245E+07	.6121E+05	.3091E+06	.1602E+06	.0614	.7752E+05
279.00	300.46	.3638E+07	.6105E+05	.3317E+06	.1708E+06	.0594	-.1097E+06
276.00	299.25	.4050E+07	.6092E+05	.3580E+06	.1832E+06	.0574	-.3499E+06

D= 300.00 M QI= .01717 M**3/SEC QS= .02681 M**3/SEC TO= 310.00 K

TI (K)	TS (K)	LOAD (J/SEC)	GPMIN (J/SEC)	GPMAX (J/SEC)	GPMAY (J/SEC)	E	FFS (J/SEC)
304.00	307.58	.4935E+06	.6996E+05	.2125E+06	.1179E+06	.0455	-.7533E+05
301.00	306.37	.7571E+06	.6961E+05	.2222E+06	.1222E+06	.0552	.3292E+05
298.00	305.15	.1033E+07	.6929E+05	.2330E+06	.1271E+06	.0604	.1132E+06
295.00	303.94	.1322E+07	.6899E+05	.2449E+06	.1325E+06	.0628	.1633E+06
292.00	302.73	.1625E+07	.6872E+05	.2582E+06	.1386E+06	.0634	.1808E+06
289.00	301.52	.1944E+07	.6847E+05	.2731E+06	.1454E+06	.0630	.1632E+06
286.00	300.31	.2279E+07	.6825E+05	.2899E+06	.1532E+06	.0620	.1075E+06
283.00	299.10	.2631E+07	.6806E+05	.3089E+06	.1628E+06	.0605	.1830E+05
280.00	297.88	.3003E+07	.6789E+05	.3307E+06	.1722E+06	.0589	-.1322E+06